Emergence and Propagation of Epistasis in Metabolic Networks

Sergey Kryazhimskiy

June 18, 2020

Abstract

Genome-wide measurements of epistasis are often used to probe functional relationships between genes. However, we lack a theory for understanding how functional relationships at the molecular level translate into epistasis measured at the level of whole-organism phenotypes, such as fitness. Here, I develop a mathematical model of a hierarchical metabolic network to address this gap. I derive how the topological relationship between reactions affected by mutations translates into epistasis and how this epistasis propagates from lower- to higher-level phenotypes in the network. An analysis of a computational model of glycolysis indicates that epistasis in more realistic metabolic networks follows similar albeit more complex patterns. These results imply that epistasis coefficients measured for high-level phenotypes carry some but not all information about the underlying functional relationships between gene products. They also suggest that pairwise inter-gene epistasis should be common and should depend on the genetic background and environment.

Life emerges from an orchestrated performance of complex regulatory and metabolic networks within cells. The blueprint for these networks is encoded in the genome. Mutations alter the genome. Some of them, once decoded by the cell, perturb cellular networks and thereby change the phenotypes important for life. Understanding how mutations affect the function of cellular networks is a central question in biology. Answering it is key to solving many practical and fundamental problems, such as finding mechanistic causes of genetic disorders [1, 2], understanding the architecture of complex traits [3–5], building artificial cells [6], explaining past and predicting future evolution [7–13]. Conversely, mutations can help us learn how cellular networks are organized [14].

To infer the wiring diagram of a cellular network that produces a certain phenotype one approach is to measure the pairwise and higher-order genetic interactions (or "epistasis") between mutations that perturb it [15–17]. Much effort has been devoted in the past 20 years to a systematic collection of such genetic interaction data for several model organisms and cell lines [17–41]. This approach is particulary powerful when the phenotypic effect of one mutation changes qualitatively depending on the presence or absence

of a second mutation in another gene, for example when a mutation has no effect on the phenotype in the wildtype background, but abolishes the phenotype when introduced together with another mutation (e.g., synthetic lethality). Such qualitative genetic interactions can often be directly interpreted in terms of a functional relationship between gene products [14, 42, 43].

Most pairs of mutations do not exhibit qualitative genetic interactions. Instead, the phenotypic effect of a mutation may change measurably but not qualitatively depending on the presence or absence of other mutations in the genome [31, 32]. The genetic interactions can in this case be quantified with one of several metrics that are termed "epistasis coefficients" [44]. While some rules have been proposed for interpreting epistasis coefficients, in particular, their sign, [45–49], the validity and robustness of these rules are unknown because there is no theory for how functional relationships translate into measurable epistasis coefficients in any system [48, 50]. To avoid this major difficulty, most large-scale empirical studies focus on correlations between epistasis coefficients rather than on their actual values. Genes with highly correlated epistasis profiles are then interpreted as being functionally related [18, 31, 32, 37, 51]. Although this approach is extremely powerful for grouping genes into protein complexes and larger functional modules [51, 52], it does not reveal the functional relationships themselves. As a result, many if not most, genetic interactions between genes and modules still await their biological interpretation [2, 32].

A theory of epistasis must resolve two challenges. First, it must specify what sort of information about the underlying biological network is contained in a matrix of epistasis coefficients. Consider a biochemical network module with an unknown internal structure and suppose that the phenotype of interest is the flux through this module. By genetically perturbing all enzymes within the module and measuring the flux in all single and double mutants, we can obtain the matrix of epistasis coefficients. In principle, we can then fit a network topology and the network parameters to this matrix. However, if we do not know what information about the network is contained in the matrix in the first place, we cannot be sure that the inferred topology and parameters are close to their true values rather than represent one of many possible solutions consistent with the data.

The second challenge is that in practice the phenotypes for which epistasis is measured are often not the ones in which we are interested. We are often interested in understanding the structure of a particular regulatory or metabolic network module. However, measuring its peformance directly is often experimentally difficult or impossible. Thus, in practice epistasis is often measured for an experimentally accessible "high-level" phenotype, such as fitness, which depends on the performance of the focal "lower-level" module, e.g., the activity of a metabolic pathway of interest, but also on other unrelated modules. If we do not know how epistasis that originally emerged in one module maps onto epistasis that is measured, it is unclear what we can infer about module's internal structure. Therefore, a theory of epistasis must describe how epistasis propagates from lower-level phenotypes where it emerges to higher-level phenotypes where it is measured.

Although there is a large body of theoretical and computational literature exploring epistasis in various biological models [18, 45, 47, 53–64], the work by Chiu et al [65] is, to my knowledge, the only attempt to develop a more general theory. Chiu et al established a fundamental connection between epistasis and the curvature of the function that maps lower-level phenotypes onto a higher-level phenotype. However, further progress is hindered by the uncertainty in what types of functions map phenotypes onto one another in real biological systems. Chiu et al considered one special case, a cost-benefit function, but the generality of this choice is unclear. Here, rather than a priori assuming a specific functional form, I consider a model of a hierarchical metabolic network and derive the class of all functions that determine how the activity of a larger metabolic module can depend on the activities of smaller constituent modules. There are several reasons to focus on metabolism. First, epistasis is often measured at the level of growth rate, at least in microbes [21, 31, 32], and metabolism fuels growth. Second, metabolic genes occupy a large fraction of most genomes [66] and the general organization of metabolism is conserved throughout life [67]. Thus, by understanding genetic interactions between metabolic genes, we will gain an understanding of a large fraction of all genetic interactions.

My general approach is based on the metabolic control analysis [45, 47, 53, 68]. I consider a hierarchical network with first-order kinetics but an arbitrary topology, and ask two questions related to the two challenges mentioned above. (1) How does an epistasis coefficient that arose at some level of the metabolic hierarchy propagate to higher levels of the hierarchy? (2) What information about the network topology is contained in the value of an epistasis coefficient observed between two mutations that affect different enzymes in this network? This model is not intended to generate predictions of epistasis for any specific organism. Instead, its purpose is to provide a baseline expectation for what kind of information about the cellular network structure may be gained from measurements of epistasis. One possible outcome of this analysis is that there may be fundamental limitations to what epistasis measurements can reveal about biology. On the other hand, if it turns out that epistasis coefficients are biologically interpretable in this simple model, then it may be worth developing more sophisticated and general models on which inference from data can be based.

Model

I consider a biochemical reaction network $\mathcal{N} = (A, \boldsymbol{x})$, where $A = \{1, 2, \ldots, n\}$ is the set of metabolites and $\boldsymbol{x} = \|x_{ij}\|_{i,j=1}^{n}$ is the matrix of reaction rates. Specifically, I assume that all reactions are reversible and first-order, i.e., the rate of the reaction converting metabolite i into metabolite j is $x_{ij}\,(S_i - S_j/K_{ij})$, where S_i, S_j are the concentrations of metabolites i and j and K_{ij} is the equilibrium constant. This assumption makes the model analytically tractable; biologically, it is equivalent to assuming that all enzymes are

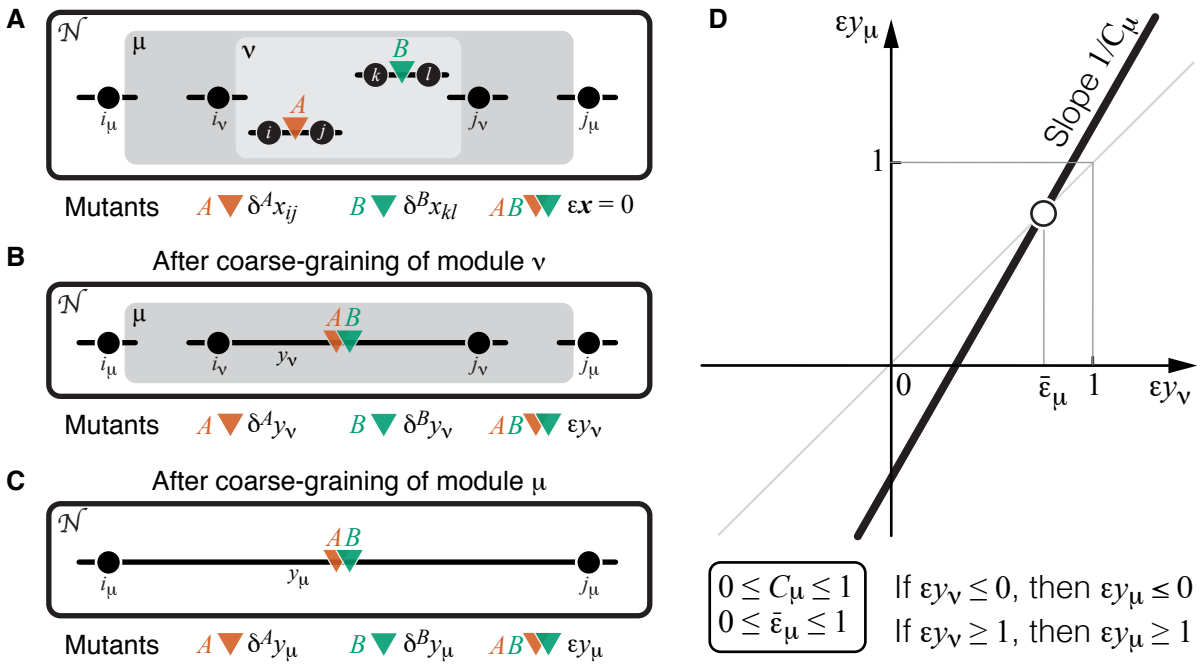

Figure 1. Structure of the model, emergence and propagation of epistasis. (A) Hierarchical metabolic network $\mathcal{N}$ containing nested modules μ and ν. A module can have an arbitrary internal structure with the constraint that its I/O metabolites are the only metabolites outside of the module to which its internal metabolites are connected. Metabolites i, j, k and ℓ are internal to both modules ν and μ; metabolites i_ν and j_ν are I/O for module ν and internal to module μ; metabolites i_μ and j_μ are I/O for module μ; other metabolites are not shown. Lines indicate reactions, and lines that terminate at only one metabolite represent potentially multiple reactions in which this metabolite participates. Mutation A perturbs reaction rate x_{ij} by $\delta^A x_{ij}$; mutation B perturbs a different reaction rate $x_{k\ell}$ by $\delta^B x_{k\ell}$; there is no epistasis between these mutations at the level of reaction rates, the lowest phenotypic level in this model. (B) At steady state, module ν can be replaced with an effective reaction with the rate constant y_ν. Epistasis between mutations A and B may emerge at the level of y_ν, a higher-level phenotype relative to the reaction rates. (C) At steady state, module μ can be replaced with an effective reaction with the rate constant y_μ. Epistasis may now propagate from the lower-level phenotype y_ν to the higher-level phenotype y_μ. (D) Properties of equation (3) that maps εy_ν onto εy_μ. Slope $1/C_\mu$ and fixed point $\bar{\varepsilon}_\mu$ depend on the topology and the reaction rates in module μ, but they are bounded, as shown. Thus, the fixed point of this map at $\bar{\varepsilon}_\mu$ is always unstable (open circle).

far from saturation. The rate constants x_{ij} depend on the concentrations and the specific activities of enzymes (and thus, can be altered by mutations) while K_{ij} characterize the fundamental chemical nature of metabolites i and j (and, as such, cannot be altered by mutations) [69]. Note that x_{ij} satisfy the Haldane relationships $x_{ji} = x_{ij}/K_{ij}$ [70]. Two metabolites i and j are said to be connected (in the graph-theoretic sense) if there exists an enzyme that catalyzes a biochemical reaction that interconverts them, i.e., if $x_{ij} > 0$.

I call a pair $\mu = (A_\mu, \boldsymbol{x}_\mu)$ a *subnetwork* of network $\mathcal{N}$ if $A_\mu \subset A$ is a subset of metabolites and $\boldsymbol{x}_\mu$ is the submatrix of $\boldsymbol{x}$ which corresponds to all reactions where both the product and the substrate belong to the set $A_\mu \cup A_\mu^{\mathrm{IO}}$. Here, A_μ^{IO} is the set of all metabolites that do not belong to A_μ but are connected to at least one metabolite from A_μ. I refer to A_μ and A_μ^{IO} as the sets of internal and "input/output" ("I/O" for short) metabolites for subnetwork μ, respectively. A subnetwork μ is called a *module* if it has two I/O metaboilites and if the matrix $\boldsymbol{x}_\mu$ has sufficiently many non-zero elements so that all internal metabolites can reach a quasi-steady state at any given concentration of the I/O metabolites (see Materials and Methods for details). I label the two I/O metabolites as i_μ and j_μ (Figures 1 and 4). One could consider modules with more than two I/O metabolites. However, mathematical calculations would become unwieldy. In addition, modules with just two I/O metabolites already capture two most salient features of metabolism: its directionality, and its complex branched topology [67]. This model is a natural generalization of a linear metabolic pathway which has been extensively studied in the previous literature [45, 47, 53, 57, 68].

The network $\mathcal{N}$ has a hierarchical structure in the sense that there is a series of nested modules $\cdots \subset \nu \subset \mu \subset \cdots$, such that $\cdots \subset A_\nu \subset A_\mu \subset \cdots$ (Figure 1).

Results

The central goal of this paper is to understand the patterns of epistasis between mutations in the hierarchical metabolic model described above. Specifically, I will address two questions. First, if two mutations exhibit epistasis at one level of the hierarchy, what can we say about epistasis between these mutations at higher levels of the hierarchy? In other words, how does the rest of the network distort an epistasis signal that arose in some module deep within the network but that is being measured at a high-level phenotype? Second, do mutations that affect different enzymes always exhibit epistasis, and, if so, what can we say about it? In other words, does epistasis carry any information about the topological structure of the module? To formulate these questions in precise mathematical terms, I first define how to quantify epistasis at different levels of the hierarchy.

Quantification of epistasis at different levels of metabolic hierarchy

Consider module ν that is at quasi-steady state at a given concentration of its I/O metabolites i_ν, j_ν. Then, in general, the flux J_ν through module ν between the I/O metabolites is a function of concentrations S_{i_ν}, S_{j_ν} and the reaction rates $\boldsymbol{x}_\nu$. However, when all reactions are first-order, it can be shown that $J_\nu = y_\nu \left(S_{i_\nu} - S_{j_\nu}/K_{i_\nu j_\nu}\right)$, where y_ν is the effective reaction rate constant of module ν, which only depends on $\boldsymbol{x}_\nu$ (Figure 1B; proof in the Materials and Methods). In other words, if the entire module ν at quasi-steady state is replaced with a single first-order biochemical reaction with rate y_ν between its two I/O metabolites, the dynamics of all metabolites outside of module ν would not change. This statement is the biochemical analog of the star-mesh transformation (and its generalization, Kron reduction) well known in the theory of electric circuits [71, 72]. The biological interpretation of this transformation is that the larger network (i.e., the cell) "cares" only about the total rate at which the I/O metabolites are interconverted but "does not care" about the details of how this conversion is enzymatically implemented. In this sense, the effective rate y_ν quantifies the function of module ν (a macroscopic parameter) while the rates $\boldsymbol{x}_\nu$ describe the specific biochemical implementation of the module (microscopic parameters).

Module ν may be embedded into a larger module μ (Figure 1A, B), which at quasi-steady state can itself be replaced with an effective first-order biochemical reaction with rate y_μ (Figure 1C). Of course, y_μ depends on the matrix $\boldsymbol{x}_\mu$ that can be decomposed into two submatrices, $\boldsymbol{x}_\nu$ and $\boldsymbol{x}_{\mu\setminus\nu}$, where the latter is the matrix of rates of reactions that belong to module μ but not to module ν. Since replacing the smaller module ν with an effective reaction does not alter the dynamics of metabolites outside of ν, y_μ must depend on $\boldsymbol{x}_\nu$ only through y_ν,

$$y_\mu = F_\mu \left(y_\nu; \boldsymbol{x}_{\mu\setminus\nu}\right), \tag{1}$$

where rates $\boldsymbol{x}_{\mu\setminus\nu}$ act as parameters of function F_μ (see Materials and Methods for details). Thus, any module μ in the metabolic hierarchy $\cdots \subset \nu \subset \mu \subset \cdots$ is characterized by its quantitative phenotype y_μ which depends on the "lower-level" quantitative phenotype y_ν through equation (1). This hierarchy of phenotypes is conceptually similar to the hierarchical "ontotype" representation of genomic data proposed recently by Yu et al [73].

Now consider mutation A that perturbs one rate constant x_{ij} and has no other effects (Figure 1A). This mutation can be quantified at the microscopic level by its relative effect $\delta^A x_{ij}$, defined as $\delta^A x_{ij} = x_{ij}^A / x_{ij}^0 - 1$, where x_{ij}^0 and x_{ij}^A are the rate constants of the wild-type and the mutant, respectively. If the reaction between metabolites i and j belongs to module ν, mutation A may affect the function of this module. Thus, mutation A can also be quantified at the level ν of the metabolic hierarchy by its relative effect $\delta^A y_\nu = y_\nu^A / y_\nu^0 - 1$ (Figure 1B).

Consider now mutation B that only perturbs the rate constant $x_{k\ell}$ of another reaction.

Since mutations A and B perturb distinct enzymes, they by definition do not genetically interact at the level of reaction rates. However, if both perturbed reactions belong to the same metabolic module ν, they may interact at the level of the function of this module in the sense that the effect of mutation B on the effective rate y_ν may depend on whether mutation A is present or not. Such genetic interaction between mutations A and B can be quantified at any level ν of the metabolic hierarchy by a number of various epistasis coefficients [44]. I will quantify it with a somewhat unconventional but mathematically convenient epistasis coefficient defined as follows.

$$\varepsilon^{AB} y_\nu = \frac{\delta^{AB} y_\nu - \delta^A y_\nu - \delta^B y_\nu}{2\,\delta^A y_\nu\,\delta^B y_\nu}, \tag{2}$$

where $\delta^{AB} y_\nu$ denotes the effect of the combination of mutations on phenotype y_ν relative to the wildtype (Figure 1A). Since I only consider two mutations A and B, I will write εy_ν instead of $\varepsilon^{AB} y_\nu$ to simplify notations. Note that other conventional epistasis coefficients can always be computed from εy_ν, $\delta^A y_\nu$ and $\delta^B y_\nu$, if necessary.

In this setup, the two questions posed at the beginning of the section can now be formulated mathematically as follows. (1) Given that two mutations A and B have an epistasis coefficient εy_ν at a lower level ν of the metabolic hierarchy, what can we say about their epistasis coefficient εy_μ at the higher level μ of the hierarchy? (2) If mutation A only perturbs the activity x_{ij} of one enzyme and mutation B only perturbs the activity $x_{k\ell}$ of another enzyme that belongs to the same module ν, then what values of εy_ν can we expect to observe based on the topological relationship within module ν between the two perturbed reactions?

Propagation of epistasis through the hierarchy of metabolic phenotypes

Assuming that the effects of both individual mutations and their combined effect at the level ν are small, it follows from equation (1), (2) that

$$\varepsilon y_\mu \;=\; \frac{\varepsilon y_\nu}{C_\mu} + \frac{H_\mu}{2\,C_\mu^2} + \text{h.o.t.}, \tag{3}$$

where $C_\mu = F'_\mu\, y_\nu / y_\mu$ and $H_\mu = F''_\mu\, y_\nu^2 / y_\mu$ are the first- and second-order control coefficients of the lower-level module ν with respect to the flux through the higher-level module μ (see Materials and Methods for details). Abbreviation "h.o.t." stands for "higher-order terms", i.e., terms that vanish as the effects of mutations tend to zero.

Equation (3) defines a linear map with slope $1/C_\mu$ and a fixed point $\bar{\varepsilon}_\mu = -H_\mu\,(2\,C_\mu\,(1 - C_\mu))^{-1}$, which both depend on the topology of module μ and the rate constants $\boldsymbol{x}_{\mu\backslash\nu}$. The first result of this paper (see Theorem 1 in the Materials and Methods) is that, for any module μ,

$$0 \le C_\mu \le 1 \text{ and } 0 \le \bar{\varepsilon}_\mu \le 1. \tag{4}$$

The full proof is given in the Materials and Methods, but its main idea is the following. Although the function F_μ in equation (1) could in principle have an infinite number of functional forms depending on the underlying topology of module μ, this is not the case. In fact, all topologies fall into three equivalence classes that differ by the topological position of the smaller module ν relative to the I/O metabolites of module μ. Thus, function F_μ can take only one of three functional forms, for which C_μ and H_μ can be explicitly calculated. The fact that $0 \leq C_\mu \leq 1$ can also be easily derived from the summation theorem of metabolic control analysis [68].

Equation (3) together with inequalities (4) show that the linear map from epistasis at a lower-level to epistasis at the higher-level has an unstable fixed point between 0 and 1 (Figure 1D). This implies that negative epistasis at one level of the metabolic hierarchy necessarily induces negative epistasis of larger magnitude at the next level of the hierarchy, i.e., $\varepsilon y_\mu \leq \varepsilon y_\nu < 0$. Therefore, once negative epistasis emerges somewhere along the hierarchy, it will induce negative epistasis at all higher levels of the hierarchy, irrespectively of the topology or the kinetic parameters of the network.

Similarly, if epistasis at the lower level of the metabolic hierarchy is positive and strong, $\varepsilon y_\nu > 1$, it will induce even stronger positive epistasis at the next level of the hierarchy, i.e., $\varepsilon y_\mu \geq \varepsilon y_\nu > 1$. Therefore, once strong positive epistasis emerges somewhere in the metabolic hierarchy, it will induce strong positive epistasis of larger magnitude at all higher levels of the hierarchy, irrespectively of the topology or the kinetic parameters of the network. If positive epistasis at a lower level of the hierarchy is weak, $0 < \varepsilon y_\nu < 1$, it could induce either negative, weak positive or strong positive epistasis at the higher level of the hierarchy, depending on the precise value of εy_ν, the topology of module μ and the microscopic rate constants $\boldsymbol{x}_{\mu\setminus\nu}$.

In summary, there are three regimes of how epistasis propagates through a hierarchical metabolic network. Negative and strong positive epistasis propagate robustly irrespectively of the topology and kinetic parameters of the metabolic network, whereas the propagation of weakly positive epistasis depends on these details.

Emergence of epistasis between mutations affecting different enzymes

Which of the three regimes described above can emerge in metabolic networks and under what circumstances? In other words, if two mutations affect the same module ν, are there any constraints on what values of epistasis can arise at the level of the functional phenotype y_ν? To address this question, I consider two mutations A and B that affect the rate constants of different single reactions within module ν.

First, I demonstrate that in a minimal module ν shown in Figure 2A the epistasis coefficient εy_ν can take values in all three domains described above. It is straightforward to obtain an analytical expression for εy_ν in this simple case (see Appendix 4). Of course, εy_ν depends on the rate constants of all reactions in this module. To demonstrate that

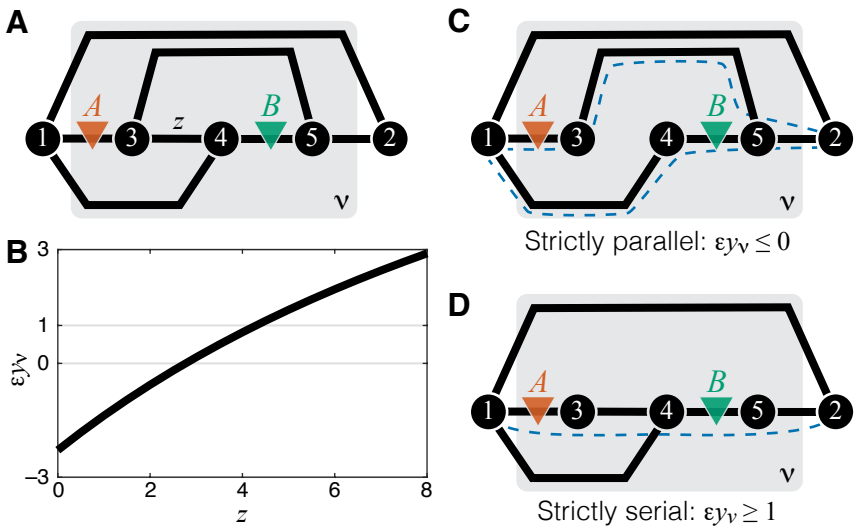

Figure 2. Emergence of epistasis and its dependence on the topological relationship between the affected reactions. (A) A minimal model of a module where negative, weak positive and strong positive epistasis can arise between two mutations A and B. (B) Epistasis between mutations A and B for the effective reaction rate y_ν through the module ν depicted in (A) as a function of the rate constant z of a third reaction. The values of other parameters of the network are given in Appendix 4. (C) An example of a module where reactions affected by mutations are strictly parallel. In such cases, epistasis for the effective rate y_ν is guaranteed to be non-positive. Dashed blue lines highlight paths that connect the I/O metabolites and each contain only one of affected reactions. (D) An example of a module where reactions affected by mutations are strictly serial. In such cases, epistasis for the effective activity y_ν is guaranteed to be ≥ 1 (strongly positive). Dashed blue line highlights the path that connects the I/O metabolites and contains both affected reactions.

εy_ν can take values anywhere from below 0 to above 1, it is convenient to keep all of the rate constants fixed except for the rate constant z of one reaction that is not affected by mutations A or B, as shown in Figure 2A. Figure 2B then shows how the epistasis coefficient εy_ν varies as a function of z. When z is small, $\varepsilon y_\nu < 0$. As z increases, it becomes weakly positive ($0 < \varepsilon y_\nu < 1$) and eventually strongly positive ($\varepsilon y_\nu > 1$). Thus, there are no fundamental constraints on the types of epistasis that can emerge between mutations that affect metabolism. This simple example also reveals that not only value but also sign of epistasis generically depends on the rates of other reactions in the network, such that other mutations or physiological changes in enzyme expression levels can modulate epistasis sign and strength. In other words, "higher-order" and "environmental" epistasis are generic features of metabolic networks.

The example above also suggests that the value of εy_ν may depend on the topological relationship between the affected reactions. Notice that when $z = 0$ the two reactions affected by mutations are parallel. On the other hand, when z is very large, most of the flux between the I/O metabolites passes through z such that the two reactions affected by mutations become effectively serial (see Appendix 4). Thus, it appears that epistasis between mutations affecting parallel reactions is negative and epistasis between mutations affecting serial reactions is positive, as previously suggested (e.g., Ref. [46]).

To formalize and mathematically prove this hypothesis, I first define two reactions as *parallel* within module ν if there exist at least two distinct non-self-intersecting (simple) paths fully contained within this module that connect the I/O metabolites, such that each path contains only one of the two focal reactions. Analogously, two reactions are *serial* within module ν if there exists at least one simple path contained within this module that connects the I/O metabolites and contains both focal reactions.

According to these definitions, two reactions can be simultaneously both parallel and serial, as, for example, the reactions affected by mutations A and B in Figure 2A. I call such reaction pairs *serial-parallel*. I say that two reactions are *strictly parallel* if they are parallel but not serial (Figure 2C) and I say that two reactions are *strictly serial* if they are serial but not parallel (Figure 2D). Thus, each pair of reactions within a module can be classified as either strictly parallel, strictly serial or serial-parallel (see Materials and Methods for details).

The second result of this paper is the following statement (see Theorem 2 in the Materials and Methods). If the two reactions affected by mutations are strictly parallel within module ν, then $\varepsilon y_\nu \leq 0$; if they are strictly serial within module ν, then $\varepsilon y_\nu \geq 1$. Here, I still assume that each mutation affects only one reaction, the two mutations affect different reactions and that their effects on the respective reaction rates are small. The full proof of this statement is given in the Materials and Methods, but its key idea is the following. Suppose that mutation A affects the rate ξ of reaction a and mutation B affects the rate η of reaction b within module ν. It is straightforward to show that in this

case

$$\varepsilon y_\nu = \frac{H_{\nu,ab}}{2\, C_{\nu,a}\, C_{\nu,b}} + \text{h.o.t.}$$

where $C_{\nu,a} = \frac{\partial F_\nu}{\partial \xi}\frac{\xi}{y_\nu}$, $C_{\nu,b} = \frac{\partial F_\nu}{\partial \eta}\frac{\eta}{y_\nu}$, $H_{\nu,ab} = \frac{\partial^2 F_\nu}{\partial \xi\, \partial \eta}\frac{\xi\eta}{y_\nu}$ are the first- and second-order control coefficient of reactions a and b with respect to the flux through the module ν (see Materials and Methods for details). In principle, the function F_ν that maps the reaction rates ξ and η onto the effective rate y_ν can have infinitely many functional forms depending on the topology of module ν. However, this is not the case. In fact, the topologies of all modules where the affected reactions a and b are strictly parallel fall into 17 equivalence classes, such that there are only 17 distinct functional forms of F_ν, all of which yield non-positive epistasis coefficients. Similarly, the topologies of all modules where the affected reactions a and b are strictly serial fall into 11 equivalence classes, such that there are only 11 distinct functional forms of F_ν, all of which yield epistasis coefficients ≥ 1.

The results of this and the previous sections together imply that the topological relationship at the microscopic level between two reactions affected by mutations constrains the values of their epistasis coefficient at all higher phenotypic levels. Specifically, if negative epistasis is detected at any phenotypic level, the affected reactions cannot be strictly serial. And conversely, if strong positive epistasis is detected at any phenotypic level, the affected reactions cannot be strictly parallel. In this model, weak positive epistasis in the absence of any additional information does not imply any specific topological relationship between the affected reactions.

Beyond first-order kinetics: epistasis in a kinetic model of glycolysis

The results of previous sections revealed a relationship between network topology and the ensuing epistasis coefficients in an analytically tractable model. However, the assumptions of this model are most certainly violated in many realistic situations. It is therefore important to know whether the same or similar rules of epistasis emergence and propagation hold beyond the scope of this model. I address this question here by analyzing a computational kinetic model of glycolysis developed by Chassagnole et al [74]. This model keeps track of the concentrations of 17 metabolites, reactions between which are catalyzed by 18 enzymes (Figures 3A and 3–figure supplement 1; see Materials and Methods for details). This model falls far outside of the analytical framework introduced in this paper: some reactions are second-order, reaction kinetics are non-linear, and in several cases the reaction rates are modulated by other metabolites [74].

Testing the predictions of the analytical theory in this computational model faces two complications. First, in a non-linear model, modules are no longer fully characterized by their effective rate constants, even at steady state. Instead, each module is described by the flux between its I/O metabolites which non-linearly depends on the concentrations of these metabolites. Consequently, the effects of mutations and epistasis coefficients also

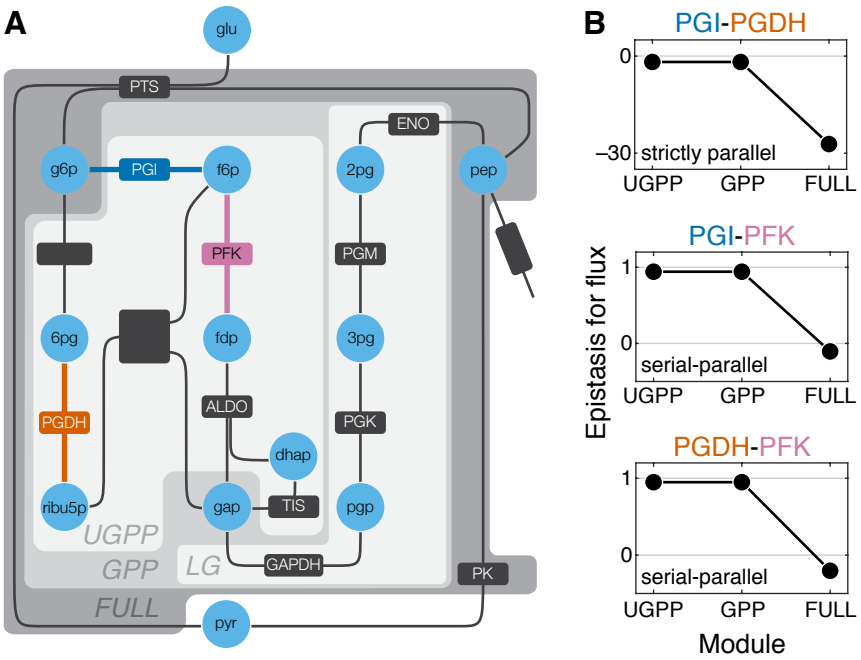

Figure 3. Epistasis in a kinetic model of *Escherichia coli* glycolysis. (*A*) Simplified schematic of the model (see Figure 3–figure supplement 1 for the full schematic). Different shades of gray in the background highlight four modules as indicated (see text). Light blue circles represent metabolites. Reactions are shown as lines with dark gray boxes. The enzymes catalyzing reactions whose control coefficients with respect to the flux through the module are positive are named; other enzyme names are ommitted for clarity (see Tables 5 and 6 for abbreviations). Three reactions, catalyzed by PGI, PFK, PGDH, for which the epistasis coefficients are shown in panel B are highlighted in dark blue, red and orange, respectively. (*B*) Epistasis coefficients for flux through each module between mutations perturbing the respective reactions, computed at steady state (see text and Materials and Methods for details). Reactions catalyzed by PGI and PGDH are strictly parallel (path g6p-f6p-fdp-gap contains only PGI, path g6p-6pg-ribu5p-gap contains only PGDH and there is no simple path in UGPP between g6p and gap that contains both PGI and PGDH). Reactions catalyzed by PGI and PFK are serial-parallel (path g6p-f6p-fdp-gap contains both reactions, path g6p-f6p-gap contains only PGI, path g6p-6pg-ribu5p-f6p-fdp-gap contains only PFK). Reactions catalyzed by PFK and PGDH are also serial-parallel (path g6p-6pg-ribu5p-f6p-fdp-gap contains both reactions, path g6p-f6p-fdp-gap contains only PFK, path g6p-6pg-ribu5p-gap contains only PGDH).

become functions of the I/O metabolite concentrations. An epistasis coefficient at the level of module ν can still be evaluated according to equation (2), with y_ν now representing the flux through module ν evaluated at a particular concentration of the I/O metabolites. For simplicity, I computationally find the steady state of the full glycolysis network and evaluate the epistasis coefficients only at this steady state, i.e., for each module, I keep the concentrations of the I/O metabolites fixed at their steady-state values for the full network (see Materials and Methods for details).

The second complication is that some control coefficients are so small that they fall below the threshold of numerical precision. Perturbing such reactions has no detectable effect on flux (Figure 3–figure supplement 2). In the analysis that follows, I ignore such reactions because the epistasis coefficient defined by equation (2) can only be computed for mutations with non-zero effects on flux. In addition, the control coefficients of some reactions are negative, which implies that an increase in the rate of such reaction decreases the flux through the module (Figure 3–figure supplement 2). I also ignore such reactions because there is no analog for them in the analytical theory presented above. After excluding 7 reactions for these reasons, I examine epistasis in 55 pairs of mutations that affect the remaining 11 reactions.

The glycolysis network shown in Figure 3A (see also Figure 3–figure supplement 1) can be naturally partitioned into four modules which I name "LG" (lower glycolysis), "UGPP" (upper glycolysis and pentose phosphate), "GPP" (glycolysis and pentose phosophate) and "FULL". Modules LG and UGPP are non-overlappng and both of them are nested in module GPP which in turn is nested in the FULL module. Thus, at least for some reaction pairs it is possible to calculate epistasis coefficients at three levels of metabolic hierarchy. There are three such pairs, and the results for them are shown in Figure 3B. Epistasis for the remaining pairs of reactions can be evaluated only at one or two levels of the hierarchy because these reactions belong to different modules at the lowest levels or because their individual effects are too small. The results for all reaction pairs are shown in Figure 3–figure supplement 3.

The strongest qualitative prediction of the analytical theory described above is that negative epistasis for a lower-level phenotype cannot turn into positive epistasis for a higher-level phenotype, while the converse is possible. Figures 3B and 3–figure supplement 3 show that the data are consistent with this prediction. Another prediction is that epistasis between strictly parallel reactions should be negative. There is only one pair of reactions that are strictly parallel, those catalyzed by glucose-6-phosphate isomerase (PGI) and 6-phosphogluconate dehydrogenase (PGDH), and indeed the epistasis coefficients between mutations affecting these reactions are negative at all levels of the hierarchy (Figures 3B). Finally, the analytical theory predicts that mutations affecting strictly serial reactions should exhibit strong positive epistasis. There are 36 reaction pairs that are strictly serial. Epistasis is positive between mutations in 33 of them, and it is strongly positive in 17 of them (Figure 3–figure supplement 3). Three pairs of strictly serial reactions (those where one reaction is catalyzed by PK and the other is catalyzed

by PGI, PGDH or PFK) exhibit negative epistasis (Figure 3–figure supplement 3). These results suggest that, although one may not be able to naively extrapolate the rules of emergence and propagation of epistasis derived in the simple analytical model to more complex networks, some generalized versions of these rules may nevertheless hold more broadly.

Discussion

Genetic interactions are a powerful tool in genetics, and they are important for our understanding of disease phenotypes and evolution. Yet, how epistasis emerges from the molecular architecture of the cell and how it propagates to various measurable phenotypes remains largely unknown. In this paper, I proposed an analytically tractable model of a hierarchical metabolic network for addressing these questions. This model revealed two simple rules. First, once epistasis emerges at some level of the hierarchy, its propagation through the levels of the hierarchy depends remarkably weakly on the details of the network. Specifically, negative epistasis at a lower level induces negative epistasis at all higher levels and strong positive epistasis induces strong positive epistasis at all higher levels, irrespectively of the topology or the kinetic parameters of the network. Second, what type of epistasis emerges in the first place depends on the topological relationship between the reactions affected by mutations. In particular, negative and strong positive epistasis emerge between mutations that affect strictly parallel and strictly serial reactions, respectively. The key conclusion from these rules is that epistasis measured for a high-level phenotype, such as fitness, carries some, albeit incomplete, information about the underlying topological relationship between the affected reactions.

These results have implications for the interpretation of empirically measured epistasis coefficients. It is often assumed that a positive epistasis coefficient between mutations that affect distinct genes signals that their gene products act in some sense serially, whereas a negative epistasis coefficient is a signal of genetic redundency, i.e., a parallel relationship between gene products [46]. My results suggest that this connection between epistasis and topology is generally correct, but more subtle. In particular, the sign of the epistasis coefficient in my model constrains but does not uniquely specify the topological relationship, such that a negative epistasis coefficients implies that the affected reactions are not strictly serial (but may or may not be strictly parallel) and an epistasis coefficient exceeding unity excludes a strictly parallel relationship (but does not necessarily imply a strictly serial relationship).

These rule establish a baseline expectation for what biologically relevant information can be robustly inferred from large-scale epistasis maps, such as those obtained for several model organisms [31, 32]. However, a major question remains whether these rules hold for more realistic biological networks and whether they can be directly used to interpret empirical epistasis coefficients. The simple model analyzed here does not capture some

biologically important phenomena, such as sign epistasis [75, 76]. Notwithstanding this limitation, my analysis of a fairly realistic computational model of glycolysis suggests that it may be possible to find general rules of propagation and emergence of epistasis in more complex networks. But it also cautions against overinterpreting empirical epistasis coefficients using the rules derived here.

My analysis offers an insight into the mechanistic origins of epistasis. It shows that the value of an epistasis coefficient measured for some particular phenotype is a result of two contributions, propagation and emergence, which correspond to two terms in equation (3). The first, propagation, term shows that if two mutations exhibit epistasis for a lower-level phenotype they also generally exhibit epistasis for a higher-level phenotype. The second contribution comes from the fact that lower-level phenotypes map onto higher-level phenotypes via non-linear functions (even in a simple model with linear kinetics). As a result, even if two mutations exhibit no epistasis at the lower-level phenotype epistasis will emerge for the higher-level phenotype, as pointed out by Chiu et al [65]. The fact that epistasis for a phenotype has these two contributions likely holds very generally.

Generic properties of epistasis in biological systems

Simple models help us identify generic phenomena—those that are shared by a large class of systems—which should inform our "null" expectations in empirical studies. Deviations from such null inform us about potentially interesting peculiarities of the examined system. The model presented here suggests that the following three features of epistasis between mutations affecting different genes in an organism are generic to metabolic networks.

Epistasis depends on the genetic background and environment. My analysis shows that the value of an epistasis statistic for a particular pair of mutations is in large part determined by the topological relationship between reactions affected by them. Since the topology of the metabolic network itself depends on the genotype and on the environment, the topological relationship between reactions might change if, for example, a third mutation knocks out a certain enzyme or if an enzyme is up- or down-regulated, as illustrated in Figure 2. Thus, we should generically expect epistasis between mutations to depend on the environment and on the presence or absence of other mutations in the genome. In other words, $G \times G \times G$ interactions (higher-oder epistasis) and $G \times G \times E$ interactions (environmental epistasis) should be common [14]. On the one hand, this fact greatly complicates the interpretation of inter-gene epistasis since the mutations in the same pair of genes can exhibit qualitatively different genetic interactions in different strains, organisms and environments, as has been observed [23, 36, 77–80]. On the other hand, comparing matrices of epistasis coefficients measured in different environments could inform us about how the organism rewires its metabolic network in response to environmental and genetic perturbations.

Propagation introduces bias towards negative epistasis. In the simple metabolic model considered here, a positive epistasis coefficient at one level of the hierarchy can turn into a negative one at a higher level, but the converse is not possible. This bias towards negative epistasis at higher-level phenotypes appears to be even stronger in networks with saturating kinetics (Figures 3 and 3–figure supplement 3). This bias could explain the excess of negative genetic interactions detected among deleterious [27, 32] and beneficial [11, 81, 82] mutations.

Inter-gene epistasis is generic. Perhaps the most important conclusion of this work is that we should expect epistasis for high-level phenotypes, such as fitness, between mutations affecting different genes to be extremely common. Consider first a unicellular organism growing exponentially. Its fitness is fully determined by its growth rate, which can be thought of as the rate constant of an effective biochemical reaction that converts external nutrients into cells [83]. In other words, growth rate is the most coarse-grained description of a metabolic network and, as such, it depends on the rate constants of all underlying biochemical reactions. This work suggests that this dependence will be generically non-linear, such that all mutations that affect growth rate individually would also exhibit epistasis for growth rate. In more complex organisms and/or in certain variable environments, it may be possible to decompose fitness into multiplicative or additive components, e.g., plant's fitness may be equal to the product of the number of seeds it produces and their germination probability [81]. Then, mutations that affect different components of fitness would exhibit no epistasis. However, such situations should be considered exceptional, as they require fitness to be decomposable and mutations to be non-pleiotropic.

If epistasis is in fact generic for high-level phenotypes, why do we not observe it more frequently? For example, a recent study that tested almost all pairs of gene knock-out mutations in yeast found genetic interactions for fitness for only about 4% of them [32]. One possibility is that many pairs of mutations exhibit epistasis that is simply to small to detect with current methods; epistasis is after all a second-order effect. As the precision of fitness measurements improves, we would then expect the fraction of interacting gene pairs to grow. Another possibility is that systematic shifts in the distribution of estimated epistasis coefficients away from zero are taken by researchers as systematic errors rather than real phenomena and are normalized out. Thus, some epistasis that is detectable may be lost during data processing.

If epistasis is indeed as ubiquituous as the present analysis suggests, it would call into question how observations of inter-gene epistasis are interpreted. In particular, contrary to a common belief, an observation of a non-zero epistasis coefficient does not necessarily imply any specific functional relationship between the components affected by mutations beyond the fact that both components somehow contribute to the measured phenotype [84]. The focus of future research should then be not merely on documenting epistasis but on developing theory and methods for a robust inference of biological relationships

from measured epistasis coefficients.

Materials and Methods

Notations and definitions

Consider a set of metabolites $A = \{1, 2, \dots\}$, which can be interconverted by biochemical reactions. All reactions are assumed to be first order and reversible. Thus, each reaction $i \leftrightarrow j$ has one substrate $i \in A$ and one product $j \in A$, and it is fully described by its rate x_{ij} which satisfies the Haldane relationship $x_{ji} = x_{ij}/K_{ij}$, where K_{ij} is the equilibrium constant. By definition, $x_{ii} = 0$. Two metabolites i and j are said to be adjacent if there is a reaction that interconverts them, i.e., $x_{ij} > 0$, and I denote the set of all reactions by $R = \{i \leftrightarrow j : i, j \in A,\ x_{ij} > 0\}$.

The biochemical reaction network $\mathcal{N}$ is defined as a pair $(A, \boldsymbol{x})$ where $\boldsymbol{x} = ||x_{ij}||$ is the matrix of all reaction rate constants. The dynamics of metabolite concentrations $S_1, \dots, S_n$ in the network are governed by equations

$$\dot{S}_i = \sum_{j=1}^{n} x_{ji}\, S_j - D_i\, S_i, \quad i \in A \tag{5}$$

where

$$D_i = \sum_{j=1}^{n} x_{ij}, \quad i \in A. \tag{6}$$

Let $A_\mu \subset A$ be a subset of metabolites. Let A_μ^{IO} be the set of all metabolites that are not in A_μ but are adjacent to at least one metabolite in A_μ. Let $R_\mu = \left\{i \leftrightarrow j \in R : i, j \in A_\mu \cup A_\mu^{\mathrm{IO}}\right\}$ be the set of all reactions where both the substrate and the product are either in A_μ or in A_μ^{IO} and let $\boldsymbol{x}_\mu$ be the rates of these reactions. The pair $\mu = (A_\mu, \boldsymbol{x}_\mu)$ is called a subnetwork of network $\mathcal{N}$. I refer to metabolites in the sets A_μ and A_μ^{IO} as internal and I/O metabolites for subnetwork μ (see Figure 4). Metabolites that are neither internal nor I/O for μ are referred to as external to subnetwork μ. The dynamics of concentrations of metabolites internal to μ are fully determined by the concentrations of the internal and I/O metabolites and by the reaction rate matrix $\boldsymbol{x}_\mu$, but they are independent of the concentrations of the external metabolites.

I call all reactions where both the substrate and the product are metabolites internal to subnetwork μ as reactions internal to subnetwork μ, and I denote the set of all such reactions by R_μ^{i}. I call all reactions where one of the metabolites is internal to μ and the other is not as the i/o reactions for subnetwork μ, and I denote the set of all such reactions by R_μ^{io}. Finally, I refer to reactions between any two I/O metabolites for subnetwork μ as bypass reactions for subnetwork μ, and I denote the set of all such reactions by R_μ^{b}. By definition, all these three sets of reactions R_μ^{i}, R_μ^{io} and R_μ^{b} are non-overlapping, and

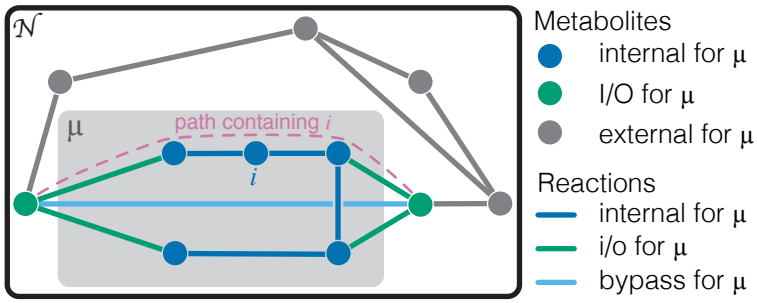

Figure 4. Illustration of the definitions. The metabolic network $\mathcal{N}$ is represented by the light-gray rectangle in the background. Subntwork μ, which is also a module, is represented by the rectangle of darker shade of gray. One metabolite internal to module μ is labelled i. Dashed line highlights a simple path that lies entirely within module μ that connects the I/O metabolites and contains the internal metabolite i.

$R_\mu = R_\mu^{\mathrm{i}} \cup R_\mu^{\mathrm{io}} \cup R_\mu^{\mathrm{b}}$. For clarity, I label metabolite types with uppercase letters "I", "I/O" and "E", and I label the reaction types with lowercase letters "i", "i/o" and "b".

Two metabolites i and j are said to be connected if there exists a simple (i.e., non-self-intersecting) path between them. I say that two metabolites i and j are connected within subnetwork μ if there exists a simple path between them such that all metabolites in this path are internal to μ (possibly excluding the terminal metabolites i and j themselves). By this definition, metabolites i and j can be connected within subnetwork μ only if they are either internal or I/O metabolites for μ. I denote simple paths connecting metabolites i and j within subnetwork μ by $p_{ij}^{\mu} = i \leftrightarrow k_1 \leftrightarrow \ldots \leftrightarrow k_m \leftrightarrow j$, where all $k_\ell \in A_\mu$. I say that each of the metabolites k_ℓ belongs to (or is contained in) path p_{ij}^{μ} (denoted by $k_\ell \in p_{ij}^{\mu}$). Similarly, I say that each of the reactions $k_\ell \leftrightarrow k_{\ell+1}$ belongs to (or is contained in) path p_{ij}^{μ} (denoted by $k_\ell \leftrightarrow k_{\ell+1} \in p_{ij}^{\mu}$). I will drop superindex μ if it is clear what subnetwork is being referred to.

Definition 1. *A subnetwork μ is called a module if (a) it has two I/O metabolites and (b) for each internal metabolite $i \in A_\mu$, there exists a simple path within μ which connects its I/O metabolits and to which metabolite i belongs.*

Figure 4 illustrates this definition. As I will show below, this definition ensures that (a) the module is fully connected (i.e., there are no subnetworks within this module that are not connected to the larger network) and (b) there are no "dangling" metabolites or sets of metabolites that would accumulate until they reach their chemical equilibrium.

Coarse-graining of a metabolic network

The "coarse-graining" procedure for network $\mathcal{N}$ outlined in this section serves three purposes. First, it is a way to obtain the steady-state concentrations for all internal metabolites within a module. Second, when all internal metabolites are at steady state, it provides

and algorithm for replacing a module with a single effective reaction whose rate can be thought of as module's quantitative phenotype. Third, the coarse-graining procedure maps the original network $\mathcal{N}$ onto a series of simpler (coarse-grained) networks, which are in some sense equivalent to $\mathcal{N}$. This mapping forms the basis of two main results of this paper formulated in Theorems 1 and 2.

1-step coarse-graining procedure

Suppose that module $\mu = (A_\mu, \boldsymbol{x}_\mu)$ contains m internal metabolites. I define the <u>1-step coarse-graining procedure that eliminates metabolite k</u> ($k \in A_\mu$) as a map

$$\mathrm{CG}^{\{k\}} : \mathcal{N} \mapsto \mathcal{N}^{\{k\}} = \left(A^{\{k\}}, \boldsymbol{x}^{\{k\}}\right),$$

where $A^{\{k\}} = A \setminus \{k\}$ and the $(n-1) \times (n-1)$ matrix of reaction rates $\boldsymbol{x}^{\{k\}}$ is defined by

$$x_{ij}^{\{k\}} = x_{ij} + \frac{x_{ik}\, x_{kj}}{D_k}, \quad i, j \in A^{\{k\}}, \quad i \neq j, \tag{7}$$

$$x_{ii}^{\{k\}} = 0, \quad i \in A^{\{k\}}, \tag{8}$$

where D_i is given by equation (6). Using the property of equilibrium constants $K_{ij} = K_{i\ell} K_{\ell j}$ for any metabolites i, j, ℓ, it is straightforward to show that the reaction rates $x_{ij}^{\{k\}}$ obey Haldane's relationships. Therefore, $\mathcal{N}^{\{k\}}$ is a metabolic network which contains one less metabolites than the orginial network $\mathcal{N}$. The map $\mathrm{CG}^{\{k\}}$ also maps the module μ onto a subnetwork $\mu^{\{k\}}$ of the network $\mathcal{N}^{\{k\}}$ with the metabolite set $A_{\mu^{\{k\}}} = A_\mu \setminus \{k\}$ and the corresponding reaction rate matrix $\boldsymbol{x}_{\mu^{\{k\}}}$, a submatrix of $\boldsymbol{x}^{\{k\}}$. In fact, it is easy to show that $\mu^{\{k\}}$ is a module.

Next, I will show that the dynamics of metabolites in the coarse-grained metabolic network $\mathcal{N}^{\{k\}}$ are identical to the dynamics of metabolites in the original network $\mathcal{N}$ where metabolite k is at quasi-steady state. The dynamics of metabolites in the network $\mathcal{N}^{\{k\}}$ are governed by equations

$$\dot{S}_i = \sum_{j \in A^{\{k\}}} x_{ji}^{\{k\}}\, S_j - D_i^{\{k\}}\, S_i, \quad \text{for } i \in A^{\{k\}}, \tag{9}$$

where $D_i^{\{k\}} = \sum_{j \in A^{\{k\}}} x_{ij}^{\{k\}}$. Since metabolites external to module μ are not adjacent to internal metabolites and since $x_{ij}^{\{k\}} = x_{ij}$ for all pairs of metabolites where at least one metabolite is external to module μ, equations (9) for the external metabolites are identical to equations (5) that govern the dynamics of these metabolites in the original network $\mathcal{N}$.

Now consider the dynamics of the I/O and internal metabolites for module $\mu^{\{k\}}$ in network $\mathcal{N}^{\{k\}}$, i.e., those in the set $A_\mu^{\mathrm{IO}} \cup A_\mu \setminus \{k\}$. For any such metabolite i, the sum in

the righthand side of equation (9) can be re-written as

$$\sum_{j\in A_\mu^{\mathrm{IO}}\cup A_\mu\setminus\{k\}} x_{ji}^{\{k\}}\,S_j = \sum_{j\in A_\mu^{\mathrm{IO}}\cup A_\mu\setminus\{k\}} \left(x_{ji}+\frac{x_{jk}\,x_{ki}}{D_k}\right) S_j - \frac{x_{ik}\,x_{ki}}{D_k}\,S_i$$
$$= \sum_{j\in A_\mu^{\mathrm{IO}}\cup A_\mu\setminus\{k\}} x_{ji}\,S_j + \frac{x_{ki}}{D_k}\sum_{j\in A_\mu^{\mathrm{IO}}\cup A_\mu\setminus\{k\}} x_{jk}\,S_j - \frac{x_{ik}\,x_{ki}}{D_k}\,S_i \tag{10}$$

If metabolite k is at quasi-steady state in the network $\mathcal{N}$, its concentration is given by

$$S_k = \sum_{j\in A_\mu^{\mathrm{IO}}\cup A_\mu\setminus\{k\}} \frac{x_{jk}\,S_j}{D_k}, \tag{11}$$

so that the second term in expression (10) equals $x_{ki}S_k$ and expression (10) becomes

$$\sum_{j\in A_\mu^{\mathrm{IO}}\cup A_\mu\setminus\{k\}} x_{ji}^{\{k\}}\,S_j = \sum_{j\in A_\mu^{\mathrm{IO}}\cup A_\mu} x_{ji}S_j - \frac{x_{ik}\,x_{ki}}{D_k}\,S_i. \tag{12}$$

For any metabolite $i \in A_\mu^{\mathrm{IO}} \cup A_\mu \setminus \{k\}$, the second term in the righthand side of equation (9) can be re-written as

$$D_i^{\{k\}} = \sum_{j\in A_\mu^{\mathrm{IO}}\cup A_\mu\setminus\{k\}} \left(x_{ij}+\frac{x_{ik}\,x_{kj}}{D_k}\right) - \frac{x_{ik}\,x_{ki}}{D_k} = D_i - \frac{x_{ik}\,x_{ki}}{D_k}. \tag{13}$$

Substituting equations (12) and (13) into equations (9), we see that equations (9) are in fact equivalent to equations (5) for all $i \in A \setminus \{k\}$ with S_k given by equation (11). Since the 1-step coarse-graining procedure eliminating metabolite k does not alter module μ, I will simplify notations and drop the super-index $\{k\}$ when denoting the coarse-grained version of module μ whenever there is no ambiguity.

p-step coarse-graining procedure

Suppose that a set $E \subseteq A_\mu$ contains p metabolites. I define the <u>p-step coarse-graining procedure that eliminates a set of metabolites $E \subseteq A_\mu$</u> as a map

$$\mathrm{CG}^E : \mathcal{N} \mapsto \mathcal{N}^E = \left(A^E, \boldsymbol{x}^E\right),$$

where $A^E = A \setminus E$ and the $(n-p) \times (n-p)$ matrix of reaction rates $\boldsymbol{x}^E$ defined by the following recursive relations that hold for any $E' \subseteq E$.

$$
\begin{aligned}
x_{ij}^{E'} &= x_{ij}^{E''} + \frac{x_{ik}^{E''}\, x_{kj}^{E''}}{D_k^{E''}}, \quad i,j \in A \setminus E',\ i \neq j,\ k \in E',\ E'' = E' \setminus \{k\}, && (14)\\
x_{ii}^{E'} &= 0, \quad i \in A, && (15)\\
x_{ij}^{\emptyset} &\equiv x_{ij}, \quad i,j \in A, && (16)\\
D_i^{E'} &= \sum_{j \in A \setminus E'} x_{ij}^{E'}, \quad i \in A \setminus E', && (17)\\
D_i^{\emptyset} &\equiv D_i = \sum_{j \in A} x_{ij}, \quad i \in A. && (18)
\end{aligned}
$$

Using equations (14)–(17), it is straightforward to show that for any $i \in A \setminus E'$, any $k \in E'$ and $E'' = E' \setminus \{k\}$,

$$
D_i^{E'} = D_i^{E''} - \frac{x_{ik}^{E''}\, x_{ki}^{E''}}{D_k^{E''}}, \tag{19}
$$

which becomes useful below.

For $E = \{k, \ell\}$, the effective rates are given by

$$
\begin{aligned}
x_{ij}^{\{k,\ell\}} &= x_{ij}^{\{k\}} + \frac{x_{i\ell}^{\{k\}}\, x_{\ell j}^{\{k\}}}{D_\ell^{\{k\}}}\\
&= x_{ij} + \frac{D_k\, x_{i\ell}\, x_{\ell j} + D_\ell\, x_{ik}\, x_{kj} + x_{ik}\, x_{k\ell}\, x_{\ell j} + x_{i\ell}\, x_{\ell k}\, x_{kj}}{D_k\, D_\ell - x_{k\ell}\, x_{\ell k}} && (20)\\
&= x_{ij} + \frac{x_{i\ell}\, x_{\ell j}}{D_\ell^{\{k\}}} + \frac{x_{ik}\, x_{kj}}{D_k^{\{\ell\}}} + \frac{x_{ik}\, x_{k\ell}\, x_{\ell j}}{D_k^{\{\ell\}}\, D_\ell} + \frac{x_{i\ell}\, x_{\ell k}\, x_{kj}}{D_\ell^{\{k\}}\, D_k}, && (21)\\
&\quad i,j \in A \setminus \{k,\ell\},\ i \neq j.
\end{aligned}
$$

For an arbitrary metabolite subset $E \subseteq A_\mu$ that contains p metabolites, I show in Appendix 1 that

$$
x_{ij}^E = x_{ij} + \sum_{L=1}^{p} \sum_{\{k_1,\ldots,k_L\} \subseteq E} \frac{x_{ik_1}}{1}\, \frac{x_{k_1 k_2}}{D_{k_1}^{E \setminus \{k_1\}}} \cdots \frac{x_{k_{L-1} j}}{D_{k_L}^{E \setminus \{k_1,k_2,\ldots,k_L\}}}, \quad i,j \in A \setminus E,\ i \neq j. \tag{22}
$$

Here, the second sum is over all $p!/(p-L)!$ ordered subsets of metabolites $(k_1, \ldots, k_L) \subseteq E$. Equation (22) shows that the effective reation rate x_{ij}^E does not depend on the order in which metabolites are eliminated (see also Property #1 in Appendix 2). It is also clear from this equation that $x_{ij}^E = x_{ij}$ for all pairs of metabolites i, j where at least one metabolite is external to μ^E; and $x_{ij}^E = 0$ for all pairs of metabolites i, j where one is external to μ^E and the other is internal to μ^E.

The coarse-graining procedure CG^E maps module μ within the metabolic network $\mathcal{N}$ onto a subnetwork $\mu^E = \left(A_\mu^E, \boldsymbol{x}_\mu^E\right)$ within the metabolic network $\mathcal{N}^E$, where $A_\mu^E = A_\mu \setminus E$ and $\boldsymbol{x}_\mu^E$ is the corresponding submatrix of matrix $\boldsymbol{x}^E$. It is straightforward to show that μ^E is a module.

Proposition 1. *Let E be any subset of metabolites internal to module μ. Then*

1. *There exists a joint quasi-steady state solution $\overline{S}_i$ for all metabolites $i \in E$, given the concentrations of the remaining internal and I/O metabolites for module μ.*

2. *The dynamics of all remaining metabolites in $A \setminus E$ in the coarse-grained metabolic network $\mathcal{N}^E$ are the same as in $\mathcal{N}$ where all metabolites in E are at quasi-steady state.*

Proof. I prove this statement by induction. It is clear that both claims hold for any singleton subset E (see above). Assume that both claims hold for some subset $E'' \subset A_\mu$. I will show that both claims then also hold for the subset $E' = E'' \cup \{k\}$ for any $k \in A_\mu \setminus E''$.

By assumption, all metabolites from the set E'' have quasi-steady-state concentrations in the original network $\mathcal{N}$. Denote their quasi-steady-state concentrations $\overline{S}_i$, for $i \in E''$. The dynamics of metabolites in the network $\mathcal{N}^{E''}$ are governed by equations

$$\dot{S}_i = \sum_{j \in A \setminus E''} x_{ji}^{E''} S_j - D_i^{E''} S_i, \quad \text{for } i \in A \setminus E''. \tag{23}$$

By assumption, these dynamics are identical to those in the original network $\mathcal{N}$, provided that metabolites from the set E'' are at quasi-steady state $\overline{S}_i$, $i \in E''$. Since $\mu_{E''}$ is a module, metabolite k can reach a quasi-steady state in $\mathcal{N}^{E''}$, which is given by

$$\overline{S}_k = \sum_{j \in A_\mu^{\mathrm{IO}} \cup A_\mu \setminus E''} \frac{x_{jk}^{E''} S_j}{D_k^{E''}} = \sum_{j \in A_\mu^{\mathrm{IO}} \cup A_\mu \setminus E'} \frac{x_{jk}^{E''} S_j}{D_k^{E''}}, \tag{24}$$

where the last equality holds because of equation (15) and the fact that $E' = E'' \cup \{k\}$. Since, by assumption, equations (23) are identical to equations (5), the quasi-steady-state concentration $\overline{S}_k$ given by equation (24) is also the quasi-steady-state concentration for metabolite k in the original metabolic network $\mathcal{N}$ where all metabolites $i \in E''$ are already at quasi-steady state. In other words, $\overline{S}_i$ define joint quasi-steady state concentrations for all metabolites $i \in E'$. Therefore, Claim 1 of the Proposition 1 holds for the subset E'.

Now, the dynamics of metabolites in the network $\mathcal{N}^{E'}$ are governed by equations

$$\dot{S}_i = \sum_{j \in A \setminus E'} x_{ji}^{E'} S_j - D_i^{E'} S_i, \quad i \in A \setminus E'. \tag{25}$$

Clearly, equations (25) for metabolites that are external to $\mu^{E'}$ are identical to equations (5) for these metabolites in the original network $\mathcal{N}$ (see equation (22)). For metabolites that are internal and I/O for module $\mu^{E'}$, I use equations (14), (15) and (19) to obtain

$$\begin{aligned}
\dot{S}_i &= \sum_{j\in A_\mu^{\rm IO}\cup A_\mu\setminus E'} x_{ji}^{E'}\, S_j - D_i^{E'}\, S_i \\
&= \sum_{j\in A_\mu^{\rm IO}\cup A_\mu\setminus E'} \left(x_{ji}^{E''} + \frac{x_{jk}^{E''}\, x_{ki}^{E''}}{D_k^{E''}} \right) S_j - \frac{x_{ik}^{E''}\, x_{ki}^{E''}}{D_k^{E''}}\, S_i - \left(D_i^{E''} - \frac{x_{ik}^{E''}\, x_{ki}^{E''}}{D_k^{E''}} \right) S_i \\
&= \sum_{j\in A_\mu^{\rm IO}\cup A_\mu\setminus E'} x_{ji}^{E''}\, S_j + x_{ki}^{E''}\, \overline{S}_k - D_i^{E''}\, S_i, \quad i \in A_\mu^{\rm IO}\cup A_\mu\setminus E'.
\end{aligned}$$

These equations are identical to equations (23) with $\overline{S}_k$ given by equation (24). Hence, they are also identical to equations (5) where metabolites from the set E' have quasi-steady state concentrations $\overline{S}_i,\ i\in E'$. Therefore, Claim 2 of the Proposition 1 holds for subset E'. □

Corollary 1. *If at least one of the I/O metabolites for module μ has a non-zero concentration, there exists a unique quasi-steady state $\overline{S}_i > 0$ for all $i \in A_\mu$. Theses concentrations can be obtained as follows. First, arbitrarily order the internal metabolites $k_1, k_2, \ldots k_m$, and define $E_1 = \{k_1\},\ E_2 = E_1 \cup \{k_2\}, \ldots, E_\ell = E_{\ell-1} \cup \{k_\ell\}, \ldots, E_m = A_\mu$. Second, calculate $x_{ij}^{E_\ell}$ for all $\ell = 1, \ldots, m-1$ and $i, j \in A_\mu^{\rm IO} \cup A_\mu \setminus E_\ell$ using equations* (14)–(17). *Third, recursively apply equation*

$$\overline{S}_{k_\ell} = \sum_{j\in A_\mu^{\rm IO}} \frac{x_{jk_\ell}^{E_{\ell-1}}\, S_j}{D_{k_\ell}^{E_{\ell-1}}} + \sum_{j\in A_\mu\setminus E_\ell} \frac{x_{jk_\ell}^{E_{\ell-1}}\, \overline{S}_j}{D_{k_\ell}^{E_{\ell-1}}}$$

for $\ell = m, m-1, \ldots, 1$.

Corollary 2. *Any module μ can be replaced with a single effective reaction between its I/O metabolites, whose rate is given by $y_\mu \equiv x_{ij}^{A_\mu}$ that can be recursively calculated using equations* (14)–(17). *The dynamics of all metabolites in the coarse-grained metabolic network $\mathcal{N}^\mu \equiv \mathcal{N}^{A_\mu}$ are identical to their dynamics in the original network $\mathcal{N}$ where all metabolites internal to module μ are at the quasi-steady state determined by the concentrations of its I/O metabolites.*

Composition of coarse-graining procedures. Consider two coarse-graining procedures CG^{E_1} and CG^{E_2} for $E_1 \subset A_\mu$ and $E_2 \subset A_\mu$. CG^{E_2} is well defined for any metabolic network that contains module μ and such that $E_2 \subset A_\mu$. In particular, if $E_1 \cap E_2 = \emptyset$, CG^{E_2} is defined for the network $\mathcal{N}^{E_1}$ which itself is the result of applying CG^{E_1} to the original network $\mathcal{N}$. Such sequential application of coarse graining procedures CG^{E_1} and CG^{E_2} defines a new coarse-graining procedure $\mathrm{CG}^{E_1} \circ \mathrm{CG}^{E_2}$ of the original network $\mathcal{N}$ which is called the composition of coarse-graining prcedures CG^{E_1} and CG^{E_2}.

Single-marked modules

Consider module $\mu = (A_\mu, \boldsymbol{x}_\mu)$ and let $a = i_a \leftrightarrow j_a$ be one reaction from its set of reactions R_μ. I denote by $\boldsymbol{x}_{\mu\backslash a}$ the matrix of rates of all reactions in the set R_μ other than a. I call a pair (μ, a) a single-marked module, and I refer to reaction a as marked within module μ. I denote the set of all single-marked modules by $\mathcal{M}_1$. For convenience, I adopt the following metabolite labelling conventions:

(i) The I/O metabolites are labelled 1 and 2 and the internal metabolites are labelled $3, 4, \ldots$;

(ii) $i_a < j_a$;

(iii) If a is a bypass reaction, then $i_a = 1$ and $j_a = 2$;

(iv) If a is an i/o reaction, then $i_a = 1$ and $j_a = 3$;

(v) If a is an internal reaction, then $i_a = 3$ and $j_a = 4$.

The set of all single-marked modules $\mathcal{M}_1$ can be partitioned into three non-overlapping topological classes which I denote $\mathcal{M}^{\mathrm{b}}$, $\mathcal{M}^{\mathrm{io}}$ and $\mathcal{M}^{\mathrm{i}}$, depending on whether reaction a is a bypass, i/o or internal reaction, respectively (see Notations and definitions). The three classes of single-marked modules are illustrated in Figure 5 (left column).

Suppose that the rate of reaction $a = i_a \leftrightarrow j_a$ is ξ, i.e., $x_{i_a\, j_a} = \xi$. The coarse-graining procedure $\mathrm{CG}^\mu \equiv \mathrm{CG}^{A_\mu}$ maps the reaction rate matrix $\boldsymbol{x}_\mu$ onto the effective reaction rate y_μ via equation (A2.2). Consider y_μ as a function of ξ. The form of this function is, in general, determined by the topology of module μ, the location of the marked reaction a within module μ, and the values of reaction rates $\boldsymbol{x}_{\mu\backslash a}$, so that in principle there could be an infinte number of functional forms of this function. However, the following proposition shows that this is in fact not the case.

Proposition 2. *Let (μ, a) be a single-marked module, and let the rate of reaction a be ξ. The coarse-graining procedure CG^μ maps ξ onto y_μ via function $F_{(\mu,a)}$ whose functional form depends only on the topological class of (μ, a). Specifically,*

$$F_{(\mu,a)} = u, \quad \textit{if}\, (\mu, a) \in \mathcal{M}^{\mathrm{b}}, \tag{26}$$

$$F_{(\mu,a)} = w_{12} + \frac{u\, w_{32}}{u/K_{13} + w_{32}}, \quad \textit{if}\, (\mu, a) \in \mathcal{M}^{\mathrm{io}}, \tag{27}$$

$$F_{(\mu,a)} = w_{12} + \frac{D_3\, w_{14}\, w_{42} + D_4\, w_{13}\, w_{32} + w_{13}\, w_{42}\, u + w_{14}\, w_{32}\, u/K_{34}}{D_3\, D_4 - u^2/K_{34}}, \quad \textit{if}\, (\mu, a) \in \mathcal{M}^{\mathrm{i}}, \tag{28}$$

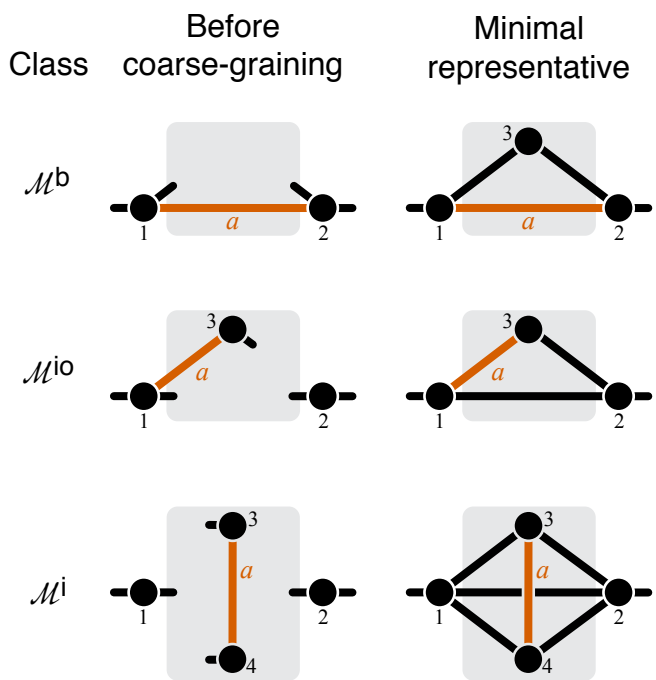

Figure 5. Classification of single-marked modules. Left column shows a general module from each topological class. The right column shows a fully connected module with the minimal number of internal metabolites from each topological class (see text for details). Modules are represented by gray rectangles (the rest of the network not shown). Circles represent metabolites; only the I/O metabolites and the metabolites that participate in the marked reaction are shown. Metabolites are labelled according to the conventions listed in the text. Lines represent reactions; short lines that have only one terminal metabolite represent all other reactions in which this metabolite participates. The marked reaction is colored orange and labelled a.

where

$$\begin{aligned} u &= \xi + \alpha, \\ D_3 &= w_{31} + w_{32} + u, \\ D_4 &= w_{41} + w_{42} + u/K_{34}, \end{aligned}$$

and all $w_{ij} \geq 0$ *and* $\alpha \geq 0$ *are independent of* ξ *but depend on* (μ, a) *and parameters* $\boldsymbol{x}_{\mu\backslash a}$.

Proof. Since any single-marked module (μ, a) belongs to exactly one of three classes $\mathcal{M}^{\mathrm{b}}$, $\mathcal{M}^{\mathrm{io}}$ and $\mathcal{M}^{\mathrm{io}}$, I consider these three cases one by one.

Class $(\mu, a) \in \mathcal{M}^{\mathrm{b}}$. By definition of the class $\mathcal{M}^{\mathrm{b}}$ and according to the labelling conventions outlined above, $a = 1 \leftrightarrow 2$ (see Figure 5). Equation (26) follows directly from Property #3 of the coarse-graining procedure (see Appendix 2).

Case $(\mu, a) \in \mathcal{M}^{\mathrm{io}}$. By definition of the class $\mathcal{M}^{\mathrm{io}}$ and according to the labelling conventions outlined above, $a = 1 \leftrightarrow 3$ (see Figure 5). According to Property #1 of the coarse-graining procedure (see Appendix 2), module μ can be coarse-grained in two stages, by first eliminating metabolites $4, \ldots, m$ and then eliminating metabolite 3, i.e.,

$$\mathrm{CG}^{\mu} = \mathrm{CG}^{A_\mu \backslash \{3\}} \circ \mathrm{CG}^{\{3\}}.$$

The result of applying $\mathrm{CG}^{A_\mu \backslash \{3\}}$ to the metabolic network $\mathcal{N}$ is the coarse-grained network $\mathcal{N}^{A_\mu \backslash \{3\}}$ with module $\mu^{A_\mu \backslash \{3\}}$ that has a single internal metabolite 3 and at most three

effective reactions $1 \leftrightarrow 2$, $2 \leftrightarrow 3$ and $1 \leftrightarrow 3$ (Figure 5) with rates w_{12}, w_{23} and $u \equiv w_{13} = \xi + \alpha$, respectively (since $\mu^{A_\mu \setminus \{3\}}$ is a module, w_{12} can be zero, but w_{23} cannot). Importantly, neither w_{12}, not w_{23}, nor α depend on ξ (see property of coarse-graining #3). Finally, the coarse-graining procedure $\mathrm{CG}^{\{3\}}$ applied to the network $\mathcal{N}^{A_\mu \setminus \{3\}}$ eliminates the single internal metabolite 3, and we obtain equation (27).

Case $(\mu, a) \in \mathcal{M}^{\mathrm{io}}$. By definition of the class $\mathcal{M}^{\mathrm{io}}$ and according to the labelling conventions outlined above, $a = 3 \leftrightarrow 4$ (see Figure 5). Analogously to the previous case, module μ can be coarse-grained in two stages, by first eliminating metabolites $5, \ldots, m$ and then eliminating metabolite 3 and 4, i.e., as above, $\mathrm{CG}^{\mu} = \mathrm{CG}^{A_\mu \setminus \{3,4\}} \circ \mathrm{CG}^{\{3,4\}}$. The coarse-grained network $\mathcal{N}^{A_\mu \setminus \{3,4\}}$ with module $\mu^{A_\mu \setminus \{3,4\}}$ has two internal metabolites 3 and 4 and at most six effective reactions with rates w_{12}, w_{13}, w_{14}, w_{23}, w_{24}, and $u \equiv w_{34} = \xi + \alpha$ (some but not all of these rates may be zero because since $\mu^{A_\mu \setminus \{3,4\}}$ is a module). Again, α and the rates w_{ij} are all independent of ξ, except for u. Finally, the coarse-graining procedure $\mathrm{CG}^{\{3,4\}}$ applied to the network $\mathcal{N}^{A_\mu \setminus \{3,4\}}$ eliminates the single internal metabolite 3 (see equation (20)), and we obtain equation (28). □

Sequential coarse-graining of multiple nested modules. Suppose that module μ in the network $\mathcal{N}$ contains another, smaller, module ν with the metabolite set A_ν and reaction rate matrix $\boldsymbol{x}_\nu$, such that $A_\nu \subset A_\mu$ and matrix $\boldsymbol{x}_\nu$ is the corresponding submatrix of $\boldsymbol{x}_\mu$. I denote by a the effective reaction that represents module ν in the coarse-grained network $\mathcal{N}^{\nu}$ and I denote by $\boldsymbol{x}_{\mu \setminus \nu}$ the matrix of rates of all reactions in the set $R_\mu \setminus R_\nu$.

The coarse-graining procedure CG^{μ} maps module μ onto its effective reaction with rate y_μ given by the equation (A2.2). And the coarse-graining procedure CG^{ν} maps module ν onto its effective reaction with rate y_ν given by the equivalent of equation (A2.2). y_μ and y_ν are of course not independent because y_μ generally depends on all the reaction rates in $\boldsymbol{x}_\mu$, including reaction rates $\boldsymbol{x}_\nu$. To understand this dependence, let us exploit Property #1 of coarse-graining procedures (see Appendix 2) and represent CG^{μ} as a composition of two coarse-graining procedures,

$$\mathrm{CG}^{\mu} = \mathrm{CG}^{\nu} \circ \mathrm{CG}^{A_\mu \setminus A_\nu}. \tag{29}$$

Since ν is a module, CG^{ν} replaces module ν with its effective rate y_ν, without altering the rates of any other reactions.Thus, y_μ depends on all rates in $\boldsymbol{x}_\nu$ only indirectly, through y_ν. In other words, all the information about module ν is contained in its effective reaction rate y_ν (provided that module ν is at quasi-steady state). As a consequence, mutations that directly affect only enzymes within the embedded module ν affect the performance of the larger module μ only indirectly, through the aggregate performance of module ν. I will use this fact in the next section to investigate how epistasis propagates through a hierarchical metabolic network.

To understand how y_μ depends on y_ν, consider module μ^{ν}, onto which the coarse-graining procedure CG^{ν} maps module μ. (As mentioned above, I write μ instead of μ^{ν}

whenever there is no ambiguity.) Denote by a the effective reaction with rate y_ν that represents module ν. According to Proposition 2,

$$y_\mu = F_{(\mu,a)}\left(y_\nu; \boldsymbol{x}_{\mu\setminus\nu}\right), \tag{30}$$

with function $F_{(\mu,a)}$ having one of the three functional forms given by equations (26)–(28), and $\boldsymbol{x}_{\mu\setminus a}$ playing a role of its parameters. Equation (30) is equivalent to equation (1).

Double-marked modules

Consider module $\mu = (A_\mu, \boldsymbol{x}_\mu)$ and let $a = i_a \leftrightarrow j_a$ and $b = i_b \leftrightarrow j_b$ be two reactions from its set of reactions R_μ. I call a triplet (μ, a, b) <u>a double-marked module</u>, and I refer to reactions a and b as marked within module μ. I denote the set of all double-marked modules by $\mathcal{M}_2$. As with single-marked modules (see Section), I adopt the following metabolite labelling conventions:

(i) The I/O metabolites are labelled 1 and 2 and the internal metabolites are labelled $3, 4, \ldots$;

(ii) $i_a, j_a, i_b, j_b \in \{1, 2, 3, 4, 5, 6\}$;

(iii) $i_a < j_a$, $i_b < j_b$, $i_a \leq i_b$, $j_a \leq j_b$.

It is easy to see that the set $\mathcal{M}_2$ can be partitioned into 9 non-overlapping topological classes according to the types of marked reactions (bypass, i/o, or internal) and the type of metabolite that is shared by both of these reactions (I/O or internal). These classes are listed in Table 1 and illustrated in Figure 6.

Each topological class contains infinitely many double-marked modules, with various numbers of metabolites. However, for each topological class $\mathcal{M}$, there is a minimum number of internal metabolites $m_\mathcal{M}$, i.e., any double-marked module from class $\mathcal{M}$ must have at least $m_\mathcal{M}$ metabolites (see column 6 in Table 1). If the double-marked module (μ, a, b) from the topological class $\mathcal{M}$ that has the minimum number of metabolites for that class, I call it <u>minimal</u> in class $\mathcal{M}$. Note that among all mimimal modules in class $\mathcal{M}$ there is only one that is fully connected (see Figure 6).

Let the rate of reaction $a = i_a \leftrightarrow j_a$ be ξ and let the rate of reaction $b = i_b \leftrightarrow j_b$ be η, i.e., $x_{i_a j_a} = \xi$ and $x_{i_b j_b} = \eta$. The coarse-graining procedure CG^μ maps the reaction rate matrix $\boldsymbol{x}_\mu$ onto the effective kinetic parameter y_μ via equation (A2.2). As in the previous section, consider y_μ as a function of two variable ξ and η,

$$y_\mu = F_{(\mu,a,b)}\left(\xi, \eta; \boldsymbol{x}_{\mu\setminus\{a,b\}}\right), \tag{31}$$

where $\boldsymbol{x}_{\mu\setminus\{a,b\}}$ refers to all reaction rates in $\boldsymbol{x}_\mu$ except a and b. The following proposition shows that the form of this function depends only on the topological class of the double-marked module (μ, a, b) while the reaction rates $\boldsymbol{x}_{\mu\setminus a}$ play the role of parameters of this function.

Class	a	b	Shared metab.	Verbal description	$m_{\mathcal{M}}$	$A_{\mathcal{M}}$
$\mathcal{M}^{\text{b,io,IO}}$	$(1,2)$	$(1,3)$	1	bypass and i/o reactions, shared I/O metabolite	1	$\{1,2,3\}$
$\mathcal{M}^{\text{b,i,}\emptyset}$	$(1,2)$	$(3,4)$	–	bypass and internal reactions, no shared metabolies	2	$\{1,2,3,4\}$
$\mathcal{M}^{\text{io,io,I}}$	$(1,3)$	$(2,3)$	3	i/o reactions, shared internal metabolite	1	$\{1,2,3\}$
$\mathcal{M}^{\text{io,io,IO}}$	$(1,3)$	$(1,4)$	1	i/o reactions, shared I/O metabolite	2	$\{1,2,3,4\}$
$\mathcal{M}^{\text{io,io,}\emptyset}$	$(1,3)$	$(2,4)$	–	i/o reactions, no shared metabolites	2	$\{1,2,3,4\}$
$\mathcal{M}^{\text{io,i,I}}$	$(1,3)$	$(3,4)$	3	i/o and internal reactions, shared internal metabolite	2	$\{1,2,3,4\}$
$\mathcal{M}^{\text{io,i,}\emptyset}$	$(1,3)$	$(4,5)$	–	i/o and internal reactions, no shared metabolites	3	$\{1,2,3,4,5\}$
$\mathcal{M}^{\text{i,i,I}}$	$(3,4)$	$(3,5)$	3	internal reactions, share internal metabolite	3	$\{1,2,3,4,5\}$
$\mathcal{M}^{\text{i,i,}\emptyset}$	$(3,4)$	$(5,6)$	–	internal reactions, no shared metabolites	4	$\{1,2,3,4,5,6\}$

Table 1. Classification of double-marked modules. Metabolites are labelled according to conventions described in the text. $m_{\mathcal{M}}$ is the minimum number of internal metabolites in a module from class $\mathcal{M}$. $A_{\mathcal{M}}$ is the set of internal and I/O metabolites in all minimal modules in class $\mathcal{M}$.

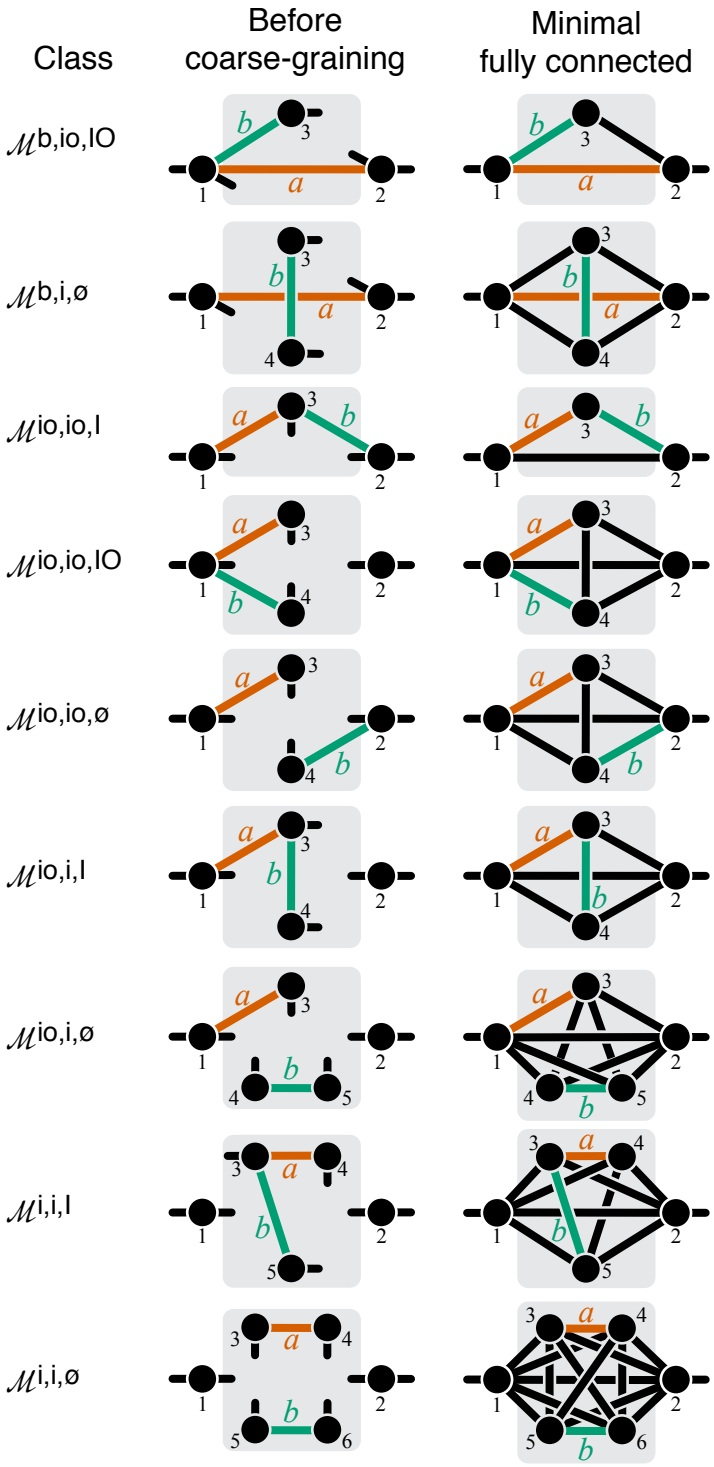

Figure 6. Classification of double-marked modules. Notations as in Figure 5.

Proposition 3. *Let (μ, a, b) be a double-marked module that belongs to the topological class $\mathcal{M}$, and let the rates of reaction a and b be ξ and η, respectively. Let $A_{(\mu,a,b)} = A_\mu \setminus \{i_a, j_a, i_b, j_b\}$ be the subset of all metabolites internal to module μ that do not participate in reactions a or b. The coarse-graining procedure $\mathrm{CG}^{(\mu,a,b)} \equiv \mathrm{CG}^{A_{(\mu,a,b)}}$ that eliminates all such metabolites maps module μ onto module μ', such that (μ', a, b) is minimal in $\mathcal{M}$ and the rates of reactions a and b in module μ' are given by*

$$u = \xi + \alpha, \tag{32}$$

$$v = \eta + \beta, \tag{33}$$

respectively, where α and β are non-negative constants that do no depend on ξ or η. Furthermore, all other effective reaction rates in module μ' are independent of ξ and η.

Proof. Let $m_{\mathcal{M}}$ be the mimimal number of internal metabolites in class $\mathcal{M}$ (see Table 1). According to the metabolite labelling conventions outlined above, $A_{(\mu,a,b)} = \{n_{\mathcal{M}}+3, n_{\mathcal{M}}+4, \dots\}$. The coarse-graining procedure $\mathrm{CG}^{(\mu,a,b)}$ eliminates all metabolites that belong to $A_{(\mu,a,b)}$, which implies that only those internal metabolites are left that participate in reactions a or b. Therefore, (μ', a, b) is minimal in class $\mathcal{M}$ (Figure 6). According to Property #3 of the coarse-graining procedure (see Appendix 2), $\mathrm{CG}^{(\mu,a,b)}$ maps the rates ξ and η of reactions a and b in module μ onto the effective rates u and v of these reactions in module μ' via linear relationships (32), (33). Finally, according to Property #3 of the coarse-graining procedure (see Appendix 2), the remaining effective reaction rates w_{ij} in the module μ' are independent of ξ and η. □

Corollary 3. *For any double-marked module $(\mu, a, b) \in \mathcal{M}$, there exists an effective reaction rate matrix $\boldsymbol{w}$ and constants $\alpha \geq 0$ and $\beta \geq 0$, such that $y_\mu = F_{\mathcal{M}}(u, v; \boldsymbol{w})$, where u and v are given by equations (32), (33) and the explicit expressions for the functional forms for $F_{\mathcal{M}}$ are given in Appendix 3.*

Epistasis for a higher-level phenotype between mutations affecting lower-level phenotypes

Consider a higher-level phenotype y, such as the effective activity of a module, which is function of a multivariate lower-level phenotype $\boldsymbol{x} = (x_1, x_2, \dots, x_n)$, such as the rates of individual reactions within the module, $y = F(\boldsymbol{x})$. Denote the wildtype values of the phenotypes as $\boldsymbol{x}^0 = (x_1^0, x_2^0, \dots, x_n^0)$ and $y^0 = F(\boldsymbol{x}^0)$. Consider a mutation that multiplicatively perturbes these values, i.e., the phenotype values in the mutant are $\boldsymbol{x}' = (x_1', x_2', \dots, x_n')$, where $x_i' = x_i^0(1 + \delta x_i)$ with all $\|\delta x_i\| \ll 1$ and $\|\cdot\|$ denotes the Eucledian norm. Then, the value of the phenotype y' in the mutant is approximately

$$y' = y^0 \left(1 + \sum_{i=1}^{n} C_i \, \delta x_i + \frac{1}{2} \sum_{i,j=1}^{n} H_{ij} \, \delta x_i \, \delta x_j \right) + o\left(\|\delta \boldsymbol{x}\|^2 \right). \tag{34}$$

where

$$C_i = \frac{x_i^0}{y^0} \left.\frac{\partial F}{\partial x_i}\right|_{\boldsymbol{x}=\boldsymbol{x}^0}, \quad i = 1, \ldots, n, \tag{35}$$

$$H_{ij} = \frac{x_i^0 x_j^0}{y^0} \left.\frac{\partial^2 F}{\partial x_i \, \partial x_j}\right|_{\boldsymbol{x}=\boldsymbol{x}^0}, \quad i, j = 1, \ldots, n, \tag{36}$$

which I refer to as first- and second-order control coefficients, respectively.

Now consider two single mutants, A and B, and the double-mutant AB. Each mutation A and B and their combination perturb all x_i phenotypes such that

$$\begin{aligned} x_i^A &= x_i^0 \left(1 + \delta^A x_i\right), \\ x_i^B &= x_i^0 \left(1 + \delta^B x_i\right), \\ x_i^{AB} &= x_i^0 \left(1 + \delta^{AB} x_i\right). \end{aligned}$$

Assuming that $\left\|\delta^A \boldsymbol{x}\right\| \ll 1$, $\left\|\delta^B \boldsymbol{x}\right\| \ll 1$ and $\left\|\delta^{AB} \boldsymbol{x}\right\| \ll 1$, using the approximation (34) and the definition of εx_i (equation (2)), I obtain

$$\delta^A y = \sum_{i=1}^{n} C_i \, \delta^A x_i + o\left(\left\|\delta^A \boldsymbol{x}\right\|\right), \tag{37}$$

$$\delta^B y = \sum_{i=1}^{n} C_i \, \delta^B x_i + o\left(\left\|\delta^B \boldsymbol{x}\right\|\right), \tag{38}$$

$$\varepsilon y = \frac{\sum_{i=1}^{n} C_i \, \varepsilon x_i \, \delta^A x_i \, \delta^B x_i + \frac{1}{2} \sum_{i,j=1}^{n} H_{ij} \, \delta^A x_i \, \delta^B x_j}{\sum_{i=1}^{n} \sum_{j=1}^{n} C_i \, C_j \, \delta^A x_i \, \delta^B x_j} + o\left(1\right), \tag{39}$$

where $o(1)$ refers to terms that are vanishingly small as all $\delta^A x_i \to 0$, $\delta^B x_i \to 0$, $i = 1, \ldots n$.

Two special cases of expressions (37)–(39) are used in this work. In the first special case, both mutations affect a single phenotype x_k, i.e., when all $\delta^A x_i = 0$ and all $\delta^B x_i = 0$ except for $i = k$, expressions (37)–(39) simplify to

$$\delta^A y = C_k \, \delta^A x_k + o\left(\left|\delta^A x_k\right|\right), \tag{40}$$

$$\delta^B y = C_k \, \delta^B x_k + o\left(\left|\delta^B x_k\right|\right), \tag{41}$$

$$\varepsilon y = \frac{\varepsilon x_k}{C_k} + \frac{H_{kk}}{2 \, C_k^2} + o\left(1\right). \tag{42}$$

This special case is used in the section "Propagation of epistasis".

The second special case when mutations A and B each affect different single phenotypes x_k and x_ℓ ($k \neq \ell$), respectively, i.e., all $\delta^A x_i = 0$ except for $i = k$, all $\delta^B x_i = 0$

except for $i = \ell$, and all $\varepsilon x_i = 0$. Then expressions (37)–(39) simplify to

$$\delta^A y = C_k \, \delta^A x_k + o\left(\left|\delta^A x_k\right|\right), \tag{43}$$

$$\delta^B y = C_\ell \, \delta^B x_\ell + o\left(\left|\delta^B x_\ell\right|\right), \tag{44}$$

$$\varepsilon y = \frac{H_{k\ell}}{2\, C_k \, C_\ell} + o\,(1)\,. \tag{45}$$

This second special case was previously considered by Chiu et al [65], who derived the equivalent of equation (45). This special case is used in the section "Emergence of epistasis between mutations affecting different enzymes".

Propagation of epistasis

In this section, I apply the general equations for the propagation of mutational effects and epistasis coefficients obtained above to the metabolic network model described in the "Model" section to understand how the effects of mutations A and B and epistasis between them propagate from one level of metabolic hierarchy to the next one.

Suppose that module ν is embedded into a larger module μ, and suppose that reaction a represents module ν in the coarse-grained network $\mathcal{N}^\nu$. Consider two mutations A and B that directly affect only enzymes within module ν. Let their effects on the effective reaction rate y_ν of module ν be $\delta^A y_\nu$ and $\delta^B y_\nu$ and their epistasis coefficient be εy_ν. We would like to know their effects $\delta^A y_\mu$ and $\delta^B y_\mu$ and epistasis εy_μ for the effective reaction rate y_μ of the larger module μ. Applying equations (30) and (40)–(42) we have

$$\delta^A y_\mu = C_\mu \, \delta^A y_\nu + \text{h.o.t.}, \tag{46}$$

$$\delta^B y_\mu = C_\mu \, \delta^B y_\nu + \text{h.o.t.}, \tag{47}$$

$$\varepsilon y_\mu = \frac{\varepsilon y_\nu}{C_\mu} + \frac{H_\mu}{2\, C_\mu^2} + \text{h.o.t.}, \tag{48}$$

where

$$C_\mu = \frac{y_\nu^0}{y_\mu^0} \frac{dF_{(\mu,a)}}{dy_\nu},$$

$$H_\mu = \frac{\left(y_\nu^0\right)^2}{y_\mu^0} \frac{d^2 F_{(\mu,a)}}{dy_\nu^2}$$

are the first and second-order control coefficients of the effective reaction a with respect to the flux through module μ (taken at the wildtype value y_ν^0). Equation (48) is identical to equation (3). The slope of the line that maps εy_ν onto εy_μ is $1/C_\mu$ and the fixed point of this map is given by

$$\bar{\varepsilon}_\mu = -\frac{H_\mu}{2\, C_\mu \, (1 - C_\mu)}.$$

Theorem 1. *For any module μ*

$$0 \leq C_\mu \leq 1 \tag{49}$$

and

$$0 \leq \bar{\varepsilon}_\mu \leq 1. \tag{50}$$

Proof. To keep notations simple, I denote the effective reaction rate of module ν by ξ, I denote the effective reaction rate of module μ by y, and I denote the function that maps ξ onto y by F. We need to show that

$$0 \leq C \leq 1 \quad \text{where} \quad C = \frac{\xi}{y} F'(\xi) \tag{51}$$

and

$$0 \leq \bar{\varepsilon} \leq 1, \quad \text{where} \quad \bar{\varepsilon} = -\frac{H}{2\,C\,(1-C)} \quad \text{and} \quad H = \frac{\xi^2}{y} F''(\xi) \tag{52}$$

for any values of the kinetic parameters of module μ and any $\xi \geq 0$. According to Proposition 2, the functionional from of F depends only on the topological class of the single-marked module (μ, a). So, I consider the three classes one by one.

Class $(\mu, a) \in \mathcal{M}^{\mathrm{b}}$. In this case (see equation (26)),

$$y = \xi + \alpha,$$

where $\alpha \geq 0$. Therefore, we have

$$\begin{aligned} C &= \frac{\xi}{y}, \\ H &= 0, \end{aligned}$$

and inequalities (51) and (52) hold.

Case $(\mu, a) \in \mathcal{M}^{\mathrm{io}}$. In this case (see equation (27))

$$y = w_{12} + \frac{u\, w_{32}}{D}$$

where $D = u/K_{13} + w_{32}$, $u = \xi + \alpha$, and $\alpha \geq 0$, $w_{12} \geq 0$ and $w_{32} \geq 0$. This yields

$$C = \frac{\xi}{y} \left(\frac{w_{32}}{D}\right)^2, \tag{53}$$

$$H = -2\,\frac{\xi^2}{y}\,\frac{w_{32}^2}{D^3}\,\frac{1}{K_{13}} = -2\,C\,\frac{\xi/K_{13}}{D}. \tag{54}$$

From equation (53), it is clear that $C \geq 0$. It follows from the summation theorem [68] that $C \leq 1$. This fact can also be seen directly fomr expression (53), re-written as

$$C = \left(\frac{\xi\, w_{32}/D}{y}\right) \left(\frac{w_{32}}{D}\right),$$

since both ratios in this expression do not exceed 1.

From equation (54) and the fact that $0 \leq C \leq 1$, it follows that $\bar{\varepsilon} \geq 0$. To show that $\bar{\varepsilon} \leq 1$, note that

$$D\,(1-C) = \frac{u}{K_{13}} + w_{32}\left(1 - \frac{\xi\, w_{32}/D}{y}\right) \geq \frac{\xi}{K_{13}}.$$

Therefore,

$$\bar{\varepsilon} = \frac{\xi/K_{13}}{D\,(1-C)} \leq 1.$$

Hence, inequalities (51) and (52) hold.

<u>Case $(\mu, a) \in \mathcal{M}^{\text{io}}$.</u> In this case (see equation (28))

$$y = w_{12} + \frac{D_3\, w_{14}\, w_{42} + D_4\, w_{13}\, w_{32} + w_{13}\, w_{42}\, u + w_{14}\, w_{32}\, u/K_{34}}{D_3\, D_4 - u^2/K_{34}}, \tag{55}$$

where $u = \xi + \alpha$, $D_3 = w_{31} + w_{32} + u$, $D_4 = w_{41} + w_{42} + u/K_{34}$, $\alpha \geq 0$ and all $w_{ij} \geq 0$. After rearranging terms, equation (55) becomes

$$y = w_{12} + \frac{\tilde{A}\, u + \tilde{B}}{D},$$

with

$$\begin{aligned}
D &= \tilde{C}\, u + \tilde{D}, \\
\tilde{A} &= w_{14}\, w_{42} + w_{13}\, w_{32}/K_{34} + w_{13}\, w_{42} + w_{14}\, w_{32}/K_{34}, \\
\tilde{B} &= (w_{31} + w_{32})\, w_{14}\, w_{42} + (w_{41} + w_{42})\, w_{13}\, w_{32}, \\
\tilde{C} &= (w_{31} + w_{32})/K_{34} + (w_{41} + w_{42}), \\
\tilde{D} &= (w_{31} + w_{32})(w_{41} + w_{42}),
\end{aligned}$$

which yields

$$C = \frac{\xi}{y}\frac{\tilde{A}\tilde{D} - \tilde{B}\tilde{C}}{D^2}, \tag{56}$$

$$H = -2\frac{\xi^2}{y}\frac{\left(\tilde{A}\tilde{D} - \tilde{B}\tilde{C}\right)\tilde{C}}{D^3} = -2\,C\,\frac{\tilde{C}\,\xi}{D}. \tag{57}$$

Next, it is straightforward to show that

$$\tilde{A}\tilde{D} - \tilde{B}\tilde{C} = \frac{1}{K_{31}}\left(w_{41}\, w_{32} - w_{31}\, w_{42}\right)^2 \geq 0,$$

which implies that $C \geq 0$. It follows from the summation theorem [68] that $C \leq 1$. This fact can also be demonstrated directly, as follows. Expanding equation (56), we have

$$C = \frac{\xi \left(\tilde{A}\,\tilde{D} - \tilde{B}\,\tilde{C}\right)}{w_{12}\,D^2 + \left(\tilde{A}\,u + \tilde{B}\right)\left(\tilde{C}\,u + \tilde{D}\right)}.$$

The numerator cannot exceed the denominator because the numerator and both terms in the denominator are non-negative and

$$\left(\tilde{A}\,u + \tilde{B}\right)\left(\tilde{C}\,u + \tilde{D}\right) \geq u\,\left(\tilde{A}\,\tilde{D} + \tilde{B}\,\tilde{C}\right) \geq \xi\left(\tilde{A}\,\tilde{D} - \tilde{B}\,\tilde{C}\right).$$

The fact that $\bar{\varepsilon} \geq 0$ follows directly from equation (57) together with $C \leq 1$. To show that $\bar{\varepsilon} \leq 1$, first note that

$$y = w_{12} + \frac{\tilde{A}\,\xi}{D} + \frac{\tilde{A}\,\alpha + \tilde{B}}{D} \geq \frac{\tilde{A}\,\xi}{D}.$$

Therefore,

$$D\,(1 - C) = \tilde{C}\,\xi + \tilde{C}\,\alpha + \tilde{D}\left(1 - \frac{\tilde{A}\,\xi/D}{y}\right) + \frac{\xi}{D}\,\frac{\tilde{B}\,\tilde{C}}{y} \geq \tilde{C}\,\xi.$$

Hence,

$$\bar{\varepsilon} = \frac{\tilde{C}\,\xi}{D(1 - C)} \leq 1.$$

Therefore, inequalities (51) and (52) hold in this case as well, which completes the proof. □

Emergence of epistasis between mutations affecting different enzymes

In this section, I establish how the topological relationship between reactions affected by mutations determines epistasis that emerges between these mutations at the level of the metabolic module.

Classification of double-marked modules with respect to the topological relationship between the marked reactions

Consider module μ. Without loss of generality, its I/O metabolites are labelled 1 and 2. As described in section "Notations and definitions", a simple path connecting two metabolites i and j within module μ is denoted by $p^{\mu}_{ij} = i \leftrightarrow k \leftrightarrow \ldots \leftrightarrow \ell \leftrightarrow j$. If

such path contains reactions $a_1, a_2, \dots$ and does not contain reactions $b_1, b_2, \dots$, I denote it as $p^{\mu}_{ij}(a_1, a_2, \dots, \bar{b}_1, \bar{b}_2, \dots)$. I denote the set of all paths $p^{\mu}_{ij}(a_1, a_2, \dots, \bar{b}_1, \bar{b}_2, \dots)$ by $\mathcal{P}^{\mu}_{ij}(a_1, a_2, \dots, \bar{b}_1, \bar{b}_2, \dots)$.

According to Lemma 1 proven in Appendix 5, $\mathcal{P}^{\mu}_{12}(a) \neq \emptyset$ for any reaction $a \in R_\mu$. Thus, we can define different topological relationships between any two reactions within a module based on whether or not there exist paths that contain both of them. Consequently, we can classify any double-marked module (μ, a, b) based on the toplogocial relationship between its marked reactions. This classification is orthogonal to that given in Table 1.

Definition 2. *Two distinct reactions $a \in R_\mu$ and $b \in R_\mu$ are called* <u>*parallel*</u> *within module μ if there exist at least two simple paths $p^{\mu}_{12}(a, \bar{b})$ and $p^{\mu}_{12}(b, \bar{a})$.*

Definition 3. *Two distinct reactions $a \in R_\mu$ and $b \in R_\mu$ are called* <u>*serial*</u> *within module μ if there exist at least one simple path $p^{\mu}_{12}(a, b)$.*

Definition 4. *Two reactions $a \in R_\mu$ and $b \in R_\mu$ are called* <u>*strictly parallel*</u> *within module μ if they are parallel but not serial.*

Definition 5. *Two reactions $a \in R_\mu$ and $b \in R_\mu$ are called* <u>*strictly serial*</u> *within module μ if they are serial but not parallel.*

Definition 6. *Two reactions $a \in R_\mu$ and $b \in R_\mu$ are called* <u>*serial-parallel*</u> *within module μ if they are both serial and parallel.*

If reactions a and b are serial, parallel, strictly serial, strictly parallel or serial-parallel within module μ, I also refer to the double-marked module (μ, a, b) as serial, parallel, etc.

Proposition 4. *Let (μ, a, b) be a double-marked module. Then reactions a and b are either strictly serial, or strictly parallel, or serial-parallel.*

Proof. The definition of parallel reactions is equivalent to the fact that both $\mathcal{P}^{\mu}_{12}(a, \bar{b}) \neq \emptyset$ and $\mathcal{P}^{\mu}_{12}(b, \bar{a}) \neq \emptyset$. Similarly, the definition of serial reactions is equivalent to the fact that $\mathcal{P}^{\mu}_{12}(a, b) \neq \emptyset$.

Now, all simple paths that connect the I/O metabolites and contain reaction a either do or do not contain the reaction b, i.e., $\mathcal{P}^{\mu}_{12}(a) = \mathcal{P}^{\mu}_{12}(a, b) \cup \mathcal{P}^{\mu}_{12}(a, \bar{b})$. According to Lemma 1, $\mathcal{P}^{\mu}_{12}(a) \neq \emptyset$. Therefore, either $\mathcal{P}^{\mu}_{12}(a, b) \neq \emptyset$ or $\mathcal{P}^{\mu}_{12}(a, \bar{b}) \neq \emptyset$ or both. Applying Lemma 1 to the reaction b, we conclude that either $\mathcal{P}^{\mu}_{12}(a, b) \neq \emptyset$ or $\mathcal{P}^{\mu}_{12}(b, \bar{a}) \neq \emptyset$ or both.

Therefore, there are three mutually exclusive possibilities.

1. $\mathcal{P}^{\mu}_{12}(a, b) = \emptyset$. Then both $\mathcal{P}^{\mu}_{12}(a, \bar{b}) \neq \emptyset$ and $\mathcal{P}^{\mu}_{12}(\bar{a}, b) \neq \emptyset$, implying that reactions a and b are strictly parallel.

2. $\mathcal{P}^{\mu}_{12}(a, b) \neq \emptyset$, $\mathcal{P}^{\mu}_{12}(a, \bar{b}) \neq \emptyset$, and $\mathcal{P}^{\mu}_{12}(\bar{a}, b) \neq \emptyset$, which implies that reactions a and b are serial-parallel.

3. $\mathcal{P}_{12}(a,b) \neq \emptyset$, and either $\mathcal{P}_{12}(a,\bar{b}) = \emptyset$ or $\mathcal{P}_{12}(\bar{a},b) = \emptyset$ (not exclusively), which implies that reactions a and b are strictly serial.

□

Corollary 4. *Reactions a and b are strictly serial if and only if they are not parallel. Reactions a and b are strictly parallel if and only if they are not serial.*

Coarse-graining preserves the topological relationship between reactions

According to Proposition 3, the coarse-graining procedure $\mathrm{CG}^{(\mu,a,b)}$ maps the double-marked module (μ,a,b) from the topological class $\mathcal{M}$ onto a minimal double-marked module (μ',a,b) from the same class $\mathcal{M}$. The following proposition establishes how this procedure changes the topological relationship between two reactions.

Proposition 5. *Let (μ,a,b) be a double-marked module from the topological class $\mathcal{M}$ (Table 1) and let (μ',a,b) be the minimal double-marked module in $\mathcal{M}$ onto which (μ,a,b) is mapped by the coarse-graining procedure $\mathrm{CG}^{(\mu,a,b)}$.*

1. *Reactions a and b are serial in (μ',a,b) if and only if they are serial in (μ,a,b).*

2. *If reactions a and b are parallel in (μ',a,b), then they are also parallel in (μ,a,b).*

Proof. Denote $a = i \leftrightarrow j$ and $b = k \leftrightarrow \ell$. Metabolites i,j,k,ℓ may be I/O or internal and the two reaction may share a metabolite as described in Table 1. I prove both claims in the case when all metabolites i,j,k,ℓ are internal to module μ and distinct from each other. Other cases can be proven analogously.

Suppose that reactions a and b are serial in (μ,a,b). Then, by definition, there exists a simple path (up to a relabelling of metabolites):

$$p_{12}(a,b) = 1 \leftrightarrow \cdots \leftrightarrow \underbrace{i \leftrightarrow j}_{=a} \leftrightarrow \cdots \leftrightarrow \underbrace{k \leftrightarrow \ell}_{=b} \leftrightarrow \cdots \leftrightarrow 2, \tag{58}$$

where all metabolites other than 1 and 2 are internal to μ. Therefore, all metabolites in this path other than $1,2,i,j,k,\ell$ are eliminated by the coarse-graining procedure. Then, according to Property #8 of the coarse-graining procedure (see Appendix 2), there exists a path

$$p'_{12}(a,b) = 1 \leftrightarrow \underbrace{i \leftrightarrow j}_{=a} \leftrightarrow \underbrace{k \leftrightarrow \ell}_{=b} \leftrightarrow 2 \tag{59}$$

in module μ', i.e., reactions a and b are serial in module μ'.

Suppose that reactions a and b are serial in (μ',a,b). Then there exists a simple path $p'_{12}(a,b)$ in μ', which can be represented by equation (59) (possibly after a relabelling of metabolites). According to Property #8 of the coarse-graining procedure (see Appendix 2), there exist simple paths $1 \leftrightarrow \cdots \leftrightarrow i$, $j \leftrightarrow \cdots \leftrightarrow k$, $\ell \leftrightarrow \cdots \leftrightarrow 2$ in μ, such

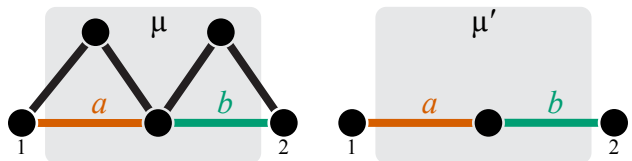

Figure 7. A counter example illustrating that the converse to claim 2 in Proposition 5 may not be true. Reactions a and b are parallel in (μ, a, b). The coarse-graining procedure maps the double-marked module (μ, a, b) onto the minimal double-marked module (μ', a, b) where reactions a and b are not parallel.

that each is either a direct reaction between terminal metabolites or a path where none of the non-terminal metabolites are in $\{1, 2, i, j, k, \ell\}$. Thus, there exists a simple path described by equation (58) in μ. Therefore, reactions a and b are serial in μ.

Consider (μ', a, b) where reactions a and b are parallel. Then there exists a simple path $p'_{12}(a, \bar{b})$ in μ'. In this path, there must be a segment connecting the I/O metabolite 1 with one of the metabolites i or j, and there must be a segment connecting the I/O metabolite 2 with the other metabolite participating in reaction a. For the sake of concretness, let these segments be $p'_{1i}(\bar{a}, \bar{b})$ and $p'_{2j}(\bar{a}, \bar{b})$, respectively (otherwise, we can relabel metabolites appropriately). Since module μ' is the minimal module in its topological class, $p'_{1i}(\bar{a}, \bar{b})$ is either a direct reaction $1 \leftrightarrow i$ or a path that contains two reactions $1 \leftrightarrow k' \leftrightarrow i$ where $k' \in \{k, \ell\}$. If $p'_{1i}(\bar{a}, \bar{b}) = 1 \leftrightarrow i$, Property #8 of the coarse-graining procedure (see Appendix 2) implies then that there exists a simple path p_{1i} in module μ which either is a direct reaction $1 \leftrightarrow i$ or contains only the eliminated metabolites, i.e. it does not contain reactions a or b. If $p'_{1i}(\bar{a}, \bar{b}) = 1 \leftrightarrow k' \leftrightarrow i$, the same logic applies to both segments of this path. Thus, there exists a simple path $p_{1i}(\bar{a}, \bar{b})$ in μ. By the same logic, there exists a simple path $p_{2j}(\bar{a}, \bar{b})$ in μ. Stiching $p_{1i}(\bar{a}, \bar{b})$, reaction a and $p_{2j}(\bar{a}, \bar{b})$ together, we have constructed a path $p_{12}(a, \bar{b})$ in μ.

The fact that a and b are parallel in (μ', a, b) also implies that there exists a simple path $p'_{12}(\bar{a}, b)$ in μ'. By the same logic as above, there exists a path $p_{12}(\bar{a}, b)$ in μ. Therefore, reactions a and b are parallel in μ. □

Note that the converse of the second claim in Proposition 5 is not true. In other words, if two reactions a and b are parallel in (μ, a, b), they may not be parallel in (μ', a, b). Figure 7 shows a counter-example illustrating this.

Corollary 5. *1. If reactions a and b are strictly serial in (μ, a, b), they are also strictly serial in (μ', a, b).*

2. If reactions a and b are strictly parallel in (μ, a, b), they are also strictly parallel in (μ', a, b).

3. If reactions a and b are serial-parallel in (μ, a, b), they are either strictly serial or serial-parallel in (μ', a, b).

Epistasis and the topological relationship between reactions

Consider a module μ. According to Corollary 2, module μ can be replaced with an effective reaction with rate y_μ. Suppose that there are two mutations A and B that affect the rates of reactions within module μ. Specifically, mutation A affects only the rate ξ of reaction a and mutation B affects only the rate η of reaction b so that $\left|\delta^A \xi\right| \ll 1$, $\left|\delta^B \eta\right| \ll 1$. Since these mutations affect different reactions, there is no epistasis between them at the level of individual reaction rates, i.e., $\varepsilon x_{ij} = 0$ for all reactions in module μ. However, y_μ depends on ξ and η, so that epistasis between mutations A and B could emerge at the level of the effective reaction rate y_μ. The goal of this section is to understand how this epistasis depends on the topological relationship between the reactions affected by mutations.

Mutations A and B define a double-marked module (μ, a, b). In general, epistasis εy_μ depends on the function $F_{(\mu,a,b)}$ that maps ξ and η onty y_μ (equation (31)) and on the perturbations $\delta^A \xi$ and $\delta^B \eta$ (equation (39)). However, in the special case when each mutation affects only one reaction rate, epistasis εy_μ does not depend on $\delta^A \xi$ and $\delta^B \eta$, as long as they are small (equation (45)). In other words, εy_μ is a property of the function $F_{(\mu,a,b)}$ alone. According to Proposition 4, the marked reactions a and b are either strictly parallel, strictly serial, or serial-parallel. The main claim (Theorem 2 below) is that, whenever a and b are strictly parallel, the function $F_{(\mu,a,b)}$ has the property $\varepsilon y_\mu \leq 0$ and whenever a and b are strictly serial, the function $F_{(\mu,a,b)}$ has the property $\varepsilon y_\mu \geq 1$.

The logic of the proof of Theorem 2 is the following. Suppose that the double-marked module (μ, a, b) belongs to the topological class $\mathcal{M}$ (Table 1). According to Proposition 3, the coarse-graining procedure $\mathrm{CG}^{(\mu,a,b)}$ maps (μ, a, b) onto the double-marked module (μ', a, b) that is minimal in $\mathcal{M}$, such that mutations A and B still affect the same reations a and b, respectively (and no other reactions) and the rates of reactions a and b in module μ' are given by equations (32), (33). It then follows from Corollary 3 that epistasis εy_μ between mutations A and B in the original double-marked module (μ, a, b) is the same as in the minimal double-marked module (μ', a, b). Furthermore, according to Corollary 5, if a and b are strictly serial in (μ, a, b), they are also strictly serial in (μ', a, b); and if a and b are strictly parallel in (μ, a, b), they are also strictly parallel in (μ', a, b). Therefore, to show that epistasis between any pair of strictly serial reactions is non-negative, it is sufficient to show that epistasis is non-negative for all strictly serial minimal double-marked modules, and analogously for strictly parallel reactions.

How do we evaluate epistasis for all strictly parallel and strictly serial minimal double-marked modules? Whether two reactions are strictly serial or strictly parallel does not depend of the specific values of reaction rates in the module, but only on module topology. Since the number of topologically distinct minimal double-marked modules is finite, all strictly serial and strictly parallel topologies can be explicitly enumerated. Unfortunately, the number of distinct topologies even for the minimal double-marked modules is very large, so finding all of them and evaluating epistasis for each of them would be quite

cumbersome. However, the task is dramatically simplified by Proposition 6 which states that a strictly serial or strictly parallel relationship between two reactions cannot be altered by removing a third reaction from the module. This leads to the realization that there exists a relatively small set of distinct "generating" module topologies, such that every strictly serial minimal module can be produced from some strictly serial generating module by setting certain reaction rates to zero; and similarly for every strictly parallel minimal module. In Appendix 6, I provide a simple algorithm for discovering all such generating topologies. Thus, if we can show that epistasis εy_μ is non-positive for all double-marked module with strictly parallel generating topologies (that is, irrespectively of the values of the reaction rate matrix $\boldsymbol{x}_\mu$), then epistasis must be non-positive for all strictly parallel double-marked modules. Similarly, if we can show that $\varepsilon y_\mu \geq 1$ for all minimal double-marked modules with strictly serial generating topologies, then epistasis must be greater or equal to unity for all strictly serial double-marked modules.

The rest of this section has the following structure. First, I prove Proposition 6 mentioned abvoe. I then provide formal definitions of the strictly parallel and strictly serial generating module topologies. Then, Proposition 7 shows that the topology of any minimal strictly serial double-marked module can be produced from a strictly serial generating topology by removing one or multiple reactions, and similarly for any minimal strictly parallel double-marked module. Then, Proposition 8 shows that epistasis between mutations affecting the marked reactions in any strictly parallel minimal double-marked module is ≤ 0. Analogously, Proposition 9 shows that epistasis between mutations affecting the marked reactions in a strictly serial minimal double-marked module is ≥ 1. Finally, Theorem 2 extends this argument to all modules with strictly serial and strictly parallel reactions.

Proposition 6. *Let (μ, a, b) and (μ', a, b) be two minimal double-marked modules from the same topological class whose sets of reactions are R_μ and $R_{\mu'}$, respectively, and $R_{\mu'} = R_\mu \setminus \{c\}$ where $c \in R_\mu \setminus \{a, b\}$.*

1. *If reactions a and b are strictly parallel in (μ, a, b), they are also strictly parallel in (μ', a, b).*

2. *If reactions a and b are strictly serial in (μ, a, b), they are also strictly serial in (μ', a, b).*

Proof. Denote the I/O metabolites in both modules μ and μ' by 1 and 2. Since μ' and μ are topologically identical except for μ' lacks one reaction c, $\mathcal{P}_{12}^{\mu'}(a_1, a_2, \dots, \bar{b}_1, \bar{b}_2, \dots) \subseteq \mathcal{P}_{12}^{\mu}(a_1, a_2, \dots, \bar{b}_1, \bar{b}_2, \dots)$ for any reactions $a_1, a_2, \dots, b_1, b_2, \dots$ from $R_{\mu'}$. In other words, there could only be fewer paths connecting the I/O metabolites within module μ' compared to module μ.

Suppose that reactions a and b are strictly parallel in (μ, a, b), which implies $\mathcal{P}_{12}^{\mu}(a, b) = \emptyset$. Since $\mathcal{P}_{12}^{\mu'}(a, b) \subseteq \mathcal{P}_{12}^{\mu}(a, b)$, $\mathcal{P}_{12}^{\mu'}(a, b) = \emptyset$, and reactions a and b are not serial in (μ', a, b). Thus, according to Corollary 4, they are strictly parallel in (μ', a, b).

Suppose that reactions a and b are strictly serial in (μ, a, b). Thus, either $\mathcal{P}_{12}^{\mu}(a, \bar{b}) = \emptyset$ or (not exclusively) $\mathcal{P}_{12}^{\mu}(b, \bar{a}) = \emptyset$. If $\mathcal{P}_{12}^{\mu}(a, \bar{b}) = \emptyset$, then $\mathcal{P}_{12}^{\mu'}(a, \bar{b}) = \emptyset$ because $\mathcal{P}_{12}^{\mu'}(a, \bar{b}) \subseteq \mathcal{P}_{12}^{\mu}(a, \bar{b})$; and similarly for $\mathcal{P}_{12}^{\mu'}(b, \bar{a})$. Thus, reactions a and b are not parallel in (μ', a, b). According to Corollary 4, they are strictly serial in (μ', a, b). □

Consider a double-marked module (μ, a, b) minimal in the topological class $\mathcal{M}$. I call the triplet (R_μ, a, b) a <u>topology minimal in $\mathcal{M}$</u>, where R_μ is the reaction set of module μ.I denote the complete reaction set for the minimal metabolite set $A_\mathcal{M}$ by $R_\mathcal{M}$. Thus, for any topology (R_μ, a, b) minimal in $\mathcal{M}$, $R_\mu \subseteq R_\mathcal{M}$.

Since all minimal modules in the topological class $\mathcal{M}$ have the same set of metabolites $A_\mathcal{M}$ (Table 1), the name "topology" is justified. In other words, (R_μ, a, b) fully specifies the topology of module μ and, consequently, the topological relationship between the marked reactions. If the double-marked module is strictly serial, I also call the corresponding topology strictly serial, and analogously for the strictly parallel and serial-parallel topologies. Let $\mathcal{R}_\mathcal{M}^\mathcal{S}$ be the set of all strictly serial topologies minimal in $\mathcal{M}$. Similarly, let $\mathcal{R}_\mathcal{M}^\mathcal{P}$ be the set of all strictly parallel topologies minimal in $\mathcal{M}$, and let $\mathcal{R}_\mathcal{M}^\mathcal{Q}$ be the set of all serial-parallel topologies minimal in $\mathcal{M}$.

Definition 7. *Topology (R, a, b) minimal in $\mathcal{M}$ is called a <u>strictly serial generating topology</u> in $\mathcal{M}$ if $(R, a, b) \in \mathcal{R}_\mathcal{M}^\mathcal{S}$ and either $R = R_\mathcal{M}$ or $(R_\mu \cup \{c\}, a, b) \in \mathcal{R}_\mathcal{M}^\mathcal{Q}$ for any reaction $c \in R_\mathcal{M} \setminus R_\mu$.*

Definition 8. *Topology (R, a, b) minimal in $\mathcal{M}$ is called a <u>strictly parallel generating topology</u> in $\mathcal{M}$ if $(R, a, b) \in \mathcal{R}_\mathcal{M}^\mathcal{P}$ and either $R = R_\mathcal{M}$ or $(R \cup \{c\}, a, b) \in \mathcal{R}_\mathcal{M}^\mathcal{Q}$ for any reaction $c \in R_\mathcal{M} \setminus R$.*

Definitions 7 and 8 state that a minimal topology is a generating topology if adding any reaction would make the marked reactions serial-parallel. Clearly, a topological class $\mathcal{M}$ may have multiple generating topologies, and it is easy to show that every topological class has at least one generating topology. I denote the set of all strictly serial generating topologies for the class $\mathcal{M}$ by $\mathcal{G}_\mathcal{M}^\mathcal{S}$ and I denote the set of all strictly parallel generating topologies for class $\mathcal{M}$ by $\mathcal{G}_\mathcal{M}^\mathcal{P}$. The following proposition justifies the name "generating topology". It states that any strictly serial minimal topology can be produced from some strictly serial generating topology by removing one or multiple reactions, and similarly for any strictly parallel minimal topology.

Proposition 7. *If $(R, a, b) \in \mathcal{R}_\mathcal{M}^\mathcal{P}$, then there exists $(R', a, b) \in \mathcal{G}_\mathcal{M}^\mathcal{P}$, such that $R \subseteq R'$. If $(R, a, b) \in \mathcal{R}_\mathcal{M}^\mathcal{S}$, then there exists $(R', a, b) \in \mathcal{G}_\mathcal{M}^\mathcal{S}$, such that $R \subseteq R'$.*

Proof. First, let $\mathcal{M}$ be one of the topological classes $\mathcal{M}^{\text{b,io,IO}}$, $\mathcal{M}^{\text{b,i,}\emptyset}$, or $\mathcal{M}^{\text{io,io,IO}}$. Clearly, $(R_\mathcal{M}, a, b) \in \mathcal{G}_\mathcal{M}^\mathcal{P}$. According to Proposition 6, any topology (R, a, b) minimal in $\mathcal{M}$ is strictly parallel. Since $R \subseteq R_\mathcal{M}$, the claim of Proposition 7 holds.

Second, consider the topological class $\mathcal{M}^{\mathrm{io,io,I}}$. Clearly, $(R_{\mathcal{M}^{\mathrm{io,io,I}}}, a, b) \in \mathcal{G}^{\mathcal{S}}_{\mathcal{M}}$. According to Proposition 6, any topology (R, a, b) minimal in $\mathcal{M}^{\mathrm{io,io,I}}$ is strictly serial. Since $R \subseteq R_{\mathcal{M}}$, the claim of Proposition 7 holds.

Finally, let $\mathcal{M}$ be one of the remaining topological classes $\mathcal{M}^{\mathrm{io,io,\emptyset}}$, $\mathcal{M}^{\mathrm{io,i,I}}$, $\mathcal{M}^{\mathrm{io,i,\emptyset}}$, $\mathcal{M}^{\mathrm{i,i,I}}$ or $\mathcal{M}^{\mathrm{i,i,\emptyset}}$. Then $(R_{\mathcal{M}}, a, b) \in \mathcal{R}^{\mathcal{Q}}_{\mathcal{M}}$. Suppose that $(R, a, b) \in \mathcal{R}^{\mathcal{P}}_{\mathcal{M}}$. Then R must be a strict subset of $R_{\mathcal{M}}$, so that the set $C = R_{\mathcal{M}} \setminus R$ is not empty. Then, either $R \in \mathcal{G}^{\mathcal{P}}_{\mathcal{M}}$ or $R \notin \mathcal{G}^{\mathcal{P}}_{\mathcal{M}}$. If $R \in \mathcal{G}^{\mathcal{P}}_{\mathcal{M}}$, the first statement of Proposition 7 is true. Suppose that $R \notin \mathcal{G}^{\mathcal{P}}_{\mathcal{M}}$. This implies that there exists a reaction $c_1 \in C$, such that $R_1 = R \cup \{c_1\} \in \mathcal{R}^{\mathcal{P}}_{\mathcal{M}}$ (R_1 cannot be in $\mathcal{R}^{\mathcal{S}}_{\mathcal{M}}$ due to Proposition 6). There are three possibilities.

(a) $R_1 = R_{\mathcal{M}}$.

(b) $R_1 \subset R_{\mathcal{M}}$ and $R_1 \in \mathcal{G}^{\mathcal{P}}_{\mathcal{M}}$.

(c) $R_1 \subset R_{\mathcal{M}}$ and $R_1 \notin \mathcal{G}^{\mathcal{P}}_{\mathcal{M}}$.

Option (a) is not possible since $R_1 \in \mathcal{R}^{\mathcal{P}}_{\mathcal{M}}$ while $R_{\mathcal{M}} \in \mathcal{R}^{\mathcal{Q}}_{\mathcal{M}}$. Option (b) implies that the first statement of Proposition 7 is true. Option (c) implies that there exists a reaction $c_2 \in C \setminus \{c_1\}$, such that $R_2 = R_1 \cup \{c_2\} \in \mathcal{R}^{\mathcal{P}}_{\mathcal{M}}$, and we have the same three possibilities for R_2 as above. Thus, by induction, the first statement of Proposition 7 must be true.

The proof of the second statement of Proposition 7 is analogous. □

In Appendix 6, I provide an algorithm for discovering all strictly serial and strictly parallel generating topologies. I implemented this algorithm in a Matlab code (available at `https://github.com/skryazhi/epistasis_theory`) All strictly parallel generating topologies are listed in Table 2 and all strictly serial generating topologies are listed in Table 3. They are also illustrated in Figures 6, 8–12. I label each generating topology by a four-letter combination (see column 4 in Tables 2 and 3): the first three letters denote the topological class and the last letter (F, P or S) denotes the specific generating topology within that class. Letter "F" (stands for "full") denotes the fact that the reaction set in the generating topology is complete. Letters "P" (for "parallel") and "S" (stands for "serial") denote striclty parallel and strictly serial generating topologies, respectively; if there are a multiple generating topologies within the same class, they are distinguished by subindices, e.g., $\mathrm{io, i, \emptyset, P_1}$; $\mathrm{io, i, \emptyset, P_2}$, etc.

Proposition 8. *Let (μ, a, b) be a minimal double-marked module in the topological class $\mathcal{M}$, with u and v being the rates of reactions a and b, respectively, and let y be the effective activity of this module after coarse-graining. Suppose that mutation A perturbs only reaction a by $\delta^A u$, and mutation B perturbs only reaction b by $\delta^B v$, such that $\left|\delta^A u\right| \ll 1$, $\left|\delta^B v\right| \ll 1$. If reactions a and b are strictly parallel in the minimal double-marked module (μ, a, b), then $\varepsilon y \leq 0$.*

Proof. According to equation (31) and Corollary 3, $y = f(u, v)$, where the function f depends on the topological class $\mathcal{M}$ (see Appendix 3). Since mutation A affects only

Class	Marked reactions		Generating topology		
	a	b	ID	Excluded reactions	Fig.
$\mathcal{M}^{\mathrm{b,io,IO}}$	$1 \leftrightarrow 2$	$1 \leftrightarrow 3$	$\mathrm{b, io, IO, F}$	$\emptyset$	6
$\mathcal{M}^{\mathrm{b,i,\emptyset}}$	$1 \leftrightarrow 2$	$3 \leftrightarrow 4$	$\mathrm{b, i, \emptyset, F}$	$\emptyset$	6
$\mathcal{M}^{\mathrm{io,io,IO}}$	$1 \leftrightarrow 3$	$1 \leftrightarrow 4$	$\mathrm{io, io, IO, F}$	$\emptyset$	6
$\mathcal{M}^{\mathrm{io,io,\emptyset}}$	$1 \leftrightarrow 3$	$2 \leftrightarrow 4$	$\mathrm{io, io, \emptyset, P}$	$\{3 \leftrightarrow 4\}$	8
$\mathcal{M}^{\mathrm{io,i,I}}$	$1 \leftrightarrow 3$	$3 \leftrightarrow 4$	$\mathrm{io, i, I, P}$	$\{2 \leftrightarrow 4\}$	9
$\mathcal{M}^{\mathrm{io,i,\emptyset}}$	$1 \leftrightarrow 3$	$4 \leftrightarrow 5$	$\mathrm{io, i, \emptyset, P_1}$	$\{3 \leftrightarrow 4, 3 \leftrightarrow 5\}$	10
			$\mathrm{io, i, \emptyset, P_2}$	$\{2 \leftrightarrow 5, 3 \leftrightarrow 5\}$	
			$\mathrm{io, i, \emptyset, P_3}$	$\{2 \leftrightarrow 4, 2 \leftrightarrow 5\}$	
$\mathcal{M}^{\mathrm{i,i,I}}$	$3 \leftrightarrow 4$	$3 \leftrightarrow 5$	$\mathrm{i, i, I, P_1}$	$\{2 \leftrightarrow 4, 2 \leftrightarrow 5\}$	11
			$\mathrm{i, i, I, P_2}$	$\{1 \leftrightarrow 5, 2 \leftrightarrow 5\}$	
$\mathcal{M}^{\mathrm{i,i,\emptyset}}$	$3 \leftrightarrow 4$	$5 \leftrightarrow 6$	$\mathrm{i, i, \emptyset, P_1}$	$\{3 \leftrightarrow 5, 3 \leftrightarrow 6, 4 \leftrightarrow 5, 4 \leftrightarrow 6\}$	12
			$\mathrm{i, i, \emptyset, P_2}$	$\{1 \leftrightarrow 5, 1 \leftrightarrow 6, 2 \leftrightarrow 5, 2 \leftrightarrow 6\}$	
			$\mathrm{i, i, \emptyset, P_3}$	$\{2 \leftrightarrow 4, 2 \leftrightarrow 6, 3 \leftrightarrow 6, 4 \leftrightarrow 5, 4 \leftrightarrow 6\}$	
			$\mathrm{i, i, \emptyset, P_4}$	$\{2 \leftrightarrow 4, 2 \leftrightarrow 5, 2 \leftrightarrow 6, 4 \leftrightarrow 5, 4 \leftrightarrow 6\}$	
			$\mathrm{i, i, \emptyset, P_5}$	$\{1 \leftrightarrow 6, 2 \leftrightarrow 4, 2 \leftrightarrow 5, 2 \leftrightarrow 6, 4 \leftrightarrow 6\}$	
			$\mathrm{i, i, \emptyset, P_6}$	$\{1 \leftrightarrow 4, 1 \leftrightarrow 6, 2 \leftrightarrow 4, 2 \leftrightarrow 6, 4 \leftrightarrow 6\}$	
			$\mathrm{i, i, \emptyset, P_7}$	$\{1 \leftrightarrow 4, 1 \leftrightarrow 5, 2 \leftrightarrow 3, 2 \leftrightarrow 6, 3 \leftrightarrow 5, 4 \leftrightarrow 6\}$	

Table 2. Strictly parallel generating topologies.

Class	Marked reactions		Generating topologies		
	a	b	ID	Excluded reactions	Fig.
$\mathcal{M}^{\mathrm{io,io,I}}$	$1 \leftrightarrow 3$	$2 \leftrightarrow 3$	$\mathrm{io}, \mathrm{io}, \mathrm{I}, \mathrm{F}$	$\emptyset$	6
$\mathcal{M}^{\mathrm{io,io,\emptyset}}$	$1 \leftrightarrow 3$	$2 \leftrightarrow 4$	$\mathrm{io}, \mathrm{io}, \emptyset, \mathrm{S}$	$\{2 \leftrightarrow 3\}$	8
$\mathcal{M}^{\mathrm{io,i,I}}$	$1 \leftrightarrow 3$	$3 \leftrightarrow 4$	$\mathrm{io}, \mathrm{i}, \mathrm{I}, \mathrm{S}_1$	$\{2 \leftrightarrow 3\}$	9
			$\mathrm{io}, \mathrm{i}, \mathrm{I}, \mathrm{S}_2$	$\{1 \leftrightarrow 4\}$	
$\mathcal{M}^{\mathrm{io,i,\emptyset}}$	$1 \leftrightarrow 3$	$4 \leftrightarrow 5$	$\mathrm{io}, \mathrm{i}, \emptyset, \mathrm{S}_1$	$\{1 \leftrightarrow 4, 1 \leftrightarrow 5\}$	10
			$\mathrm{io}, \mathrm{i}, \emptyset, \mathrm{S}_2$	$\{2 \leftrightarrow 3, 2 \leftrightarrow 4, 3 \leftrightarrow 5\}$	
			$\mathrm{io}, \mathrm{i}, \emptyset, \mathrm{S}_3$	$\{1 \leftrightarrow 5, 2 \leftrightarrow 3, 2 \leftrightarrow 5\}$	
$\mathcal{M}^{\mathrm{i,i,I}}$	$3 \leftrightarrow 4$	$3 \leftrightarrow 5$	$\mathrm{i}, \mathrm{i}, \mathrm{I}, \mathrm{S}_1$	$\{1 \leftrightarrow 3, 2 \leftrightarrow 3\}$	11
			$\mathrm{i}, \mathrm{i}, \mathrm{I}, \mathrm{S}_2$	$\{2 \leftrightarrow 3, 2 \leftrightarrow 5, 4 \leftrightarrow 5\}$	
$\mathcal{M}^{\mathrm{i,i,\emptyset}}$	$3 \leftrightarrow 4$	$5 \leftrightarrow 6$	$\mathrm{i}, \mathrm{i}, \emptyset, \mathrm{S}_1$	$\{2 \leftrightarrow 3, 2 \leftrightarrow 5, 2 \leftrightarrow 6, 4 \leftrightarrow 5, 4 \leftrightarrow 6\}$	12
			$\mathrm{i}, \mathrm{i}, \emptyset, \mathrm{S}_2$	$\{1 \leftrightarrow 3, 1 \leftrightarrow 6, 2 \leftrightarrow 3, 2 \leftrightarrow 6, 4 \leftrightarrow 6\}$	

Table 3. Strictly serial generating topologies.

reaction rate u and mutation B only affects reaction rate v, the expression for εy is given by equation (45), i.e.,

$$\varepsilon y = \frac{H_{ab}}{2\,C_a\,C_b}, \tag{60}$$

where

$$C_a = \frac{u}{y}\frac{\partial f}{\partial u}, \tag{61}$$

$$C_b = \frac{v}{y}\frac{\partial f}{\partial v}, \tag{62}$$

$$H_{ab} = \frac{u\,v}{y}\frac{\partial^2 f}{\partial u\,\partial v}. \tag{63}$$

According to Theorem 1, $0 \le C_a \le 1$ and $0 \le C_b \le 1$. And since all $y > 0$, $u > 0$, $v > 0$, to prove Lemma 8, it is sufficient to show that $\frac{\partial^2 f}{\partial u\,\partial v} \le 0$ for any minimal double-marked module (μ, a, b) from any topological class $\mathcal{M}$ where reactions a and b are strictly parallel. According to Proposition 7, the reaction set R_μ must be a subset of the reaction set of at least one of the strictly parallel generating topologies listed in Table 2. Therefore, to show that $\varepsilon y \le 0$ for (μ, a, b), it is sufficient to show that $\varepsilon y \le 0$ for any double-marked module (μ, a, b) with any strictly parallel generating topology.

Generating topologies b, io, IO, F and b, i, $\emptyset$, F (Figure 6). According to equations (A3.1) and (A3.2),

$$y = f(u, v) = u + \phi(v),$$

where $\phi(v)$ is independent of u, which implies that $\frac{\partial^2 f}{\partial u\,\partial v} = 0$.

Generating topology io, io, IO, F (Figure 6). According to equation (A3.4),

$$y = f(\xi, \eta) = w_{12} + \frac{A\,u\,v + B\,u + B\,v}{D(u, v)},$$

where

$$\begin{aligned}
D(\xi, \eta) &= E\,u\,v + F\,u + G\,v + B, \\
A &= \frac{w_{42}}{K_{13}} + \frac{w_{32}}{K_{14}}, \\
B &= w_{32}\,w_{42} + w_{32}\,w_{43} + w_{34}\,w_{42}, \\
E &= \frac{1}{K_{13}\,K_{14}}, \\
F &= \frac{w_{42} + w_{43}}{K_{13}}, \\
G &= \frac{w_{32} + w_{34}}{K_{14}}.
\end{aligned}$$

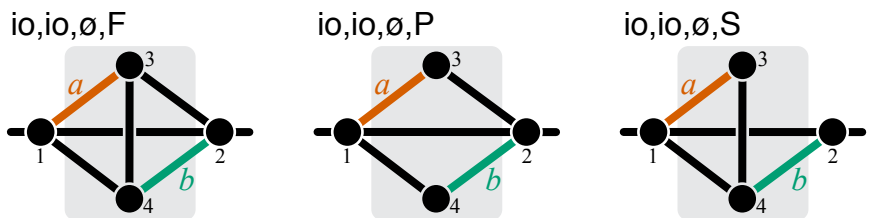

Figure 8. Graphical representation of strictly serial and strictly parallel generating topologies in the class $\mathcal{M}^{\mathrm{io,io,\emptyset}}$. Topology with the complete reaction set io, io, $\emptyset$, F is shown for reference (same as in Figure 6).

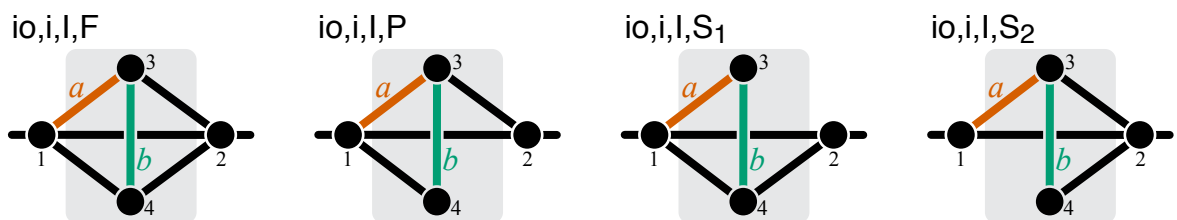

Figure 9. Graphical representation of strictly serial and strictly parallel generating topologies in class $\mathcal{M}^{\mathrm{io,i,I}}$. Topology with the complete reaction set io, i, I, F is shown for reference (same as in Figure 6).

Therefore,

$$\frac{\partial^2 f}{\partial u\,\partial v} = -2\,\frac{w_{34}}{K_{14}}\,\frac{(w_{32}\,v/K_{14}+B)\;(w_{42}\,u/K_{13}+B)}{\big(D(u,v)\big)^3} \leq 0.$$

Generating topology io, io, $\emptyset$, P (Figure 8). According to equation (A3.5),

$$y = f(u,v) = w_{12} + \phi(u) + \psi(v),$$

where $\phi(u)$ is independent of v an $\psi(v)$ is independent of u. Therefore, $\frac{\partial^2 f}{\partial u\,\partial v} = 0$.

Generating topology io, i, I, P (Figure 9). Notice that metabolite 4 together with reactions $1 \leftrightarrow 4$, a and b form a double-marked module (μ', a, b) whose I/O metabolites are 1 and 3 and which is minimal in the topological calss $\mathcal{M}^{\mathrm{b,io,IO}}$. Denote the effective reaction rate of module μ' by y'. Therefore, $\varepsilon y' = 0$, as shown above. Since module μ' is contained in μ, by Theorem 1, $\varepsilon y \leq 0$.

Generating topology io, i, $\emptyset$, P_1 (Figure 10). According to Property 1 of the coarse-graining procedure (see Appendix 2), we can coarse-grain module μ by first eliminating metabolite 3. By Property 3 of the coarse-graining procedure (see Appendix 2), mutation A perturbs only the reaction rate u' of the effective reaction $a' \equiv 1 \leftrightarrow 2$ in module μ' after the elimination of metabolite 3. According to equation (46) and Theorem 1, $\left|\delta^A u'\right| \ll 1$. After eliminating metabolite 3, the double-marked module (μ', a', b) is minimal in the topological class $\mathcal{M}^{\mathrm{b,i,\emptyset}}$ which implies that $\varepsilon y = 0$, as shown above.

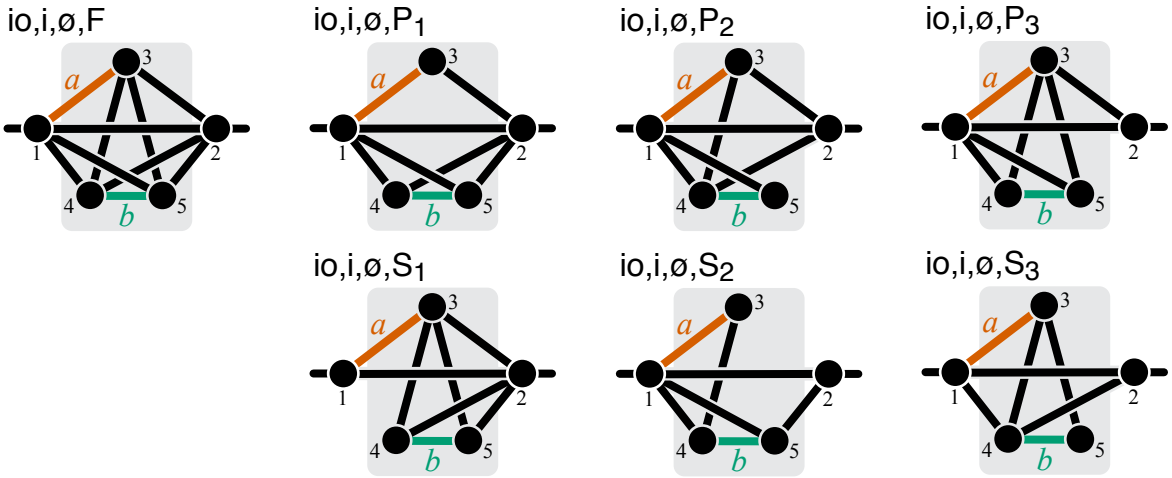

Figure 10. Graphical representation of strictly serial and strictly parallel generating topologies in class $\mathcal{M}^{\mathrm{io,i,\emptyset}}$. Topology with the complete reaction set $\mathrm{io, i, \emptyset, F}$ is shown for reference (same as in Figure 6).

Generating topology $\mathrm{io, i, \emptyset, P_2}$ (Figure 10). We can coarse-grain module μ by first eliminating metabolite 5, which will result in a double-marked module (μ', a, b') that is minimal in the topological class $\mathcal{M}^{\mathrm{io,io,IO}}$. The rest of the proof for this topology is analogous to that for the topology $\mathrm{io, i, \emptyset, P_1}$.

Generating topology $\mathrm{io, i, \emptyset, P_3}$ (Figure 10). Notice that metabolites 4 and 5 together with reactions a, b, $1 \leftrightarrow 4$, $1 \leftrightarrow 5$, $3 \leftrightarrow 4$ and $3 \leftrightarrow 5$ form a double-marked module (μ', a, b) whose I/O metabolites are 1 and 3 and which is minimal in the topological calss $\mathcal{M}^{\mathrm{b,i,\emptyset}}$. The rest of the proof for this topology is analogous to that for the topology $\mathrm{io, i, I, P}$.

Generating topology $\mathrm{i, i, I, P_1}$ (Figure 11). Notice that metabolites 4 and 5 together with reactions a, b, $1 \leftrightarrow 3$, $1 \leftrightarrow 4$, $1 \leftrightarrow 5$ and $4 \leftrightarrow 5$ form a double-marked module (μ', a, b) whose I/O metabolites are 1 and 3 and which is minimal in the topological calss $\mathcal{M}^{\mathrm{io,io,IO}}$. The rest of the proof for this topology is analogous to that for the topology $\mathrm{io, i, I, P}$.

Generating topology $\mathrm{i, i, I, P_2}$ (Figure 11). Notice that metabolite 5 together with reactions a, b, and $4 \leftrightarrow 5$ form a double-marked module (μ', a, b) whose I/O metabolites are 3 and 4 and which is minimal in the topological calss $\mathcal{M}^{\mathrm{b,io,IO}}$. The rest of the proof for this topology is analogous to that for the topology $\mathrm{io, i, I, P}$.

Generating topology $\mathrm{i, i, \emptyset, P_1}$ (Figure 12). According to equation (A3.9),

$$y = f(u, v) = x_{12} + \phi(u) + \psi(v).$$

where $\phi(u)$ is independent of v and $\psi(v)$ is independent of u. Therefore, $\frac{\partial^2 f}{\partial u \, \partial v} = 0$.

Generating topology $\mathrm{i, i, \emptyset, P_2}$ (Figure 12). Notice that metabolites 5 and 6 together with reactions a, b, $3 \leftrightarrow 5$, $3 \leftrightarrow 6$, $4 \leftrightarrow 5$ and $5 \leftrightarrow 6$ form a double-marked module (μ', a, b)

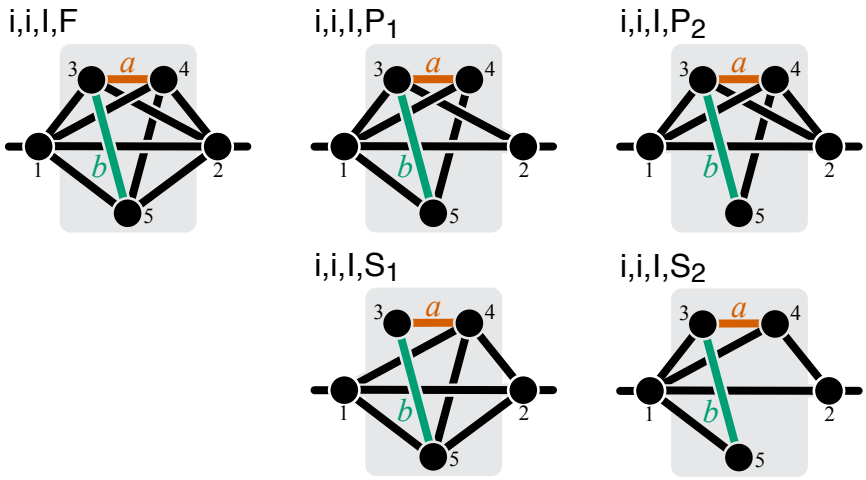

Figure 11. Graphical representation of strictly serial and strictly parallel generating topologies in class $\mathcal{M}^{\mathrm{i,i,I}}$. Topology with the complete reaction set $\mathrm{i}, \mathrm{i}, \mathrm{I}, \mathrm{F}$ is shown for reference (same as in Figure 6).

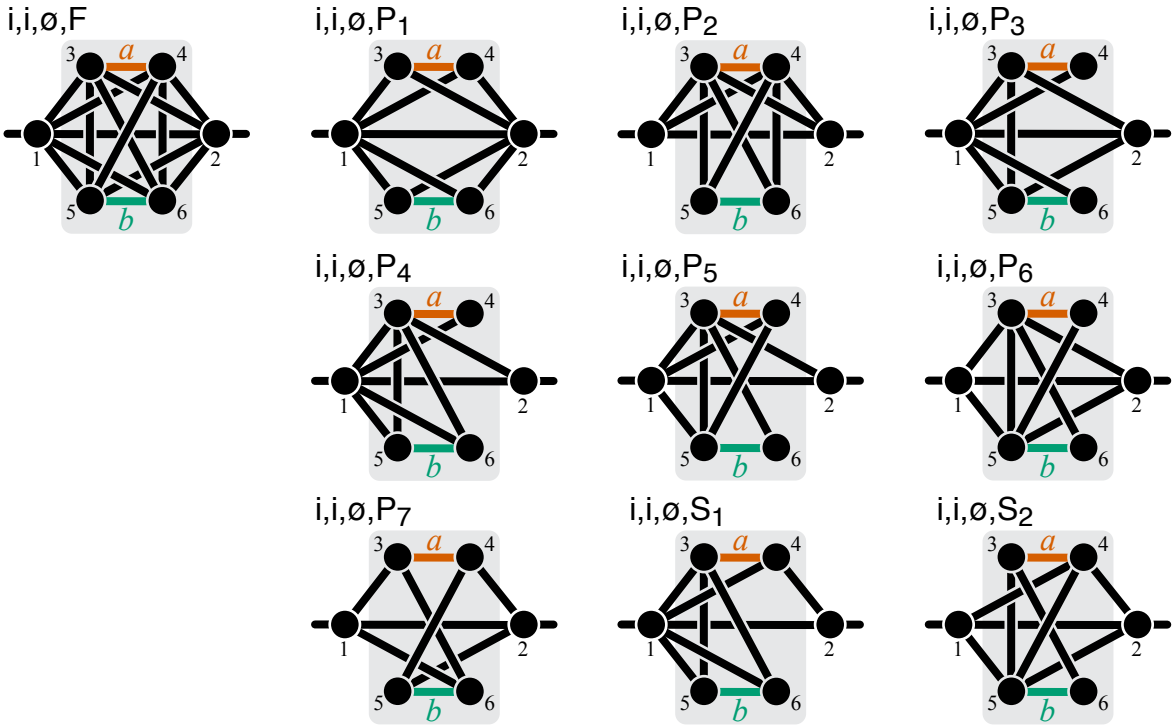

Figure 12. Graphical representation of strictly serial and strictly parallel generating topologies in class $\mathcal{M}^{\mathrm{i,i,\emptyset}}$. Topology with the complete reaction set $\mathrm{i}, \mathrm{i}, \emptyset, \mathrm{F}$ is shown for reference (same as in Figure 6).

whose I/O metabolites are 3 and 4 and which is minimal in the topological calss $\mathcal{M}^{\mathrm{b,i,\emptyset}}$. The rest of the proof for this topology is analogous to that for the topology $\mathrm{io,i,I,P}$.

Generating topology $\mathrm{i,i,\emptyset,P_3}$ (Figure 12). We can coarse-grain module μ by first eliminating metabolites 4 and 6, which will result in a double-marked module (μ', a', b') that is minimal in the topological class $\mathcal{M}^{\mathrm{io,io,IO}}$. The rest of the proof for this topology is analogous to that for the topology $\mathrm{io,i,\emptyset,P_1}$.

Generating topology $\mathrm{i,i,\emptyset,P_4}$ (Figure 12). We can coarse-grain module μ by first eliminating metabolite 4, which will result in a double-marked module (μ', a', b) that is minimal in the topological class $\mathcal{M}^{\mathrm{io,i,\emptyset}}$ with a strictly parallel generating topology $\mathrm{io,i,\emptyset,P_3}$. The rest of the proof for this topology is analogous to that for the topology $\mathrm{io,i,\emptyset,P_1}$.

Generating topology $\mathrm{i,i,\emptyset,P_5}$ (Figure 12). We can coarse-grain module μ by first eliminating metabolite 6, which will result in a double-marked module (μ', a, b') that is minimal in the topological class $\mathcal{M}^{\mathrm{i,i,I}}$ with a strictly parallel generating topology $\mathrm{io,i,\emptyset,P_1}$. The rest of the proof for this topology is analogous to that for the topology $\mathrm{io,i,\emptyset,P_1}$.

Generating topology $\mathrm{i,i,\emptyset,P_6}$ (Figure 12). Notice that metabolites 4 and 6 together with reactions a, b, $3 \leftrightarrow 5$, $3 \leftrightarrow 6$, $4 \leftrightarrow 5$ form a double-marked module (μ', a, b) whose I/O metabolites are 3 and 5 and which is minimal in the topological calss $\mathcal{M}^{\mathrm{io,io,\emptyset}}$. The rest of the proof for this topology is analogous to that for the topology $\mathrm{io,i,I,P}$.

Generating topology $\mathrm{i,i,\emptyset,P_7}$ (Figure 12). Using equation (A3.9), I show in Appendix 7 that

$$\frac{\partial^2 y}{\partial u\, \partial v} = \frac{2\,\beta}{K_{31}}\, \frac{(A_u\, v + B_u)\, (A_v\, u + B_v)}{(E_u\, v + F_u)^3}, \tag{64}$$

where A_v, B_v, E_u, F_u are all non-negative constants (independent of u and v) and $\beta \leq 0$. □

Proposition 9. *Let (μ, a, b) be a minimal double-marked module in the topological class $\mathcal{M}$, with u and v being the rates of reactions a and b, respectively, and let y be the effective activity of this module after coarse-graining. Suppose that mutation A perturbs only reaction a by $\delta^A u$, and mutation B perturbs only reaction b by $\delta^B v$, such that $\left|\delta^A u\right| \ll 1$, $\left|\delta^B v\right| \ll 1$. If reactions a and b are strictly serial in the minimal double-marked module (μ, a, b), then $\varepsilon y \geq 1$.*

Proof. As described in the proof of Proposition 8, $y = f(u, v)$, where the function f depends on the topological class $\mathcal{M}$ (see Appendix 3), and εy is given by the equations (60)–(63). Similarly to the proof of Proposition 8, I prove Proposition 9 by showing that $\varepsilon y \geq 1$ for any minimal double-marked module (μ, a, b) whose topology is a strictly serial generating topology listed in Table 3. Proposition 7 would then imply that Proposition 9 holds for any strictly serial minimal double-marked module (μ, a, b).

Generating topology set $\mathrm{io,io,I,F}$ (Figure 6). According to equation (A3.3), we have

$$y = w_{12} + \frac{u\, v}{D} \tag{65}$$

where $D = u/K_{13} + v$. Therefore,

$$\begin{aligned} C_a &= \left(\frac{v}{D}\right)^2 \frac{u}{y}, \\ C_b &= \frac{1}{K_{12}} \left(\frac{u}{D}\right)^2 \frac{v}{y}, \\ H_{ab} &= \frac{2}{K_{12}} \frac{1}{y\,D} \left(\frac{u\,v}{D}\right)^2. \end{aligned}$$

Substituting these expressions into equation (60), I obtain,

$$\varepsilon y = \frac{y}{u\,v/D} \geq 1$$

because, according to equation (65), $y \geq u\,v/D$.

Generating topology $\mathrm{io}, \mathrm{io}, \emptyset, \mathrm{S}$ (Figure 8). According to Property 1 of the coarse-graining procedure (see Appendix 2), we can coarse-grain module μ by first eliminating metabolite 3. By Property 3 of the coarse-graining procedure (see Appendix 2), mutation A perturbs only the rate u' of the effective reaction $a' \equiv 1 \leftrightarrow 4$ in resulting module μ'. According to equation (46) and Theorem 1, $\left|\delta^A u'\right| \ll 1$. After eliminating metabolite 3, the double-marked module (μ', a', b) is minimal in the topological class $\mathcal{M}^{\mathrm{io,io,I}}$ which implies that $\varepsilon y \geq 1$, as shown above.

Generating topology $\mathrm{io}, \mathrm{i}, \mathrm{I}, \mathrm{S}_1$ (Figure 9). INotice that metabolite 3 together with reactions a, b, and $1 \leftrightarrow 4$ form a double-marked module (μ', a, b) whose I/O metabolites are 1 and 4 and which is minimal in the topological calss $\mathcal{M}^{\mathrm{io,io,I}}$. Therefore, if the effective reaction rate of module μ' is y', $\varepsilon y' \geq 1$, as shown above. According to equations (46), (47) and Theorem 1, $\left|\delta^A y'\right| \ll 1$, $\left|\delta^B y'\right| \ll 1$. Since module μ' is contained in μ, by Theorem 1, $\varepsilon y \geq 1$.

Generating topology $\mathrm{io}, \mathrm{i}, \mathrm{I}, \mathrm{S}_2$ (Figure 9). We can coarse-grain module μ by first eliminating metabolite 4, which will result in a double-marked module (μ', a, b') which is minimal in the topological class $\mathcal{M}^{\mathrm{io,io,I}}$. The rest of the proof for this topology is analogous to that for the topology $\mathrm{io}, \mathrm{io}, \emptyset, \mathrm{S}$.

Generating topology $\mathrm{io}, \mathrm{i}, \emptyset, \mathrm{S}_1$ (Figure 10). If the reaction set of (μ, a, b) is a subset of the strictly serial generating topology $\mathrm{io}, \mathrm{i}, \emptyset, \mathrm{S}_1$, then $w_{14} = w_{15} = 0$ (Table 3, Figure 10). We can coarse-grain module μ by first eliminating metabolites 4 and 5, which will result in a double-marked module (μ', a, b') which is minimal in the topological class $\mathcal{M}^{\mathrm{io,io,I}}$. The rest of the proof for this topology is analogous to that for the topology $\mathrm{io}, \mathrm{io}, \emptyset, \mathrm{S}$.

Generating topology $\mathrm{io}, \mathrm{i}, \mathrm{I}, \mathrm{S}_2$ (Figure 9). Notice that metabolites 3 and 4 together with reactions a, b, $1 \leftrightarrow 4$, $1 \leftrightarrow 5$ and $3 \leftrightarrow 4$ form a double-marked module (μ', a, b) whose I/O metabolites are 1 and 5 and which is minimal in the topological calss $\mathcal{M}^{\mathrm{io,io,\emptyset}}$ and whose reaction set is the strictly serial generating set $\mathrm{io}, \mathrm{io}, \emptyset, \mathrm{S}$. The rest of the proof for this topology is analogous to that for the topology $\mathrm{io}, \mathrm{i}, \mathrm{I}, \mathrm{S}_1$.

Generating topology $\mathrm{io}, \mathrm{i}, \mathrm{I}, \mathrm{S}_3$ (Figure 9). Notice that metabolites 3 and 5 together with reactions a, b, $1 \leftrightarrow 4$, $3 \leftrightarrow 4$ and $3 \leftrightarrow 5$ form a double-marked module (μ', a, b) whose I/O metabolites are 1 and 4 and which is minimal in the topological calss $\mathcal{M}^{\mathrm{io},\mathrm{io},\emptyset}$ and whose reaction set is the strictly serial generating set $\mathrm{io}, \mathrm{io}, \emptyset, \mathrm{S}$. The rest of the proof for this topology is analogous to that for the topology $\mathrm{io}, \mathrm{i}, \mathrm{I}, \mathrm{S}_1$.

Generating topology $\mathrm{i}, \mathrm{i}, \mathrm{I}, \mathrm{S}_1$ (Figure 11). Notice that metabolite 3 together with reactions a, b, and $4 \leftrightarrow 5$ form a double-marked module (μ', a, b) whose I/O metabolites are 4 and 5 and which is minimal in the topological calss $\mathcal{M}^{\mathrm{io},\mathrm{io},\mathrm{I}}$. The rest of the proof for this topology is analogous to that for the topology $\mathrm{io}, \mathrm{i}, \mathrm{I}, \mathrm{S}_1$.

Generating topology $\mathrm{i}, \mathrm{i}, \mathrm{I}, \mathrm{S}_2$ (Figure 11). Notice that metabolites 3 and 5 together with reactions a, b, $1 \leftrightarrow 3$, $1 \leftrightarrow 4$ and $1 \leftrightarrow 5$ form a double-marked module (μ', a, b) whose I/O metabolites are 1 and 4 and which is minimal in the topological calss $\mathcal{M}^{\mathrm{io},\mathrm{i},\mathrm{I}}$ and whose reaction set is the strictly serial generating set $\mathrm{io}, \mathrm{i}, \mathrm{I}, \mathrm{S}_2$. The rest of the proof for this topology is analogous to that for the topology $\mathrm{io}, \mathrm{i}, \mathrm{I}, \mathrm{S}_1$.

Generating topology $\mathrm{i}, \mathrm{i}, \emptyset, \mathrm{S}_1$ (Figure 12). We can coarse-grain module μ by first eliminating metabolites 5 and 6, which will result in a double-marked module (μ', a, b') which is minimal in the topological class $\mathcal{M}^{\mathrm{io},\mathrm{i},\mathrm{I}}$ with the strictly serial generating topology $\mathrm{io}, \mathrm{i}, \mathrm{I}, \mathrm{S}_1$. The rest of the proof for this topology is analogous to that for the topology $\mathrm{io}, \mathrm{io}, \emptyset, \mathrm{S}$.

Generating topology $\mathrm{i}, \mathrm{i}, \emptyset, \mathrm{S}_2$ (Figure 12). We can coarse-grain module μ by first eliminating metabolite 6, which will result in a double-marked module (μ', a, b') which is minimal in the topological class $\mathcal{M}^{\mathrm{i},\mathrm{i},\mathrm{I}}$ with the strictly serial generating topology $\mathrm{i}, \mathrm{i}, \mathrm{I}, \mathrm{S}_1$. The rest of the proof for this topology is analogous to that for the topology $\mathrm{io}, \mathrm{io}, \emptyset, \mathrm{S}$. □

Theorem 2. *Let (μ, a, b) be a double-marked module, with ξ and η being the rates of reactions a and b, respectively, and let y_μ be the effective activity of this module after coarse-graining. Suppose that mutation A perturbs only reaction a by $\delta^A\xi$, and mutation B perturbs only reaction b by $\delta^B\eta$, such that $\left|\delta^A\xi\right| \ll 1$, $\left|\delta^B\eta\right| \ll 1$. If reactions a and b are strictly parallel in the double-marked module (μ, a, b), then $\varepsilon y_\mu \leq 0$. If reactions a and b are strictly serial in the double-marked module (μ, a, b), then $\varepsilon y_\mu \geq 1$.*

Proof. According to Proposition 3, the coarse-graining procedure $\mathrm{CG}^{(\mu,a,b)}$ maps (μ, a, b) onto a double-marked module (μ', a, b) that is minimal in the same topological class as (μ, a, b), and the rates of reactions a and b in μ' are given by linear relations (32) and (33). Clearly, $\left|\delta^A u\right| \ll 1$ and $\left|\delta^B v\right| \ll 1$. Furthermore, none of the other reaction rates w_{ij} in μ' depend on ξ or η, so that $\delta^A w_{ij} = 0$ and $\delta^B w_{ij} = 0$ for all w_{ij} other than u and v, and $\varepsilon w_{ij} = 0$ for all w_{ij} including u and v. It then follows from Corollary 3 that $\varepsilon y_\mu \equiv \varepsilon y_{\mu'}$.

Now, according to Corollary 5, if reactions a and b are strictly parallel in (μ, a, b), they are also strictly parallel in (μ', a, b). Therefore, by Proposition 8, $\varepsilon y_{\mu'} \leq 0$. Analogously, if reactions a and b are strictly serial in (μ, a, b), they are also strictly serial in (μ', a, b). Therefore, by Proposition 9, $\varepsilon y_{\mu'} \geq 1$. □

Kinetic model of glycolysis

I downloaded the kinetic metabolic model of *E. coli* glycolysis by Chassagnole *et al* [74] from the BioModels database [85] on September 15, 2015 (model ID BIOMD0000000051). I used the Matlab SimBiology toolbox to interpret the model. To validate the model, I simulated it for 40 seconds and reproduced Figures 4 and 5 from Ref. [74]. The Matlab code is available at `https://github.com/skryazhi/epistasis_theory`.

Modifications to the original model. Next, I simplified and modified the model by (a) fixing the concentrations of ATP, ADP, AMP, NADPH, NADP, NADH, NAD at their steady-state values given in Table V of Ref. [74] and (b) removing dilution by growth. I then created four models of sub-modules of glycolysis by retaining the subsets of metabolites and enzymes shown in Figure 3–figure supplement 1 and Table 4 and removing other metabolites and enzymes. Each sub-module has one input and one output metabolite. Note that, since some reactions are irreversible, it is important to distinguish the input metabolite from the output metabolite. The concentrations of the input and the output metabolites in each model are held constant at their steady-state values given in Table 4. I defined the flux through the sub-module as the flux towards the output metabolite contributed by the sub-module (Table 4). This flux is the equivalent of the quantitative phenotype y_μ of a module in the analytical model. In addition, I made the following modifications specific to individual sub-modules.

1. In the FULL model, the stoichiometry of the PTS reaction was changed to

$$[\text{Ext glu}] + [\text{pep}] \leftrightarrow [\text{g6p}] + [\text{pyr}]$$

   and the value of the constant $K_{\text{PTS,a1}}$ was set to 0.02 mM, based on the values found in the literature [86, 87].

2. In all models other than FULL, the extracellular compartment was deleted.

3. In all models, the concentrations of the I/O metabolites were set to values shown in Table 4, which are the steady-state concentrations achieved in the FULL model with the concentration of extracellular glucose being 2 µM and pyruvate concentration being 10 µM.

Calculation of flux control coefficients and epistasis coefficients. I calculate the first- and second-order flux control coefficients (FCC) C_i and H_{ij} for flux J with respect to reactions i and j as follows (see equations (35), (36)). I perturb the $r_{\max,i}$ of reaction i by factor between 0.75 and 1.25 (10 values in a uniformly-spaced grid), such that $\delta r_{\max,i} \in [-0.25, 0.25]$. Then, I obtain the steady-state flux J' in each perturbed

Model	Internal metabolites	Concentrations of I/O metabolites	Reactions	Output flux
UGPP	6pg, dhap, e4p, f6p, fdp, rib5p, ribu5p, sed7p, xyl5p	[g6p] = 3.82 mM, [gap] = 0.44 mM	ALDO, G6PDH, PFK, PGDH, PGI, Ru5P, R5PI, TA, TIS, TKa, TKb	$J_{\mathrm{ALDO}} + J_{\mathrm{TIS}} + J_{\mathrm{TKb}} + J_{\mathrm{TKa}} - J_{\mathrm{TA}}$
LG	2pg, 3pg, pgp	[gap] = 0.44 mM, [pep] = 0.08 mM	ENO, GAPDH, PGK, PGM	J_{ENO}
GPP	all in UGPP and in LG, gap	[g6p] = 3.82 mM, [pep] = 0.08 mM	all in UGPP and in LG	J_{ENO}
FULL	all in GPP, g6p, pep	[Ext glu] = 2 µM, [pyr] = 10 µM	all in GPP, PTS, PK, PEPCxyl	$J_{\mathrm{PK}} + J_{\mathrm{PTS}}$

Table 4. Definition of modules in the glycolysis network shown in Figure 3–figure supplement 1. Enzyme abbreviations are listed in Table 6. Metabolite abbreviations are listed in Table 5.

2pg	2-phosphoglycerate
3pg	3-phosphoglycerate
6pg	6-phosphogluconate
dhap	dihydroxyacetonephosphate
e4p	erythrose-4-phosphate
f6p	fructose-6-phosphate
fdp	fructose-1,6-bisphosphate
g6p	glucose-6-phosphate
gap	glyceraldehyde-3-phosphate
glu	glucose
pep	phosphoenolpyruvate
pgp	1,3-diphosphoglycerate
pyr	pyruvate
rib5p	ribose-5-phosphate
ribu5p	ribulose-5-phosphate
sed7p	sedoheptulose-7-phosphate
xyl5p	xylulose-5-phosphate

Table 5. Names of metabolites used in the kinetic model of glycolysis.

ALDO	aldolase
ENO	enolase
G6PDH	glucose-6-phosphate dehydrogenase
GAPDH	glyceraldehyde-3-phosphate dehydrogenase
PFK	phosphofructokinase
PGDH	6-phosphogluconate dehydrogenase
PGI	glucose-6-phosphateisomerase
PGK	phosphoglycerate kinase
PGM	phosphoglycerate mutase
PEPCxyl	PEP carboxylase
PK	pyruvate kinase
PTS	phosphotransferase system
R5PI	ribose-phosphateisomerase
Ru5P	ribulose-phosphate epimerase
TA	transaldolase
TIS	triosephosphate isomerase
TKa	transketolase, reaction a
TKb	transketolase, reaction b

Table 6. Names of enzymes used in the kinetic model of glycolysis.

model and calculate the flux perturbations $\delta J = J'/J^0 - 1$, where J^0 is the corresponding flux in the unperturbed model. Then, to obtain C_i and H_{ii}, I fit the linear model

$$\delta J \sim C_i \, (\delta r_{\max,i}) + \frac{H_{ii}}{2} \, (\delta r_{\max,i})^2$$

by least squares. If the estimated value of C_i was below 10^{-4} for a given sub-module, I set C_i to zero and exclude this reaction from further consideration in that sub-module because it does not affect flux to the degree that is accurately measurable. If the estimated value of H_{ii} is below 10^{-4}, I set H_{ii} to zero.

To calculate the non-diagonal second-order control coefficients H_{ij}, I create a 4×4 grid of perturbations of $\delta r_{\max,i}$ and $\delta r_{\max,j}$ and calculate the resulting flux perturbations δJ (16 perturbations total). Since C_i, C_j, H_{ii} and H_{jj} are known, I obtain H_{ij}, by regressing

$$\delta J - \left(C_i \, (\delta r_{\max,i}) + \frac{H_{ii}}{2} \, (\delta r_{\max,i})^2 \right) - \left(C_j \, (\delta r_{\max,j}) + \frac{H_{jj}}{2} \, (\delta r_{\max,j})^2 \right)$$

against

$$(\delta r_{\max,i}) \, (\delta r_{\max,j}) \, .$$

If the estimated value of H_{ij} is below 10^{-4}, I set H_{ij} to zero. I estimate the epistasis coefficient εJ between mutations affecting reactions i and j as

$$\varepsilon J = \frac{H_{ij}}{2 \, C_i \, C_j}.$$

Establishing the topological relationships between pairs of reactions. To establish the topological relationship (strictly serial, strictly parallel or serial-parallel) between two reactions, I consider the smallest module (LG, UGPP, GPPP or FULL) which contains both reactions. I then manually identify whether there exists a simple path connecting the input metabolite with the output metabolite for that module that passes through both reactions. (Note that, since some reactions are irreversible in this model, it is important to distinguish the input metabolite from the output metabolite). If such path does not exist, I classify the topological relationship between the two reactions as strictly parallel. If such path exists, I check if there are two paths connecting the input to the output metabolites such that each path contains only one of the two focal reactions. If such paths do not exist, I classify the topological relationship between the two reactions as strictly serial. Otherwise, I classify it as serial-parallel.

Acknowledgements

I thank Chris Marx for discussions that stimulated this work, David McCandlish for making me aware of the Kron reduction, Daniel P. Rice and the Kryazhimskiy lab for

feedback on the manuscript. This work was supported by the BWF Career Award at Scientific Interface (Grant 1010719.01), the Alfred P. Sloan Foundation (Grant FG-2017-9227), the Hellman Foundation and NIH (Grant 1R01GM137112).

References

[1] Hu T, Sinnott-Armstrong NA, Kiralis JW, Andrew AS, Karagas MR, Moore JH. Characterizing genetic interactions in human disease association studies using statistical epistasis networks. BMC bioinformatics. 2011;12(1):364.

[2] Fang G, Wang W, Paunic V, Heydari H, Costanzo M, Liu X, et al. Discovering genetic interactions bridging pathways in genome-wide association studies. Nat Commun. 2019;10(1):1–18.

[3] Zuk O, Hechter E, Sunyaev SR, Lander ES. The mystery of missing heritability: Genetic interactions create phantom heritability. Proc Natl Acad Sci USA. 2012;109(4):1193–1198.

[4] Mackay TF. Epistasis and quantitative traits: using model organisms to study gene–gene interactions. Nat Rev Genet. 2014;15(1):22–33.

[5] Wei WH, Hemani G, Haley CS. Detecting epistasis in human complex traits. Nature Reviews Genetics. 2014;15(11):722–733.

[6] Hutchison CA, Chuang RY, Noskov VN, Assad-Garcia N, Deerinck TJ, Ellisman MH, et al. Design and synthesis of a minimal bacterial genome. Science. 2016;351(6280).

[7] Blount ZD, Borland CZ, Lenski RE. Historical contingency and the evolution of a key innovation in an experimental population of Escherichia coli. Proc Natl Acad Sci USA. 2008;105(23):7899–7906.

[8] Wiser MJ, Ribeck N, Lenski RE. Long-term dynamics of adaptation in asexual populations. Science. 2013;342(6164):1364–1367.

[9] De Visser JAG, Krug J. Empirical fitness landscapes and the predictability of evolution. Nat Rev Genet. 2014;15(7):480–490.

[10] Harms MJ, Thornton JW. Historical contingency and its biophysical basis in glucocorticoid receptor evolution. Nature. 2014;512(7513):203–207.

[11] Kryazhimskiy S, Rice DP, Jerison ER, Desai MM. Global epistasis makes adaptation predictable despite sequence-level stochasticity. Science. 2014;344(6191):1519–1522.

[12] Sailer ZR, Harms MJ. High-order epistasis shapes evolutionary trajectories. PLoS Comput Biol. 2017;13(5):e1005541.

[13] Sohail M, Vakhrusheva OA, Sul JH, Pulit SL, Francioli LC, van den Berg LH, et al. Negative selection in humans and fruit flies involves synergistic epistasis. Science. 2017;356(6337):539–542.

[14] Phillips PC. Epistasisthe essential role of gene interactions in the structure and evolution of genetic systems. Nature Reviews Genetics. 2008;9(11):855–867.

[15] Taylor MB, Ehrenreich IM. Higher-order genetic interactions and their contribution to complex traits. Trends in genetics. 2015;31(1):34–40.

[16] Sailer ZR, Harms MJ. Detecting high-order epistasis in nonlinear genotype-phenotype maps. Genetics. 2017;205(3):1079–1088.

[17] New AM, Lehner B. Harmonious genetic combinations rewire regulatory networks and flip gene essentiality. Nat Commun. 2019;10(1):1–12.

[18] Segre D, DeLuna A, Church GM, Kishony R. Modular epistasis in yeast metabolism. Nat Genet. 2005;37(1):77–83.

[19] Kelley R, Ideker T. Systematic interpretation of genetic interactions using protein networks. Nat Biotech. 2005;23(5):561–566.

[20] Lehner B, Crombie C, Tischler J, Fortunato A, Fraser AG. Systematic mapping of genetic interactions in Caenorhabditis elegans identifies common modifiers of diverse signaling pathways. Nat Genet. 2006;38(8):896–903.

[21] Jasnos L, Korona R. Epistatic buffering of fitness loss in yeast double deletion strains. Nat Genet. 2007;39(4):550–554.

[22] Collins SR, Miller KM, Maas NL, Roguev A, Fillingham J, Chu CS, et al. Functional dissection of protein complexes involved in yeast chromosome biology using a genetic interaction map. Nature. 2007;446(7137):806–810.

[23] St Onge RP, Mani R, Oh J, Proctor M, Fung E, Davis RW, et al. Systematic pathway analysis using high-resolution fitness profiling of combinatorial gene deletions. Nat Genet. 2007;39(2):199–206.

[24] Typas A, Nichols RJ, Siegele DA, Shales M, Collins SR, Lim B, et al. High-throughput, quantitative analyses of genetic interactions in E. coli. Nat Methods. 2008;5(9):781.

[25] Roguev A, Bandyopadhyay S, Zofall M, Zhang K, Fischer T, Collins SR, et al. Conservation and rewiring of functional modules revealed by an epistasis map in fission yeast. Science. 2008;322(5900):405–410.

[26] Costanzo M, Baryshnikova A, Bellay J, Kim Y, Spear ED, Sevier CS, et al. The genetic landscape of a cell. Science. 2010;327(5964):425–431.

[27] Szappanos B, Kovács K, Szamecz B, Honti F, Costanzo M, Baryshnikova A, et al. An integrated approach to characterize genetic interaction networks in yeast metabolism. Nat Genet. 2011;43(7):656–662.

[28] Huang W, Richards S, Carbone MA, Zhu D, Anholt RR, Ayroles JF, et al. Epistasis dominates the genetic architecture of Drosophila quantitative traits. Proc Natl Acad Sci USA. 2012;109(39):15553–15559.

[29] Roguev A, Talbot D, Negri GL, Shales M, Cagney G, Bandyopadhyay S, et al. Quantitative genetic-interaction mapping in mammalian cells. Nat Methods. 2013;10(5):432.

[30] Bassik MC, Kampmann M, Lebbink RJ, Wang S, Hein MY, Poser I, et al. A systematic mammalian genetic interaction map reveals pathways underlying ricin susceptibility. Cell. 2013;152(4):909–922.

[31] Babu M, Arnold R, Bundalovic-Torma C, Gagarinova A, Wong KS, Kumar A, et al. Quantitative genome-wide genetic interaction screens reveal global epistatic relationships of protein complexes in Escherichia coli. PLoS Genet. 2014;10(2).

[32] Costanzo M, VanderSluis B, Koch EN, Baryshnikova A, Pons C, Tan G, et al. A global genetic interaction network maps a wiring diagram of cellular function. Science. 2016;353(6306):aaf1420.

[33] Van Leeuwen J, Pons C, Mellor JC, Yamaguchi TN, Friesen H, Koschwanez J, et al. Exploring genetic suppression interactions on a global scale. Science. 2016;354(6312):aag0839.

[34] Skwark MJ, Croucher NJ, Puranen S, Chewapreecha C, Pesonen M, Xu YY, et al. Interacting networks of resistance, virulence and core machinery genes identified by genome-wide epistasis analysis. PLoS Genet. 2017;13(2).

[35] Du D, Roguev A, Gordon DE, Chen M, Chen SH, Shales M, et al. Genetic interaction mapping in mammalian cells using CRISPR interference. Nat Methods. 2017;14(6):577.

[36] Heigwer F, Scheeder C, Miersch T, Schmitt B, Blass C, Jamnani MVP, et al. Time-resolved mapping of genetic interactions to model rewiring of signaling pathways. eLife. 2018;7:e40174.

[37] Horlbeck MA, Xu A, Wang M, Bennett NK, Park CY, Bogdanoff D, et al. Mapping the genetic landscape of human cells. Cell. 2018;174(4):953–967.

[38] Norman TM, Horlbeck MA, Replogle JM, Alex YG, Xu A, Jost M, et al. Exploring genetic interaction manifolds constructed from rich single-cell phenotypes. Science. 2019;365(6455):786–793.

[39] Liu X, Liu Z, Dziulko AK, Li F, Miller D, Morabito RD, et al. iSeq 2.0: A Modular and Interchangeable Toolkit for Interaction Screening in Yeast. Cell Systems. 2019;8(4):338–344.

[40] Kuzmin E, VanderSluis B, Wang W, Tan G, Deshpande R, Chen Y, et al. Systematic analysis of complex genetic interactions. Science. 2018;360(6386):eaao1729.

[41] Celaj A, Gebbia M, Musa L, Cote AG, Snider J, Wong V, et al. Highly Combinatorial Genetic Interaction Analysis Reveals a Multi-Drug Transporter Influence Network. Cell Syst. 2020;10(1):25–38.

[42] Tong AHY, Evangelista M, Parsons AB, Xu H, Bader GD, Pagé N, et al. Systematic genetic analysis with ordered arrays of yeast deletion mutants. Science. 2001;294(5550):2364–2368.

[43] Davierwala AP, Haynes J, Li Z, Brost RL, Robinson MD, Yu L, et al. The synthetic genetic interaction spectrum of essential genes. Nat Genet. 2005;37(10):1147–1152.

[44] Mani R, Onge RPS, Hartman JL, Giaever G, Roth FP. Defining genetic interaction. Proc Natl Acad Sci USA. 2008;105(9):3461–3466.

[45] Szathmary E. Do deleterious mutations act synergistically? Metabolic control theory provides a partial answer. Genetics. 1993;133(1):127–132.

[46] Dixon SJ, Costanzo M, Baryshnikova A, Andrews B, Boone C. Systematic mapping of genetic interaction networks. Ann Rev Genet. 2009;43:601–625.

[47] MacLean R. Predicting epistasis: an experimental test of metabolic control theory with bacterial transcription and translation. J Evol Biol. 2010;23(3):488–493.

[48] Lehner B. Molecular mechanisms of epistasis within and between genes. Tr Genet. 2011;27(8):323–331.

[49] Baryshnikova A, Costanzo M, Myers CL, Andrews B, Boone C. Genetic interaction networks: toward an understanding of heritability. Annu Rev of Genomics Hum Genet. 2013;14:111–133.

[50] Domingo J, Baeza-Centurion P, Lehner B. The causes and consequences of genetic interactions (epistasis). Annu Rev of Genomics Hum Genet. 2019;20:433–460.

[51] Bellay J, Atluri G, Sing TL, Toufighi K, Costanzo M, Ribeiro PSM, et al. Putting genetic interactions in context through a global modular decomposition. Genome Res. 2011;21(8):1375–1387.

[52] Michaut M, Baryshnikova A, Costanzo M, Myers CL, Andrews BJ, Boone C, et al. Protein complexes are central in the yeast genetic landscape. PLoS Comput Biol. 2011;7(2).

[53] Bagheri-Chaichian H, Hermisson J, Vaisnys JR, Wagner GP. Effects of epistasis on phenotypic robustness in metabolic pathways. Math Biosci. 2003;184(1):27–51.

[54] Bagheri HC, Wagner GP. Evolution of dominance in metabolic pathways. Genetics. 2004;168(3):1713–1735.

[55] Wong SL, Zhang LV, Tong AH, Li Z, Goldberg DS, King OD, et al. Combining biological networks to predict genetic interactions. Proceedings of the National Academy of Sciences. 2004;101(44):15682–15687.

[56] Martin G, Elena SF, Lenormand T. Distributions of epistasis in microbes fit predictions from a fitness landscape model. Nature genetics. 2007;39(4):555–560.

[57] Sanjuán R, Nebot MR. A network model for the correlation between epistasis and genomic complexity. PLoS One. 2008;3(7).

[58] Gertz J, Gerke JP, Cohen BA. Epistasis in a quantitative trait captured by a molecular model of transcription factor interactions. Theoretical population biology. 2010;77(1):1–5.

[59] Pumir A, Shraiman B. Epistasis in a model of molecular signal transduction. PLoS computational biology. 2011;7(5).

[60] Macía J, Solé RV, Elena SF. The causes of epistasis in genetic networks. Evolution. 2012;66(2):586–596.

[61] Velenich A, Gore J. The strength of genetic interactions scales weakly with mutational effects. Genome biology. 2013;14(7):R76.

[62] Weinreich DM, Knies JL. Fisher's geometric model of adaptation meets the functional synthesis: data on pairwise epistasis for fitness yields insights into the shape and size of phenotype space. Evolution. 2013;67(10):2957–2972.

[63] Wagner GP. Two rules for the detection and quantification of epistasis and other interaction effects. In: Epistasis. Springer; 2015. p. 145–157.

[64] Poelwijk FJ, Krishna V, Ranganathan R. The context-dependence of mutations: a linkage of formalisms. PLoS computational biology. 2016;12(6).

[65] Chiu HC, Marx CJ, Segrè D. Epistasis from functional dependence of fitness on underlying traits. Proc R Soc B. 2012;279(1745):4156–4164.

[66] Orth JD, Conrad TM, Na J, Lerman JA, Nam H, Feist AM, et al. A comprehensive genome-scale reconstruction of Escherichia coli metabolism–2011. Mol Syst Biol. 2011;7(1).

[67] Csete M, Doyle J. Bow ties, metabolism and disease. Tr Biotech. 2004;22(9):446–450.

[68] Kacser H, Burns JA. The control of flux. Symp Soc Exp Biol. 1973;32:65–104.

[69] Savageau MA. Biochemical systems analysis. A study of function and design in molecular biology. Reading, MA: Addison-Wesley Publishing Company, Inc.; 1976.

[70] Cornish-Bowden A. Fundamentals of enzyme kinetics. John Wiley & Sons; 2013.

[71] Versfeld L. Remarks on star-mesh transformation of electrical networks. Electron Lett. 1970;6(19):597–599.

[72] Dorfler F, Bullo F. Kron reduction of graphs with applications to electrical networks. IEEE Transactions on Circuits and Systems I: Regular Papers. 2013;60(1):150–163.

[73] Yu MK, Kramer M, Dutkowski J, Srivas R, Licon K, Kreisberg JF, et al. Translation of genotype to phenotype by a hierarchy of cell subsystems. Cell Syst. 2016;2(2):77–88.

[74] Chassagnole C, Noisommit-Rizzi N, Schmid JW, Mauch K, Reuss M. Dynamic modeling of the central carbon metabolism of *Escherichia coli*. Biotechnol Bioeng. 2002;79(1):53–73.

[75] Chou HH, Delaney NF, Draghi JA, Marx CJ. Mapping the fitness landscape of gene expression uncovers the cause of antagonism and sign epistasis between adaptive mutations. PLoS Genet. 2014;10(2).

[76] Ewald J, Bartl M, Dandekar T, Kaleta C. Optimality principles reveal a complex interplay of intermediate toxicity and kinetic efficiency in the regulation of prokaryotic metabolism. PLoS Comput Biol. 2017;13(2).

[77] Musso G, Costanzo M, Huangfu M, Smith AM, Paw J, San Luis BJ, et al. The extensive and condition-dependent nature of epistasis among whole-genome duplicates in yeast. Genome Res. 2008;18(7):1092–1099.

[78] Tischler J, Lehner B, Fraser AG. Evolutionary plasticity of genetic interaction networks. Nat, Genet. 2008;40(4):390–391.

[79] Dowell RD, Ryan O, Jansen A, Cheung D, Agarwala S, Danford T, et al. Genotype to phenotype: a complex problem. Science. 2010;328(5977):469–469.

[80] Li X, Lalić J, Baeza-Centurion P, Dhar R, Lehner B. Changes in gene expression predictably shift and switch genetic interactions. Nature communications. 2019;10(1):1–15.

[81] Khan AI, Dinh DM, Schneider D, Lenski RE, Cooper TF. Negative epistasis between beneficial mutations in an evolving bacterial population. Science. 2011;332(6034):1193–1196.

[82] Chou HH, Chiu HC, Delaney NF, Segrè D, Marx CJ. Diminishing returns epistasis among beneficial mutations decelerates adaptation. Science. 2011;332(6034):1190–1192.

[83] Scott M, Gunderson CW, Mateescu EM, Zhang Z, Hwa T. Interdependence of cell growth and gene expression: origins and consequences. Science. 2010;330(6007):1099–1102.

[84] Boyle EA, Li YI, Pritchard JK. An expanded view of complex traits: from polygenic to omnigenic. Cell. 2017;169(7):1177–1186.

[85] Malik-Sheriff RS, Glont M, Nguyen TVN, Tiwari K, Roberts MG, Xavier A, et al. BioModels15 years of sharing computational models in life science. Nucleic Acids Research. 2019 11;Gkz1055. Available from: `https://doi.org/10.1093/nar/gkz1055`.

[86] Stock JB, Waygood EB, Meadow N, Postma P, Roseman S. Sugar transport by the bacterial phosphotransferase system. The glucose receptors of the *Salmonella typhimurium* phosphotransferase system. J Biol Chem. 1982;257(23):14543–14552.

[87] Natarajan A, Srienc F. Dynamics of glucose uptake by single *Escherichia coli* cells. Metabolic engineering. 1999;1(4):320–333.

Figure supplements

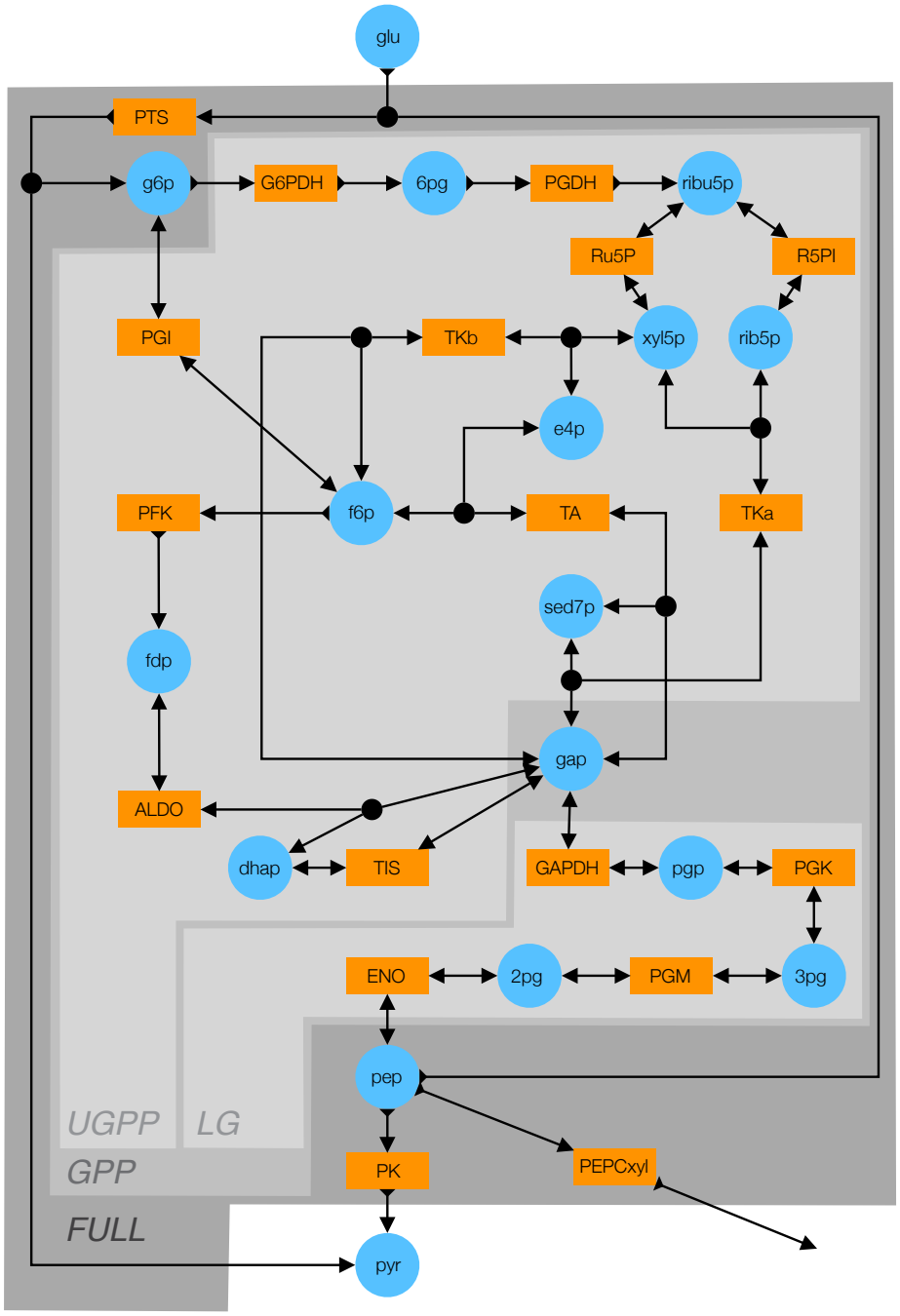

Figure 3–figure supplement 1. Simplified model by Chassagnole et al. (Ref. [74]). Blue circles indicate metabolites (see Table 5 for abbreviations). Orange rectangles indicate enzymes (see Table 6 for abbreviations). Double-arrows indicate reversible reactions. Arrows with a fletch indicate irreversible reactions. Black circles indicate reactions with multiple substrates or products. Different shades of gray indicate the FULL, GPP, UGPP and LG models defined in Table 4.

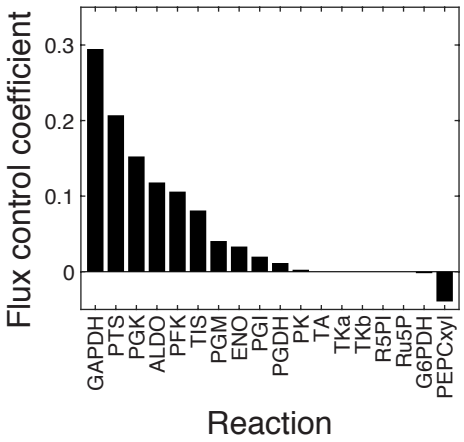

Figure 3–figure supplement 2. Control coefficients for the output flux in the FULL module. The first-order flux control coefficients (FCCs) of all 18 reactions with respect to the output flux in the unpperturbed FULL model are shown. 11 out of 18 reactions have positive FCCs, five (TA, TKa, TKb, R5PI, Ru5P) have zero FCCs and two (G6PDH and PEPCxyl) have negative FCCs. The 11 reactions with positive FCCs were retained for further analysis, the others were excluded. For these 11 reactions, the FCCs and epistasis coefficients with respect to fluxes through all modules (FULL, GPP, UGPP, LG) are shown in Figure 3–figure supplement 3.

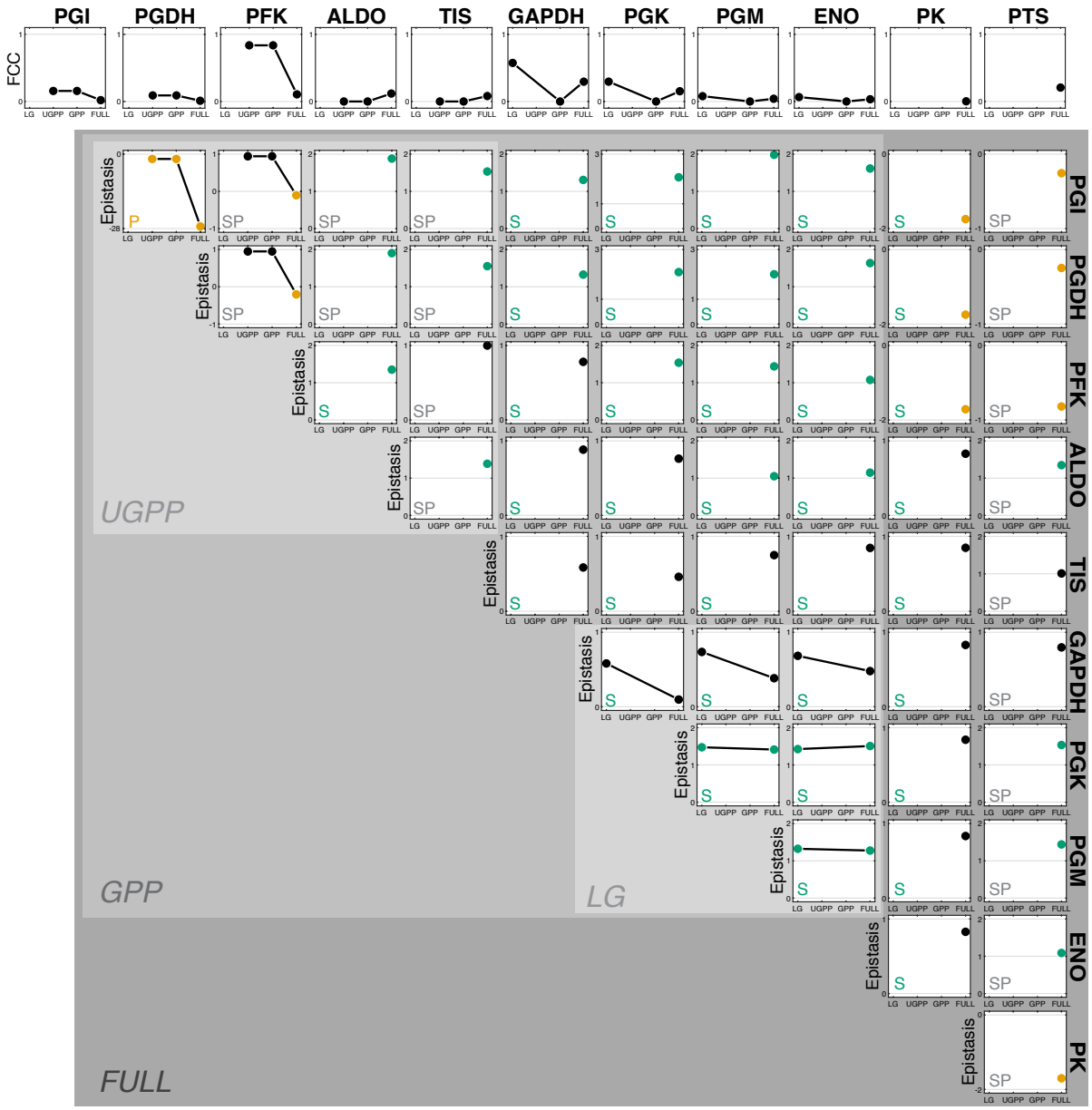

Figure 3–figure supplement 3. Control and epistasis coefficients for the fluxes through multiple sub-modules within glycolysis. The top row shows the FCCs of 11 reactions whose FCCs in the FULL model are positive (see Figure 3–figure supplement 2). The matrix below shows the epistasis coefficients for each pair of these reactions. The topological relationship between reactions is indicated in the lower left corner of each panel ("P", strictly parallel; "S", strictly serial; "SP" serial-parallel). Points are colored orange (green) if the epistasis coefficient is less than zero (greater than one). Backgrounds of different shades of gray indicate the sub-modules, as in Figure 3–figure supplement 1.

Additional files

- **Supplementary file 1.** Mathematica notebook "Case i,i,emptyset,P7.nb" for evaluating epistasis for the generating topology $\mathrm{i}, \mathrm{i}, \emptyset, \mathrm{P}_7$.
- **Supplementary file 2.** PDF version of the Mathematica notebook "Case i,i,emptyset,P7.nb".

Appendix 1 Derivation of equation (22)

First, the terms in equation (22) can be re-arranged as follows

$$
\begin{aligned}
x_{ij}^{E} &= x_{ij} + \frac{x_{ik_1}\, x_{k_1 j}}{D_{k_1}^{E\setminus\{k_1\}}} + \frac{x_{ik_2}\, x_{k_2 j}}{D_{k_2}^{E\setminus\{k_2\}}} + \cdots \\
&+ \frac{x_{ik_1}\, x_{k_1 k_2}\, x_{k_2 j}}{D_{k_1}^{E\setminus\{k_1\}}\, D_{k_2}^{E\setminus\{k_1,k_2\}}} + \cdots + \frac{x_{ik_2}\, x_{k_2 k_1}\, x_{k_1 j}}{D_{k_2}^{E\setminus\{k_2\}}\, D_{k_1}^{E\setminus\{k_1,k_2\}}} + \cdots \\
&= x_{ij} + \frac{x_{ik_1}}{D_{k_1}^{E\setminus\{k_1\}}} \underbrace{\left(x_{k_1 j} + \frac{x_{k_1 k_2}\, x_{k_2 j}}{D_{k_2}^{E\setminus\{k_1,k_2\}}} + \cdots \right)}_{=x_{k_1 j}^{E\setminus\{k_1\}}} \\
&+ \frac{x_{ik_2}}{D_{k_2}^{E\setminus\{k_2\}}} \underbrace{\left(x_{k_2 j} + \frac{x_{k_2 k_1}\, x_{k_1 j}}{D_{k_1}^{E\setminus\{k_1,k_2\}}} + \cdots \right)}_{=x_{k_2 j}^{E\setminus\{k_2\}}} + \cdots \\
&= x_{ij} + \sum_{\ell\in E} \frac{x_{i\ell}\, x_{\ell j}^{E\setminus\{\ell\}}}{D_{\ell}^{E\setminus\{\ell\}}}. \qquad \text{(A1.1)}
\end{aligned}
$$

Next, I will demonstrate the validity of equation (A1.1) by induction. It is clear, for $E = \{k\} \subset A_\mu$, equation (22) reduces to equation (7). Let E'' be a subset of A_μ. Let $k \in A_\mu \setminus E''$ be an internal metabolite that does not belong to E'', and let $E' = E'' \cup \{k\} \subseteq A_\mu$. Now suppose that equation (A1.1) holds for E'', i.e.,

$$
x_{ij}^{E''} = x_{ij} + \sum_{\ell\in E''} \frac{x_{i\ell}\, x_{\ell j}^{E''\setminus\{\ell\}}}{D_{\ell}^{E''\setminus\{\ell\}}}. \qquad \text{(A1.2)}
$$

I will now show that equation (A1.1) also holds for E', i.e.,

$$
x_{ij}^{E'} = x_{ij} + \sum_{\ell\in E'} \frac{x_{i\ell}\, x_{\ell j}^{E'\setminus\{\ell\}}}{D_{\ell}^{E'\setminus\{\ell\}}}. \qquad \text{(A1.3)}
$$

To do that, I use the definition of $x_{ij}^{E'}$ (equation (14)) and apply equation (A1.2) to

expand terms $x_{ij}^{E''}$ and $x_{ik}^{E''}$ as follows.

$$\begin{aligned} x_{ij}^{E'} &= x_{ij}^{E''} + \frac{x_{ik}^{E''}\, x_{kj}^{E''}}{D_k^{E''}} \\ &= x_{ij} + \sum_{\ell \in E''} \frac{x_{i\ell}\, x_{\ell j}^{E''\setminus\{\ell\}}}{D_\ell^{E''\setminus\{\ell\}}} + \frac{x_{ik}\, x_{kj}^{E''}}{D_k^{E''}} + \sum_{\ell \in E''} \frac{x_{i\ell}\, x_{\ell k}^{E''\setminus\{\ell\}}\, x_{kj}^{E''}}{D_\ell^{E''\setminus\{\ell\}}\, D_k^{E''}} \\ &= x_{ij} + \sum_{\ell \in E''} \frac{x_{i\ell}}{D_\ell^{E''\setminus\{\ell\}}} \left(x_{\ell j}^{E''\setminus\{\ell\}} + \frac{x_{\ell k}^{E''\setminus\{\ell\}}\, x_{kj}^{E''}}{D_k^{E''}} \right) + \frac{x_{ik}\, x_{kj}^{E''}}{D_k^{E''}}. \end{aligned} \tag{A1.4}$$

Recalling that $E' = E'' \setminus \{k\}$, I also re-write equation (A1.3) as

$$x_{ij}^{E'} = x_{ij} + \sum_{\ell \in E''} \frac{x_{i\ell}\, x_{\ell j}^{E'\setminus\{\ell\}}}{D_\ell^{E'\setminus\{\ell\}}} + \frac{x_{ik}\, x_{kj}^{E''}}{D_k^{E''}}. \tag{A1.5}$$

To demonstrate that equations (A1.4) and (A1.5) are identical, it is sufficient to show that for any $\ell \in E''$,

$$\frac{1}{D_\ell^{E''\setminus\{\ell\}}} \left(x_{\ell j}^{E''\setminus\{\ell\}} + \frac{x_{\ell k}^{E''\setminus\{\ell\}}\, x_{kj}^{E''}}{D_k^{E''}} \right) = \frac{x_{\ell j}^{E'\setminus\{\ell\}}}{D_\ell^{E'\setminus\{\ell\}}}. \tag{A1.6}$$

To show that equation (A1.6) holds, I first use equations (14) and (19) to express $x_{kj}^{E''}$ and $D_k^{E''}$ in terms of effective reaction rates after the elimination of the metabolite set $E'' \setminus \{\ell\}$,

$$\begin{aligned} x_{kj}^{E''} &= x_{kj}^{E''\setminus\{\ell\}} + \frac{x_{k\ell}^{E''\setminus\{\ell\}}\, x_{\ell j}^{E''\setminus\{\ell\}}}{D_\ell^{E''\setminus\{\ell\}}} \\ D_k^{E''} &= D_k^{E''\setminus\{\ell\}} - \frac{x_{k\ell}^{E''\setminus\{\ell\}}\, x_{\ell k}^{E''\setminus\{\ell\}}}{D_\ell^{E''\setminus\{\ell\}}}, \end{aligned} \tag{A1.7}$$

which imply that

$$\frac{1}{D_\ell^{E''\setminus\{\ell\}}} \left(x_{\ell j}^{E''\setminus\{\ell\}} + \frac{x_{\ell k}^{E''\setminus\{\ell\}}\, x_{kj}^{E''}}{D_k^{E''}} \right) = \frac{x_{\ell j}^{E''\setminus\{\ell\}}\, D_k^{E''\setminus\{\ell\}} + x_{\ell k}^{E''\setminus\{\ell\}}\, x_{kj}^{E''\setminus\{\ell\}}}{D_\ell^{E''\setminus\{\ell\}}\, D_k^{E''}} = \frac{D_k^{E''\setminus\{\ell\}}\, x_{\ell j}^{E'\setminus\{\ell\}}}{D_\ell^{E''\setminus\{\ell\}}\, D_k^{E''}}.$$

Finally, it follows from equation (A1.7) that

$$D_\ell^{E''\setminus\{\ell\}}\, D_k^{E''} = D_k^{E''\setminus\{\ell\}}\, D_\ell^{E'\setminus\{\ell\}},$$

which completes the proof of equality (A1.6). Thus, equation (A1.3) holds, thereby proving that equation (22) for any metabolite subset $E \subseteq A_\mu$.

Appendix 2 Properties of the coarse-graining procedure

The following are some properties of the p-step coarse-graining procedure CG^E eliminating metabolites in the set $E \subseteq A_\mu$.

1. It follows from equation (22) that the effective reaction rates x_{ij}^E do not depend on the order in which metabolites are eliminated. Thus, the composition of coarse-graining procedures is commutative, i.e., if $E = E_1 \cup E_2$, where E_1 and E_2 are two non-overlapping subsets of A_μ, then

$$\mathrm{CG}^{E_1} \circ \mathrm{CG}^{E_2} = \mathrm{CG}^{E_2} \circ \mathrm{CG}^{E_1} = \mathrm{CG}^E.$$

2. If at least one of the metabolites i or j is not adjacent to any of the eliminated metabolites, then $x_{ij}^E = x_{ij}$. This follows directly from equation (22).

3. If both metabolites i and j are adjacent to at least one eliminated metabolite, then

$$x_{ij}^E = x_{ij} + \alpha, \tag{A2.1}$$

   where $\alpha \geq 0$ depends only on the rates of reactions each of which involves at least one eliminated metabolite, but it does not depend on any of the reactions that involve only metabolites in $A \setminus E$. This follows directly from equation (22). In particular, if both k and ℓ are from $A \setminus E$, then x_{ij}^E is independent of $x_{k\ell}$.

4. If, in the original network $\mathcal{N}$, metabolites i and j are adjacent or connected by a simple path that contains only the eliminated metabolites, then metabolites i and j are adjacent in the coarse-grained network $\mathcal{N}^E$. This follows from equation (22).

5. Let $B = \{\ell_1, \ell_2, \ldots, \ell_m\} \subset A \setminus E$ be a subset of distinct metabolites that have not been eliminated by the coarse-graining procedure CG^E. If for each $i = 1, \ldots, m-1$, either ℓ_i and ℓ_{i+1} are adjacent or there exists a simple path $\ell_i \leftrightarrow \cdots \leftrightarrow \ell_{i+1}$ all of whose non-terminal metabolites are from E, then there exists a simple path $p_{\ell_1 \ell_m} = \ell_1 \leftrightarrow \cdots \leftrightarrow \ell_2 \leftrightarrow \cdots \leftrightarrow \ell_m$ in $\mathcal{N}^E$. This follows from Property #4 of the coarse-graining procedure (see Appendix 2).

6. If, in the metabolic network $\mathcal{N}$, metabolites i and j are not adjacent (i.e., $x_{ij} = 0$) and no simple path exists within the set E (i.e., such that all non-terminal metabolites in this path are from E) that connects metabolites i and j, then metabolites i and j are also not adjacent in the coarse-grained network $\mathcal{N}^E$ (i.e., $x_{ij}^E = 0$). This follows directly from equation (22).

7. Let $B = \{\ell_1, \ell_2, \ldots, \ell_m\} \subset A \setminus E$ be a subset of distinct metabolites which have not been eliminated by the coarse-graining procedure CG^E. For a simple path $p_{\ell_1\,\ell_m} = \ell_1 \leftrightarrow \ell_2 \leftrightarrow \cdots \leftrightarrow \ell_m$ to exist in $\mathcal{N}^E$, it is neccessary that for each $i = 1, \ldots, m-1$, either ℓ_i and ℓ_{i+1} are adjacent or there exists a simple path $\ell_i \leftrightarrow \cdots \leftrightarrow \ell_{i+1}$ all of whose non-terminal metabolites are from E. This follows from Property #6 of the coarse-graining procedure (see Appendix 2).

8. Properties #5 and #7 imply that for a simple path $p_{\ell_1\,\ell_m} = \ell_1 \leftrightarrow \ell_2 \leftrightarrow \cdots \leftrightarrow \ell_m$ to exist in $\mathcal{N}^E$, it is neccessary and sufficient that, in the original network $\mathcal{N}$, for each $i = 1, \ldots, m-1$, either ℓ_i and ℓ_{i+1} are adjacent or there exists a simple path $\ell_i \leftrightarrow \cdots \leftrightarrow \ell_{i+1}$ all of whose non-terminal metabolites are from E.

9. If $E = A_\mu$, then its effective reaction rate y_μ depends on the reaction rates $\boldsymbol{x}_\mu$ but does not depend on any other reaction rates or any of the metabolite concentrations, i.e.,
$$y_\mu = F_\mu\left(\boldsymbol{x}_\mu\right). \tag{A2.2}$$
This follows directly from equation (22).

Appendix 3 Functions mapping the rates of two reactions onto module's effective reaction rate

$$F_{\mathrm{b,io,IO}}(u,v) \;=\; u + \frac{v\,w_{32}}{v/K_{13} + w_{32}}. \tag{A3.1}$$

$$\begin{aligned} F_{\mathrm{b,i,\emptyset}}(u,v) &= u + \frac{D_3\,w_{14}\,w_{42} + D_4\,w_{13}\,w_{32} + w_{13}\,w_{42}\,v + w_{14}\,w_{32}\,v/K_{34}}{D_3\,D_4 - v^2/K_{34}}, \\ D_3 &= w_{31} + w_{32} + v, \\ D_4 &= w_{41} + w_{42} + v/K_{34}. \end{aligned} \tag{A3.2}$$

$$F_{\mathrm{io,io,I}}(u,v) \;=\; w_{12} + \frac{u\,v}{u/K_{13} + v}. \tag{A3.3}$$

$$\begin{aligned} F_{\mathrm{io,io,IO}}(u,v) &= w_{12} + \frac{D_3\,v\,w_{42} + D_4\,u\,w_{32} + u\,w_{34}\,w_{42} + v\,w_{43}\,w_{32}}{D_3\,D_4 - w_{34}\,w_{43}}, \\ D_3 &= u/K_{13} + w_{32} + w_{34}, \\ D_4 &= v/K_{14} + w_{42} + w_{43}. \end{aligned} \tag{A3.4}$$

$$
\begin{aligned}
F_{\mathrm{io,io},\emptyset}(u,v) &= w_{12} + \frac{D_3\, w_{14}\, v/K_{24} + D_4\, u\, w_{32} + u\, w_{34}\, v/K_{24} + w_{14}\, w_{43}\, w_{32}}{D_3\, D_4 - w_{34}\, w_{43}}, \\
D_3 &= u/K_{13} + w_{32} + w_{34}, \\
D_4 &= w_{41} + v/K_{24} + w_{43}.
\end{aligned} \tag{A3.5}
$$

$$
\begin{aligned}
F_{\mathrm{io,i,I}}(u,v) &= w_{12} + \frac{D_3\, w_{14}\, w_{42} + D_4\, u\, w_{32} + u\, v\, w_{42} + w_{14}\, w_{32}\, v/K_{34}}{D_3\, D_4 - v^2/K_{34}}, \\
D_3 &= u/K_{13} + w_{32} + v, \\
D_4 &= w_{41} + w_{42} + v/K_{43}.
\end{aligned} \tag{A3.6}
$$

$$
\begin{aligned}
F_{\mathrm{io,i},\emptyset}(u,v) &= W_{12} + \frac{W_{13}\, W_{32}}{W_{31} + W_{32}}, \\
W_{ij} &= w_{ij} + \frac{D_4\, w_{i5}\, w_{5j} + D_5\, w_{i4}\, w_{4j} + w_{i4}\, v\, w_{5j} + w_{i5}\, w_{4j}\, v/K_{45}}{D_4\, D_5 - v^2/K_{45}}, \\
D_4 &= w_{41} + w_{42} + w_{43} + v, \\
D_5 &= w_{51} + w_{52} + w_{53} + v/K_{45}, \\
w_{13} &\equiv u.
\end{aligned} \tag{A3.7}
$$

$$
\begin{aligned}
F_{\mathrm{i,i,I}}(u,v) &= W_{12} + \frac{D_3\, W_{14}\, W_{42} + D_4\, W_{13}\, W_{32} + W_{13}\, W_{34}\, W_{42} + W_{14}\, W_{43}\, W_{32}}{D_3\, D_4 - W_{34}\, W_{43}}, \\
W_{ij} &= w_{ij} + \frac{w_{i5}\, w_{5j}}{D_5}, \\
D_3 &= W_{31} + W_{32} + W_{34}, \\
D_4 &= W_{41} + W_{42} + W_{43}, \\
D_5 &= w_{51} + w_{52} + w_{53} + w_{54}, \\
w_{34} &\equiv u, \\
w_{35} &\equiv v.
\end{aligned} \tag{A3.8}
$$

$$
\begin{aligned}
F_{\mathrm{i,i},\emptyset}(u,v) &= W_{12} + \frac{D_3\, W_{14}\, W_{42} + D_4\, W_{13}\, W_{32} + W_{13}\, W_{34}\, W_{42} + W_{14}\, W_{43}\, W_{32}}{D_3\, D_4 - W_{34}\, W_{43}}, \\
W_{ij} &= w_{ij} + \frac{D_5\, w_{i6}\, w_{6j} + D_6\, w_{i5}\, w_{5j} + w_{i5}\, w_{6j}\, v + w_{i6}\, w_{5j}\, v/K_{56}}{D_5\, D_6 - v^2/K_{56}}, \\
D_3 &= W_{31} + W_{32} + W_{34}, \\
D_4 &= W_{41} + W_{42} + W_{43}, \\
D_5 &= w_{51} + w_{52} + w_{53} + w_{54} + v, \\
D_6 &= w_{61} + w_{62} + w_{63} + w_{64} + v/K_{56}, \\
w_{34} &\equiv u.
\end{aligned} \tag{A3.9, A3.10}
$$

In equations (A3.1)–(A3.9), u and v are given by expressions (32), (33). Effective activities $w_{ji} = w_{ij}/K_{ij} \geq 0$ are constants (except where otherwise noted) that depend on the original double-marked module (μ, a, b) and on the parameters $\boldsymbol{x}_{\mu\setminus\{a,b\}}$ but not depend on ξ and η.

Appendix 4 Epistasis in a toy metabolic network

In this section, I demonstrate that all three types of epistasis can emerge between two mutations that affect individual enzymes in a toy metablic network shown in Figure 4–figure 1 (see also Figure 2A). Mutation A perturbs the activity of the enzyme catalyzing the reaction between metabolites 1 and 3 and mutation B pertubs the activity of the enzyme catalyzing the reaction between metabolites 4 and 5. To simplify notations, I denote the rate of the affected reactions by $\xi = x_{13}$ and $\eta = x_{45}$, and I also denote $z = x_{34}$. The effects of mutations A and B at the microscopic level are $\delta^A\xi$ and $\delta^B\eta$, respectively, and there is no epistasis between them.

I label the module depicted in Figure 4–figure 1 (see also Figure 2A) as μ and label its effective reaction rate by y. I will calculate the epistasis coefficient εy between mutations A and B at the level of the effective reaction rate y, and I am specifically interested how εy depends on the reaction rate z of reaction between metabolites 3 and 4. Notice that module μ contains as smaller module ν with internal metabolites 3 and 4 and I/O metabolites 1 and 5. Denote the effective activity of module ν by u. Since both mutations affect module ν, I will calculate an epistasis coefficient εu between these mutations at the level of the effective actvity u and then propagate it to εy using expression (48).

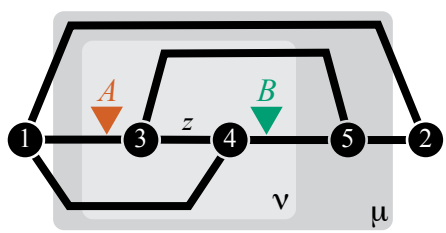

Appendix 4–figure 1. Toy metabolic network where all three epistasis regimes can emerge between mutations A and B. Same as Figure 2A, with more details.

Using expression (20), I coarse-grain module ν and obtain the effective reaction rate u between metabolites 1 and 5.

$$u = \frac{a\,\xi\,\eta + b_\xi\,\xi + b_\eta\,\eta + c}{d\,\xi\,\eta + e_\xi\,\xi + e_\eta\,\eta + f},$$

where

$$
\begin{aligned}
a &= \frac{x_{14}}{K_{13}} + x_{35} + z, \\
b_\xi &= x_{35}\left(x_{41} + \frac{z}{K_{34}}\right), \\
b_\eta &= x_{14}\left(x_{35} + z\right), \\
c &= \frac{x_{14}\, x_{35}\, z}{K_{34}}, \\
d &= \frac{1}{K_{13}}, \\
e_\xi &= \frac{1}{K_{13}}\left(x_{41} + \frac{z}{K_{34}}\right), \\
e_\eta &= x_{35} + z \\
f &= \frac{x_{35}\, z}{K_{34}} + x_{41}\, z + x_{35}\, x_{41}.
\end{aligned}
$$

I obtain the following expressions for the first- and second-order control coefficients.

$$
C_\xi = \frac{\xi}{u}\frac{\partial u}{\partial \xi} = \frac{\xi}{u}\left(\frac{(x_{35}+z)\,\eta + x_{35}\,(x_{41}+z/K_{34})}{D}\right)^2 = \frac{\xi}{u}\left(\frac{\tilde{c}_1\, z + \tilde{d}_1}{D}\right)^2, \tag{A4.1}
$$

$$
\begin{aligned}
C_\eta &= \frac{\eta}{u}\frac{\partial u}{\partial \eta} = \frac{\eta}{u}\frac{1}{K_{14}}\left(\frac{(x_{41}+z/K_{34})\,\xi/K_{43} + x_{14}\ (z + x_{35})}{D}\right)^2 \\
&= \frac{\eta}{u}\frac{1}{K_{14}}\left(\frac{\tilde{c}_2\, z + \tilde{d}_2}{D}\right)^2,
\end{aligned} \tag{A4.2}
$$

$$
H_{\xi\eta} = \frac{\xi\,\eta}{u}\frac{\partial^2 u}{\partial\xi\,\partial\eta} = \frac{\xi\,\eta}{u}\frac{2\,z}{K_{14}}\frac{\left(\tilde{c}_1\, z + \tilde{d}_1\right)\left(\tilde{c}_2\, z + \tilde{d}_2\right)}{D^3}, \tag{A4.3}
$$

where

$$
\begin{aligned}
D &= d\,\xi\,\eta + e_\xi\,\xi + e_\eta\,\eta + f, \\
\tilde{c}_1 &= \frac{1}{K_{54}}\left(x_{53} + \frac{\eta}{K_{45}}\right), \\
\tilde{d}_1 &= x_{35}\ (x_{41} + \eta), \\
\tilde{c}_2 &= \xi + x_{14}, \\
\tilde{d}_2 &= x_{14}\left(\frac{\xi}{K_{13}} + x_{35}\right).
\end{aligned}
$$

Substituting expressions (A4.1)–(A4.3) into equations (43)–(45), I obtain

$$\delta^A u = \frac{\xi}{u}\left(\frac{\tilde{c}_1\, z + \tilde{d}_1}{D}\right)^2 \delta^A \xi, \tag{A4.4}$$

$$\delta^B u = \frac{\eta}{u}\frac{1}{K_{14}}\left(\frac{\tilde{c}_2\, z + \tilde{d}_2}{D}\right)^2 \delta^B \eta. \tag{A4.5}$$

$$\varepsilon u = \frac{z\left(\tilde{a} z + \tilde{b}\right)}{\left(\tilde{c}_1\, z + \tilde{d}_1\right)\left(\tilde{c}_2\, z + \tilde{d}_2\right)}, \tag{A4.6}$$

where

$$\tilde{a} = \frac{1}{K_{54}}\left(\xi + x_{14}\right)\left(x_{53} + \frac{\eta}{K_{45}}\right) = \tilde{c}_1\, \tilde{c}_2,$$

$$\tilde{b} = \left(\frac{\xi}{K_{13}} + x_{35}\right) x_{14}\, \eta + \left(x_{41} + \eta\right) x_{35}\, \xi.$$

The mapping from u onto y can be easily obtained using expression (48). I coarse-grain module μ by eliminating the internal metabolite 5 and obtain

$$y = x_{12} + \frac{u\, x_{52}}{u/K_{15} + x_{52}}.$$

Therefore,

$$C_u = \frac{u}{y}\frac{dy}{du} = \frac{u}{y}\frac{x_{52}^2}{\left(u/K_{15} + x_{52}\right)^2} \geq 0, \tag{A4.7}$$

$$H_u = \frac{u^2}{y}\frac{d^2 y}{du^2} = -\frac{2\, u^2}{y\, K_{15}}\frac{x_{52}^2}{\left(u/K_{15} + x_{52}\right)^3} \leq 0, \tag{A4.8}$$

and

$$\varepsilon y = \frac{1}{C_u}\left(\varepsilon u + \frac{H_u}{2\, C_u}\right). \tag{A4.9}$$

Figure 2B illustrates the behavior of εy given by equation (A4.9) as a function of z. It was generated using the following matrix of rate constants:

$$\boldsymbol{x} = \begin{pmatrix} 0 & 0.378 & 0.514 & 0.237 & 0 \\ 1.810 & 0 & 0 & 0 & 1.001 \\ 42.232 & 0 & 0 & z & 2.446 \\ 7.957 & 0 & z/2.44 & 0 & 0.259 \\ 0 & 6.982 & 0.994 & 0.257 & 0 \end{pmatrix}.$$

The Matlab code is available at `https://github.com/skryazhi/epistasis_theory`.

Next, I consider several special cases of the toy network depicted in Figure 4–figure 1 that relate this network to those in Figures 2C and D in the main text.

Parallel reactions: $z = 0$. When $z = 0$, metabolic flux from metabolite 1 to metabolite 2 takes three paths: $1 \leftrightarrow 2$, $1 \leftrightarrow 2 \leftrightarrow 5 \leftrightarrow 2$ and $1 \leftrightarrow 4 \leftrightarrow 5 \leftrightarrow 2$ (see Figure 2C in the main text). Therefore, reactions $1 \leftrightarrow 3$ and $4 \leftrightarrow 5$, which are affected by mutations, are strictly parallel. In this case, according to equation (A4.6), $\varepsilon u = 0$ and hence

$$\varepsilon y = \frac{H_u}{C_u^2} \leq 0.$$

Linear pathway: $x_{12} = x_{35} = x_{14} = 0$. In this case, we have $\tilde{a} = \xi\,\eta$, $\tilde{c}_1 = \eta$, $\tilde{c}_2 = \xi$, and $\tilde{b} = \tilde{d}_1 = \tilde{d}_2 = 0$. Therefore $\varepsilon u = 1$. Moreover, equations (A4.7), (A4.8) simplify to

$$\begin{aligned} C_u &= \frac{x_{52}}{u/K_{15} + x_{52}}, \\ H_u &= -\frac{2\,u\,x_{52}}{K_{15}\,\left(u/K_{15} + x_{52}\right)^2}. \end{aligned}$$

Therefore, according to equation (A4.9), $\bar{\varepsilon} = -H_u\left[2C_u\left(1 - C_u\right)\right]^{-1} = 1$, and hence $\varepsilon y = 1$.

Effectively linear pathway: $z \to \infty$. When $z \to \infty$, module 1 becomes an effectively linear pathway because most of the metabolic flux between the I/O metabolites 1 and 5 passes through reaction $3 \leftrightarrow 4$. In this case, we have

$$\varepsilon u \to \frac{\tilde{a}}{\tilde{c}_1\,\tilde{c}_2} = 1,$$

and therefore, according to Theorem 1, $\varepsilon y \geq 1$.

Appendix 5 Existence of a simple path that contains a given reaction

Lemma 1. *For any reaction $a \in R_\mu$, there exists a simple path $p_{12}(a)$ within module μ that connects the I/O metabolites and contains this reaction, i.e., $\mathcal{P}_{12}^{\mu}(a) \neq \emptyset$.*

Proof. Reaction a is either a bypass, i/o, or internal reaction for module μ. If a is a bypass reaction, then the statement is trivially true. If a is an i/o reaction, then, without loss of generality, let $a = 1 \leftrightarrow j$. Since μ is a module, there exists a simple path $j \leftrightarrow j_1 \leftrightarrow \cdots \leftrightarrow 2$ that connects the internal metabolite j to the I/O metabolite 2. Therefore, the path $1 \leftrightarrow j \leftrightarrow j_1 \leftrightarrow \cdots \leftrightarrow 2$ connects the I/O metabolites and contains reaction a.

Suppose that $a = i \leftrightarrow j$ is an internal reaction. To prove the statement, it is sufficient to show that there exists a pair of non-intersecting paths p'_{1i} and p'_{2i}, such that one of them contains a and the other does not.

Since μ is a module, there exists a pair of non-intersecting paths p_{1i} and p_{2i} and a pair of non-intersecting paths p_{1j} and p_{2j} within module μ (I omitted super-index μ to simplify notations). Either (i) $j \in p_{1i}$ or $j \in p_{2i}$ or $i \in p_{1j}$ or $i \in p_{2j}$; or (ii) $j \notin p_{ui}$ and $i \notin p_{uj}$, $u = 1, 2$.

Consider case (i). Suppose it is the path p_{1i} that contains metabolite j. Then let

$$\begin{aligned} p'_{1i} &= \overbrace{1 \leftrightarrow \cdots \leftrightarrow \underbrace{j}_{=a}}^{\text{along } p_{1i}} \leftrightarrow i, \\ p'_{2i} &= p_{2i}, \end{aligned}$$

and the statement is true. We can analogously construct p'_{1i} and p'_{2i} in the cases when p_{2i} contains metabolite j, or p_{1j} contains metabolite i, or p_{2j} contains metabolite i. Thus, the statement is true in case (i).

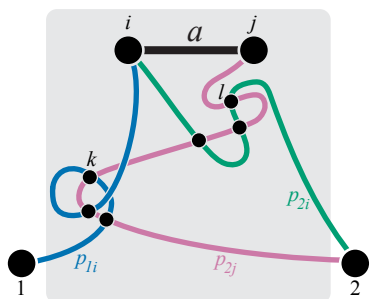

Appendix 5–figure 1. Illustration for the proof of Lemma 1.

Consider case (ii). If paths p_{2j} and p_{1i} do not intersect, then let

$$\begin{aligned} p'_{1i} &= p_{1i}, \\ p'_{2i} &= \underbrace{i \leftrightarrow j}_{=a} \overbrace{\leftrightarrow \cdots \leftrightarrow 2}^{=p_{2j}}, \end{aligned}$$

and the statement is true. Suppose paths p_{2j} and p_{1i} intersect. Then, among all metabolites that belong to both p_{1i} and p_{2j}, let metabolite k be the one closest to j along the path p_{2j} (Figure 5–figure 1). Then the segment p_{kj} of path p_{2j} and the path p_{1i} do not intersect. Let

$$p''_{1i} = \overbrace{1 \leftrightarrow \cdots \leftrightarrow k}^{\text{along } p_{1i}} \underbrace{\leftrightarrow \cdots \leftrightarrow j}_{\text{along } p_{2j}} \overbrace{\leftrightarrow i}^{=a},$$

If p''_{1i} and p_{2i} do not intersect, then the statement is true. If p''_{1i} and p_{2i} do intersect, this intersetion can only occur within the segment p_{kj} of path p''_{1i}, excluding metabolites k and j (Figure 5–figure 1). This is because the remaining segment p_{1k} of path p''_{1i} is also a segment of p_{1i}, which, by assumption, does not intersect p_{2i}. Suppose that among all metabolites that belong to both the segment p_{kj} of path p''_{1i} and the path p_{2i} metabolite ℓ is the one closest to j along the path p''_{1i}. Then let

$$\begin{aligned} p'_{1i} &= p_{1i}, \\ p'_{2i} &= \overbrace{2 \leftrightarrow \cdots \leftrightarrow \ell}^{\text{along } p_{2i}} \underbrace{\leftrightarrow \cdots \leftrightarrow j}_{\text{along } p_{2j}} \overbrace{\leftrightarrow i}^{=a}. \end{aligned}$$

The path p'_{2i} does not intersect the path p_{1i} because its first segment $p_{2\ell}$ belongs to path p_{2i} and its second segment $p_{\ell j}$ belongs to the segment p_{kj} of path p''_{1i} (and, as mentioned above, segment p_{kj} does not intersect p_{1i}). Thus, the statement holds for case (ii) as well. □

Appendix 6 Discovery of all strictly serial and strictly parallel generating topologies

How do we discover all generating topologies? Suppose that $(R, a, b) \in \mathcal{G}^{\mathcal{S}}_{\mathcal{M}}$, i.e., (R, a, b) is a strictly serial generating topology in class $\mathcal{M}$. Since $R \subseteq R_{\mathcal{M}}$ where $R_{\mathcal{M}}$ is the complete reaction set $R_{\mathcal{M}}$ for class $\mathcal{M}$, R can be discovered by sequentially removing reactions from $R_{\mathcal{M}}$. The same logic holds for all strictly parallel generating topologies. The following algorithm implements this idea.

1. **Define function** `generate_topology_list`**.** This function takes a topology $(R, a, b) \in \mathcal{R}^{\mathcal{Q}}_{\mathcal{M}}$ as input and returns a list of topologies L as output. Initialize $L = \emptyset$. For every reaction $c_i \in R \setminus \{a, b\}$, construct the reaction subset $R_i = R \setminus \{c_i\}$ and use Definition 1 to test whether R_i corresponds to a valid module. If R_i corresponds to a module, add (R_i, a, b) to list L; otherwiese, discard.[1] Return list L.

2. **Initialization.**

   (a) Pick a topological class $\mathcal{M}$.

   (b) Test whether $(R_{\mathcal{M}}, a, b) \in \mathcal{R}^{\mathcal{S}}_{\mathcal{M}}$. If so, $\mathcal{G}^{\mathcal{S}}_{\mathcal{M}} = \{(R_{\mathcal{M}}, a, b)\}$ and $\mathcal{G}^{\mathcal{P}}_{\mathcal{M}} = \emptyset$. Return $\mathcal{G}^{\mathcal{S}}_{\mathcal{M}}$, $\mathcal{G}^{\mathcal{P}}_{\mathcal{M}}$.

   (c) Test whether $(R_{\mathcal{M}}, a, b) \in \mathcal{R}^{\mathcal{P}}_{\mathcal{M}}$. If so, $\mathcal{G}^{\mathcal{P}}_{\mathcal{M}} = \{(R_{\mathcal{M}}, a, b)\}$ and $\mathcal{G}^{\mathcal{S}}_{\mathcal{M}} = \emptyset$. Return $\mathcal{G}^{\mathcal{S}}_{\mathcal{M}}$, $\mathcal{G}^{\mathcal{P}}_{\mathcal{M}}$.

[1] It can be proven that, as long as $(R, a, b) \in \mathcal{R}^{\mathcal{Q}}_{\mathcal{M}}$, there exists at least one $c_i \in R$, such that R_i corresponds to a module, i.e., $L \neq \emptyset$.

(d) Set $\mathcal{G}^{\mathcal{S}}_{\mathcal{M}} = \emptyset$, $\mathcal{G}^{\mathcal{P}}_{\mathcal{M}} = \emptyset$. Use function `generate_topology_list` with $(R_{\mathcal{M}}, a, b)$ as input and obtain the list of reaction sets L. Proceed to Step 3 with list L.

3. Take list $L = \big((R_1, a, b), (R_2, a, b), \ldots, (R_k, a, b)\big)$ as input. Set $L' = \emptyset$. Proceed to Step 3a with $i = 1$.

   (a) Test whether (R_i, a, b) belongs to $\mathcal{R}^{\mathcal{P}}_{\mathcal{M}}$, $\mathcal{R}^{\mathcal{S}}_{\mathcal{M}}$ or $\mathcal{R}^{\mathcal{Q}}_{\mathcal{M}}$. Choose one of the alternatives 3b, 3c, or 3d.

   (b) $(R_i, a, b) \in \mathcal{R}^{\mathcal{P}}_{\mathcal{M}}$. If $(R_i, a, b) \notin \mathcal{G}^{\mathcal{P}}_{\mathcal{M}}$ and if $(R_i \cup \{c\}, a, b) \in \mathcal{R}^{\mathcal{Q}}_{\mathcal{M}}$ for all $c \in R_{\mathcal{M}} \setminus R_i$, then add (R_i, a, b) to $\mathcal{G}^{\mathcal{P}}_{\mathcal{M}}$. Proceed to Step 3e.

   (c) $(R_i, a, b) \in \mathcal{R}^{\mathcal{S}}_{\mathcal{M}}$. If $(R_i, a, b) \notin \mathcal{G}^{\mathcal{S}}_{\mathcal{M}}$ and if $(R_i \cup \{c\}, a, b) \in \mathcal{R}^{\mathcal{Q}}_{\mathcal{M}}$ for all $c \in R_{\mathcal{M}} \setminus R_i$, then add (R_i, a, b) to $\mathcal{G}^{\mathcal{S}}_{\mathcal{M}}$. Proceed to Step 3e.

   (d) $(R_i, a, b) \in \mathcal{R}^{\mathcal{Q}}_{\mathcal{M}}$. Use function `generate_topology_list` with (R_i, a, b) as input and obtain the list of reaction sets L_i. Replace L' with $L' \cup L_i$. Proceed to Step 3e.

   (e) If $i = k$, proceed to Step 3f. Otherwise, proceed to Step 3a with $i + 1$.

   (f) If $L' \neq \emptyset$, then proceed to Step 3 with L' as input. Otherwise, return $\mathcal{G}^{\mathcal{S}}_{\mathcal{M}}$, $\mathcal{G}^{\mathcal{P}}_{\mathcal{M}}$.

Appendix 7 Derivation of equation (64)

In this case, equations (A3.10) simplify to

$$
\begin{aligned}
W_{12}(v) &= w_{12} + \frac{w_{16}\, w_{52}\, v/K_{56}}{D_{56}(v)}, \\
W_{13}(v) &= w_{13} + \frac{w_{16}\, w_{63}\, D_5(v)}{D_{56}(v)}, \\
W_{14}(v) &= \frac{w_{16}\, w_{54}\, v/K_{56}}{D_{56}(v)}, \\
W_{23}(v) &= \frac{w_{25}\, w_{63}\, v}{D_{56}(v)}, \\
W_{24}(v) &= w_{24} + \frac{w_{25}\, w_{54}\, D_6(v)}{D_{56}(v)}, \\
W_{34}(u, v) &= u + \frac{w_{36}\, w_{54}\, v/K_{56}}{D_{56}(v)},
\end{aligned}
$$

where

$$
\begin{aligned}
D_{56}(v) &= D_5(v)\, D_6(v) - \frac{v^2}{K_{56}}, \\
D_5(v) &= w_{52} + w_{54} + v, \\
D_6(v) &= w_{61} + w_{63} + v/K_{56}.
\end{aligned}
$$

Notice that the only effective activity that depends on u is W_{34}, and $\frac{\partial W_{34}}{\partial u} = 1$. Thus, it is easy to differentiate y, given by equation (A3.9), with respect to u, if we isolate the term W_{34} in both the numerator and the denomintor,

$$y = W_{12} + \frac{A_{56,34}\, W_{34} + B_{56,34}}{D_{56,34}}, \tag{A7.1}$$

where

$$\begin{aligned}
D_{56,34} &= E_{56,34}\, W_{34} + F_{56,34}, \\
A_{56,34} &= W_{14}\, W_{42} + \frac{W_{13}\, W_{32}}{K_{34}} + W_{13}\, W_{42} + \frac{W_{14}\, W_{32}}{K_{34}} \left(W_{13} + W_{14}\right) \left(\frac{W_{32}}{K_{34}} + W_{42}\right), \\
B_{56,34} &= W_{14}\, W_{42}\, \left(W_{31} + W_{32}\right) + W_{13}\, W_{32}\, \left(W_{41} + W_{42}\right), \\
E_{56,34} &= \frac{W_{31} + W_{32}}{K_{34}} + \left(W_{41} + W_{42}\right), \\
F_{56,34} &= \left(W_{31} + W_{32}\right) \left(W_{41} + W_{42}\right).
\end{aligned}$$

It is also useful to obtain another expression for y, which is easier to differentiate with respect to v. To do that, we can first eliminate metabolites 3 and 4 to obtain effective reaction rates

$$\begin{aligned}
V_{12}(u) &= w_{12} + \frac{w_{13}\, w_{42}\, u}{D_{34}(u)}, \\
V_{15}(u) &= \frac{w_{13}\, w_{45}\, u}{D_{34}(u)}, \\
V_{16}(u) &= w_{16} + \frac{w_{13}\, w_{36}\, D_4(u)}{D_{34}(u)}, \\
V_{25}(u) &= w_{25} + \frac{w_{24}\, w_{45}\, D_3(u)}{D_{34}(u)}, \\
V_{26}(u) &= \frac{w_{24}\, w_{36}\, u/K_{34}}{D_{34}(u)}, \\
V_{56}(u, v) &= v + \frac{w_{36}\, w_{54}\, u/K_{34}}{D_{34}(u)},
\end{aligned}$$

where

$$\begin{aligned}
D_{34}(u) &= D_3(u)\, D_4(u) - \frac{u^2}{K_{34}}, \\
D_3(u) &= w_{31} + u + w_{36}, \\
D_4(u) &= w_{42} + u/K_{34} + w_{45}.
\end{aligned}$$

The only effective activity that depends on v is V_{56}, and $\frac{\partial V_{56}}{\partial u} = 1$. Thus, isolating the term V_{56} (and recalling that $V_{65} = V_{56}/K_{56}$), we obtain the following expression for y,

which is easy to differentiate with respect to v.

$$y = V_{12} + \frac{A_{34,56}\, V_{65} + B_{34,56}}{D_{34,56}}, \tag{A7.2}$$

where

$$\begin{aligned}
D_{34,56} &= E_{34,56}\, V_{65} + F_{34,56}, \\
A_{34,56} &= (V_{16} + V_{15}) \left(\frac{V_{62}}{K_{65}} + V_{52} \right), \\
B_{34,56} &= V_{15}\, V_{52}\, (V_{61} + V_{62}) + V_{16}\, V_{62}\, (V_{51} + V_{52}), \\
E_{34,56} &= \frac{V_{61} + V_{62}}{K_{65}} + (V_{51} + V_{52}), \\
F_{34,56} &= (V_{61} + V_{62})\, (V_{51} + V_{52}).
\end{aligned}$$

Using symbolic computation it is possible to show that (see Mathematica notebook (Supplementary file 1) and Mathematica notebook pdf (Supplementary file 2), p. 2)

$$D_{56,34}\, D_{56} = D_{34,56}\, D_{34}. \tag{A7.3}$$

Also notice that, any module with the reaction set $\mathrm{i}, \mathrm{i}, \emptyset, \mathrm{P}_7$ is symmetric with respect to swapping metabolite labels 1 with 2, 3 with 5, and 4 with 6. It is easy to check that equations (A7.1), (A7.2) respect this symmetry.

Differentiating equation (A7.1) with respect to u, after some algebra I obtain

$$\frac{\partial y}{\partial u} = \frac{\partial y}{\partial W_{34}} = \frac{1}{K_{31}} \left(\frac{W_{31}\, W_{42} - W_{32}\, W_{41}}{D_{56,34}} \right)^2. \tag{A7.4}$$

Analogously, differentiating equation (A7.2) with respect to v, I obtain

$$\frac{\partial y}{\partial v} = \frac{1}{K_{56}} \frac{\partial y}{\partial V_{65}} = \frac{1}{K_{51}} \left(\frac{V_{52}\, V_{61} - V_{51}\, V_{62}}{D_{34,56}} \right)^2. \tag{A7.5}$$

Notice that equation (A7.5) can also be obtained from equation (A7.4) by symmetry with respect to the aforementioned metabolite relabelling.

Next, using symbolic computation (see Mathematica notebook (Supplementary file 1) and Mathematica notebook pdf (Supplementary file 2), p. 3), it is possible to show that

$$\frac{(W_{31}\, W_{42} - W_{32}\, W_{41})\; D_{56}}{D_{56,34}\, D_{56}} = \frac{A_u\, v + B_u}{E_u\, v + F_u}, \tag{A7.6}$$

where all coefficients

$$
\begin{aligned}
A_u &= \frac{w_{31}}{K_{56}}\,\psi + w_{42}\,\phi, \\
B_u &= \psi\,\phi \\
E_u &= u\left[\frac{w_{31}\,w_{52} + w_{31}\,w_{54} + w_{36}\,w_{52}}{K_{34}\,K_{56}} + (w_{42}\,w_{61} + w_{42}\,w_{63} + w_{45}\,w_{61})\right] + D_4(u)\,\phi + \frac{D_3(u)}{K_{56}}\,\psi \\
F_u &= u\left(\frac{w_{52} + w_{54}}{K_{34}}\,\phi + (w_{61} + w_{63})\,\psi\right) + \phi\,\psi.
\end{aligned}
$$

and

$$
\begin{aligned}
\phi &= w_{31}\,w_{61} + w_{31}\,w_{63} + w_{36}\,w_{61}, \\
\psi &= w_{42}\,w_{52} + w_{42}\,w_{54} + w_{45}\,w_{52}
\end{aligned}
$$

are independent of v and are non-negative. Similarly (see Mathematica notebook (Supplementary file 1) and Mathematica notebook pdf (Supplementary file 2), p. 4),

$$
\frac{(V_{52}\,V_{61} - V_{51}\,V_{62})\;D_{34}}{D_{34,56}\,D_{34}} = \frac{A_v\,u + B_v}{E_v\,u + F_v}, \tag{A7.7}
$$

where

$$
\begin{aligned}
A_v &= w_{61}\,\psi + \frac{w_{52}}{K_{34}}\,\phi, \\
B_v &= \psi\,\phi, \\
E_v &= v\left[(w_{42}\,w_{61} + w_{42}\,w_{63} + w_{45}\,w_{61}) + \frac{w_{31}\,w_{52} + w_{31}\,w_{54} + w_{36}\,w_{52}}{K_{34}\,K_{56}}\right] + \frac{D_5(v)}{K_{34}}\,\phi + D_6(v)\,\psi \\
F_v &= v\left((w_{42} + w_{45})\;\phi + \frac{w_{31} + w_{36}}{K_{56}}\,\psi\right) + \phi\,\psi.
\end{aligned}
$$

We can now obtain the second derivative $\frac{\partial^2 y}{\partial u\,\partial v}$, taking into account equation (A7.6). Alternatively, we can obtain $\frac{\partial^2 y}{\partial u\,\partial v}$ by differentiating $\frac{\partial y}{\partial v}$ with respect to u, taking into account equation (A7.7). The denominators in both expressions would be identical due to equation (A7.3). Therefore the expression for the second derivative must have the form given by equation (64), i.e.,

$$
\frac{\partial^2 y}{\partial u\,\partial v} = \frac{2\,\beta}{K_{31}}\,\frac{(A_u\,v + B_u)\;(A_v\,u + B_v)}{(E_u\,v + F_u)^3},
$$

where β is independent of u and v. Thus, according to equations (A7.4), (A7.6),

$$
\beta = \frac{A_u\,F_u - B_u\,E_u}{A_v\,u + B_v} = -\left(w_{36}\,\psi/K_{56} + w_{45}\,\phi\right),
$$

which is verified in Mathematica notebook (Supplementary file 1) and Mathematica notebook pdf (Supplementary file 2), p. 4. Similarly, according to equations (A7.5), (A7.7),

$$\frac{\beta}{K_{31}} = \frac{1}{K_{51}} \frac{A_v\, F_v - B_v\, E_v}{A_u\, v + B_v} = -\frac{w_{63}\, \psi + w_{54}/K_{34}\, \phi}{K_{51}}$$

which is verified in Mathematica notebook (Supplementary file 1) and Mathematica notebook pdf (Supplementary file 2), p. 5.